

# **High temperature UV-vis-NIR spectroscopy of glasses doped with polyvalent elements.**

## **Dissertation**

**zur Erlangung des akademischen Grades doctor rerum naturalium**

**(Dr. rer. nat.)**

vorgelegt dem Rat der Chemisch-Geowissenschaftlichen Fakultät  
der Friedrich-Schiller-Universität Jena

von Dipl.-Ing. Ladislav Kido

geboren am 14. Mai 1976 in Považská Bystrica, Slowakei

**Gutachter:**

1. Prof. Dr. Christian Rüssel
2. HDoz. Dr. Doris Ehrt

Tag der öffentlichen Verteidigung: 18. Mai 2005

## **Zusammenfassung.**

Polyvalente Elemente können einen beträchtlichen Einfluss auf die Eigenschaften von Glasschmelzen und fertigen Glasprodukten haben. Während bei Zimmertemperatur hauptsächlich die Färbung ein Ausdruck für abgelaufene Redoxreaktionen ist, wird bei hohen Temperaturen (in der Glasschmelze) zum Beispiel die Wärmeabsorption und -leitung wesentlich durch polyvalente Elemente beeinflusst. Trotz dieser großen praktischen Bedeutung gibt es nur relativ wenige direkte Untersuchungen zum Absorptionsverhalten polyvalenter Elemente bei hohen Temperaturen. Das Redoxverhalten polyvalenter Elemente in Glasschmelzen lässt sich durch elektrochemische Methoden direkt messen. Allerdings ist das bei Temperaturen unterhalb 800 °C nicht mehr (ohne weiteres) möglich. Hier bieten UV-vis-NIR-spektroskopische Messungen einen experimentellen Ausweg. In der vorgelegten Arbeit wird das Redoxverhalten ausgewählter, technologisch wichtiger polyvalenter Elemente in Gläsern der Zusammensetzung  $16\text{Na}_2\text{O}-10\text{CaO}-74\text{SiO}_2$  mittels Hochtemperaturspektroskopie (im vorliegenden Fall bis 800 °C) im UV-vis-NIR-Bereich zwischen 300 und 1.100 nm untersucht.

Die UV-vis-NIR-Spektroskopie bei hohen Temperaturen erfordert die Beachtung einiger Besonderheiten. Da ist zuerst die Tatsache, dass die zu untersuchenden Proben, aber auch der verwendete ‚Ofen‘ (hier ein Mikroskopheiztisch TS1500 der Firma LINKAM, GB), mit steigender Temperatur selbst Strahlung im zu untersuchenden Spektralbereich emittieren, die sich dem Messlicht überlagert. Gemäß dem PLANCK'schen Strahlungsgesetz nimmt die Intensität dieser thermischen Strahlung mit steigender Temperatur zu, und die Wellenlänge des Maximums der emittierten Strahlung verschiebt sich dabei aus dem IR- zunehmend in den sichtbaren Bereich (zu kleineren Wellenlängen). Oberhalb der Transformationstemperatur der zu untersuchenden Glasproben ist außerdem dafür Sorge zu tragen, dass es durch die zunehmende Wirksamkeit der Grenzflächenspannung nicht zu einer Verformung der Probe und damit zu einer Verfälschung der Abbildungsbedingungen kommt.

Aus diesem Grund wurden zwei unterschiedliche Messanordnungen verwendet. Für Untersuchungen im Wellenlängenbereich unter 500 nm, in dem sich die Effekte der thermischen optischen Emission unter den genannten Bedingungen praktisch noch nicht bemerkbar machen, kam ein Diodenarray-Spektrometer zum Einsatz, das zudem den Vorteil kurzer Messzeiten (< 1s) bietet. Im sichtbaren und im NIR-Bereich fand ein modulares Spektrometer mit Gittermonochromator (TRIAX320, ISA Jobin-Yvon) und Si-Detektor Verwendung. Wesentlich ist in

diesem Fall die Verwendung eines optischen Choppers, der im Strahlengang zwischen Lichtquelle (Halogenlampe) und Heiztisch mit Probe angeordnet ist, so dass nur das „gechopperte“ Licht mit Hilfe eines LockIn-Verstärkers (SR830, Stanford Research Systems, USA) ausgewertet wird.

Das  $16\text{Na}_2\text{O}-10\text{CaO}-74\text{SiO}_2$ -Grundglas ist ein in der Glasforschung häufig verwendetes Modellglas, das wesentliche physikalische Eigenschaften technischer Massengläser besitzt, aber für wissenschaftliche Untersuchungen auf einfache Weise variiert werden kann. Außerdem bietet es den Vorteil, dass es bereits ausgiebig untersucht ist und deshalb ein umfangreicher Datenbestand zu den physikalisch-chemischen Eigenschaften vorliegt.

Diesem Grundglas sind polyvalente Elemente in geringen Konzentrationen ( $< 2$  Mol-%) zugesetzt worden. Diese haben keinen Einfluss auf die optische Basizität des Grundglases, und deshalb bleiben die Position und die Halbwertsbreite der einzelnen Absorptionsbanden auch bei unterschiedlichen Konzentrationen an polyvalenten Elementen konstant. In den Gläsern mit mehr als einem polyvalenten Element sind die resultierenden Absorptionsspektren Überlagerungen der Banden der einzelnen Elemente. Aus diesem Grund werden die (auch von der Temperatur abhängigen) Parameter der GAUSS-Banden, die bei der Spektrenanalyse der nur mit einem polyvalenten Element versetzten Gläser erhalten wurden, auch für die Analyse der Spektren von Gläsern mit zwei polyvalenten Elementen genutzt.

In allen untersuchten Fällen verschob sich die UV-Absorptionskante mit steigender Temperatur in Richtung größerer Wellenlängen. Das ist auf eine verstärkte thermische Schwingung der Sauerstoffatome in der Glasstruktur zurückzuführen.

### **Mit Kupfer oder mit Kupfer und Zinn, Antimon bzw. Arsen dotierte Gläser.**

Die Spektren von CuO dotierten Gläsern zeigen eine Absorptionsbande um  $12.660\text{ cm}^{-1}$  ( ${}^2\text{E} \rightarrow {}^2\text{T}_2$ ), die ziemlich gut einer einzelnen GAUSS-Bande entspricht. Wie bereits erwähnt, bleiben die Position und die Halbwertsbreite dieser Absorptionsbande auch bestehen, wenn einem Glas zusätzlich zu CuO auch SnO, Sb<sub>2</sub>O<sub>3</sub> bzw. As<sub>2</sub>O<sub>3</sub> zugesetzt wird, und zwar bei allen hier untersuchten Konzentrationen und Temperaturen. Weder SnO noch Sb<sub>2</sub>O<sub>3</sub> bzw. As<sub>2</sub>O<sub>3</sub> absorbieren im vis-NIR-Bereich.

Mit steigender Temperatur wird die  $\text{Cu}^{2+}$ -Absorptionbande zu kleineren Wellenzahlen hin verschoben:  $11.560\text{ cm}^{-1}$  bei  $800\text{ °C}$ . Dabei wird die Bande breiter: von  $7.220\text{ cm}^{-1}$  bei  $25\text{ °C}$  auf  $7.580\text{ cm}^{-1}$  bei  $800\text{ °C}$ . In Gläsern, die nur mit  $\text{CuO}$  dotiert wurden, nimmt die Intensität der  $\text{Cu}^{2+}$ -Absorptionsbande mit steigender Temperatur nur wenig ab.

Gläser, die neben  $\text{CuO}$  auch noch mit  $\text{SnO}$  dotiert sind, zeigen bei  $25\text{ °C}$  eine verringerte Absorption im Vergleich zu Gläsern, die nur die gleiche Konzentration an  $\text{CuO}$  enthalten. Die Temperaturabhängigkeit ist aber sehr ähnlich dem oben beschriebenen Fall. Dieses Verhalten kann durch die geringe Standard-Reaktionsenthalpie von nur  $\Delta H^0_{\text{Cu/Sn}} = 8\text{ kJ}\cdot\text{mol}^{-1}$  für die Reaktion  $2\text{Cu}^+ + \text{Sn}^{4+} \leftrightarrow 2\text{Cu}^{2+} + \text{Sn}^{2+}$  erklärt werden.

Die Absorption von Gläsern die gleichzeitig  $\text{CuO}$  und  $\text{Sb}_2\text{O}_3$  enthalten, ist vergleichbar mit der von Gläsern, die  $\text{CuO}$  und  $\text{SnO}$  enthalten. Beim Aufheizen zeigen diese Gläser bis zu Temperaturen von etwa  $600\text{ °C}$  ein ebenfalls vergleichbares Verhalten, wie es oben bereits beschrieben ist. Oberhalb dieser Temperatur kommt es dann aber zu einem deutlichen Ansteigen der Intensität der  $\text{Cu}^{2+}$ -Absorptionsbande. Das lässt sich durch die in diesen Gläsern ablaufende Redoxreaktion  $2\text{Cu}^+ + \text{Sb}^{5+} \leftrightarrow 2\text{Cu}^{2+} + \text{Sb}^{3+}$  mit einem  $\Delta H^0_{\text{Cu/Sb}} = 102\text{ kJ}\cdot\text{mol}^{-1}$  erklären. Eine Temperaturniedrigung kehrt die Reaktion um und führt zu einer Verringerung der Intensität der  $\text{Cu}^{2+}$ -Bande.

Ganz ähnlich verhalten sich die mit  $\text{CuO}$  und  $\text{As}_2\text{O}_3$  dotierten Gläser: bis etwa  $600\text{ °C}$  bleibt beim Aufheizen die Intensität der  $\text{Cu}^{2+}$ -Bande mehr oder weniger konstant, oberhalb dieser Temperatur nimmt die Intensität zu. Auch läuft eine Redoxreaktion  $2\text{Cu}^+ + \text{As}^{5+} \leftrightarrow 2\text{Cu}^{2+} + \text{As}^{3+}$  mit einem  $\Delta H^0_{\text{Cu/As}} = 46\text{ kJ}\cdot\text{mol}^{-1}$  ab, die mit steigender Temperatur das Gleichgewicht auf die linke Seite verschiebt.

Thermodynamische Berechnungen auf der Basis von  $\Delta H^0$ - und  $\Delta S^0$ -Daten, die mittels Square-Wave-Voltammetrie bei höheren Temperaturen ermittelt wurden, erklären qualitativ und quantitativ die Verschiebung der Redoxverhältnisse während des Aufheizens und des Abkühlens im Temperaturbereich zwischen  $600$  und  $1.500\text{ °C}$ . Die Temperatur von  $600\text{ °C}$  wird als eine fiktive Temperatur angenommen, unterhalb derer wegen der kinetischen Hinderung keine Veränderungen im Redoxverhältnis mehr auftreten können.

## Mit Mangan oder Chrom sowie gleichzeitig mit Mangan und Chrom dotierte Gläser.

Drei Serien von Gläsern sind untersucht worden: Gläser, die nur mit Mangan dotiert wurden, Gläser, die nur mit Chrom dotiert wurden, sowie Gläser, die gleichzeitig Mangan und Chrom enthalten.

Mit steigender Temperatur nimmt die Intensität der  $\text{Cr}^{6+}$ -Bande (Übergang  $T_1(\pi) \rightarrow {}^3T_2(\pi^*)$ ), die bei 25 °C bei  $27.460 \text{ cm}^{-1}$  liegt, ab. Oberhalb 600 °C verstärkt sich diese Tendenz deutlich. Das kann durch eine Dissoziation der Chromatkomplexe erklärt werden. Damit kombiniert ist eine Synproportionierung gemäß  $2\text{Cr}^{6+} + \text{Cr}^{3+} \rightarrow 3\text{Cr}^{5+}$ , die oberhalb 600 °C in Betracht gezogen werden muss. Diese charge-transfer-Bande wird dabei nur um etwa  $570 \text{ cm}^{-1}$  zu kleineren Wellenzahlen verschoben (bei 800 °C). Gleichzeitig wird die Bande breiter: um  $1.640 \text{ cm}^{-1}$  ( $3.840 \text{ cm}^{-1}$  bei 25 °C).

Die Beschreibung der  $\text{Cr}^{3+}$ -Bande um  $22.560 \text{ cm}^{-1}$  ( ${}^4A_2 \rightarrow {}^4T_1(F)$ ) und einer Halbwertsbreite von  $3.270 \text{ cm}^{-1}$  mit GAUSS-Parametern kann nur in einem Temperaturbereich  $< 600 \text{ °C}$  erfolgen, in dem die oben genannte Synproportionierung noch nicht stattfindet, da die  $\text{Cr}^{5+}$ -Bande eine ähnliche Lage hat. Die erhaltenen Bandenparameter sind aber für die Analyse der Spektren (Zerlegung in Einzelbanden) der Gläser verwendet worden, die Chrom und Mangan enthalten.

Eine weitere  $\text{Cr}^{3+}$ -Bande liegt bei  $15.240 \text{ cm}^{-1}$ . Obwohl diese Bande eine Kombination aus zwei spin-verbotenen und einer spin-erlaubten Bande ist, wird sie hier als eine einheitliche Bande mit einer Halbwertsbreite von  $3.000 \text{ cm}^{-1}$  diskutiert. Es zeigte sich aber, dass diese zusammengesetzte Bande sich im gesamten untersuchten Temperaturbereich mit nur einer GAUSS-Bande hinreichend gut beschreiben lässt. Aus diesem Grund ist sie auch bei der Analyse der Spektren (Zerlegung in Einzelbanden) der Gläser verwendet worden, die Chrom und Mangan enthalten.

Die Absorptionsspektren der Gläser, die mit Mangan dotiert wurden, bestehen aus einer  $\text{Mn}^{3+}$ -Bande bei  $20.330 \text{ cm}^{-1}$ , Halbwertsbreite  $5.940 \text{ cm}^{-1}$  ( ${}^5E \rightarrow {}^5T_2$ ), und einer überlagerten Bande (Schulter) bei  $15.140 \text{ cm}^{-1}$  mit einer Halbwertsbreite von  $4.850 \text{ cm}^{-1}$ , die durch den JAHN-TELLER-Effekt hervorgerufen wird. Das Intensitätsverhältnis zwischen den beiden Banden ist etwa 4,3. Die Hauptbande verschiebt sich mit steigender Temperatur um etwa

1.330  $\text{cm}^{-1}$  zu kleiner Wellenzahlen hin und wird dabei breiter (8.130  $\text{cm}^{-1}$  bei 800 °C). Die Intensität nimmt dabei bis 700 °C um etwa 10% leicht ab. Die Intensität der zweiten Bande nimmt stärker ab, sie ist oberhalb 700 °C nicht mehr nachweisbar. Mit steigender Temperatur verschwindet also die durch den JAHN-TELLER-Effekt bewirkte Aufspaltung, und damit besteht das  $\text{Mn}^{3+}$ -Absorptionsspektrum nur noch aus einer GAUSS-Bande.

Die von den mit Chrom oder Mangan dotierten Gläsern erhaltenen GAUSS-Parameter (Position und Halbwertsbreite der Banden) wurden genutzt, um die Spektren von Gläsern zu beschreiben, die beide polyvalente Elemente enthalten. In diesen Gläsern werden die gleichen Absorptionsbanden gefunden wie in den Gläsern, die nur eines der beiden polyvalenten Elemente enthält. Allerdings ist die Intensität der  $\text{Cr}^{6+}$ -Bande bei 25 °C dann kleiner als in einem Glas, das nur die entsprechende Chrommenge enthält, während die Intensität der  $\text{Mn}^{3+}$ -Banden größer ist als in einem Glas mit nur der entsprechenden Menge Mangan. Das deutet auf eine Verschiebung der Redoxverhältnisse beim Abkühlen der Schmelze hin.

Während des Aufheizens eines mit Chrom und Mangan dotierten Glases nehmen die Intensitäten der betreffenden  $\text{Cr}^{6+}$ - und  $\text{Mn}^{3+}$ -Banden bis etwa 600 °C etwa in gleichem Maße ab, wie das in den nur mit Chrom bzw. nur mit Mangan dotierten Gläsern der Fall war. Bis etwa 600 °C werden die Redoxverhältnisse also nicht verändert. Oberhalb 600 °C steigt dann die Intensität der  $\text{Cr}^{6+}$ -Bande aber wieder an, während die der  $\text{Mn}^{3+}$ -Banden deutlich abnimmt. Dieses Verhalten kann durch eine Redoxreaktion  $\text{Cr}^{3+} + 3\text{Mn}^{3+} \leftrightarrow \text{Cr}^{6+} + 3\text{Mn}^{2+}$  erklärt werden.

Aus in der Literatur verfügbaren thermodynamischen Daten für des  $\text{Cr}^{6+}/\text{Cr}^{3+}$ -Redoxpaar und aus den Absorptionsspektren kann der molare Extinktionskoeffizient für die  $\text{Cr}^{6+}$ -Bande bei 27.460  $\text{cm}^{-1}$  berechnet werden. Weil der Anstieg der  $\text{Mn}^{3+}$ - und die Abnahme der  $\text{Cr}^{6+}$ -Konzentration direkt stöchiometrisch gekoppelt sind, kann auch der molare Extinktionskoeffizient für die  $\text{Mn}^{3+}$ -Bande bei 20.330  $\text{cm}^{-1}$  berechnet werden. Das ermöglicht die Berechnung der Gleichgewichtskonstante für das  $\text{Mn}^{3+}/\text{Mn}^{2+}$ -Gleichgewicht bei Temperaturen der Glas-schmelze. Aus den entsprechenden molaren Absorptionskoeffizienten, den thermodynamischen Daten für das  $\text{Cr}^{6+}/\text{Cr}^{3+}$ -Gleichgewicht, der Gleichgewichtskonstante für das  $\text{Mn}^{3+}/\text{Mn}^{2+}$ -Gleichgewicht bei 1.480 °C und der gefitteten Standard-Enthalpie von  $\Delta H^0 = 106,8 \text{ kJ}\cdot\text{mol}^{-1}$ , wurden die  $\text{Cr}^{6+}$ - und  $\text{Mn}^{3+}$ -Absorptionen berechnet.

Durch Variation der Aufheizgeschwindigkeiten zwischen 20 und 1 K·min<sup>-1</sup> war es möglich neue, wichtige Kenntnisse über die Kinetik der Reaktion zwischen Chrom- und Manganionen in Gläsern zu erhalten. Mit Hilfe des Diodenarray-Spektrometers können aufgrund der kurzen Messzeiten (0,3 s) die Änderungen im Redoxverhältnis exakt als Funktion der Temperatur und der Zeit verfolgt werden.

Mit sich ändernder Temperatur wird > 520 °C eine Redoxreaktion beobachtet. Mit steigender Temperatur verschiebt sich diese Reaktion auf die Seite von Cr<sup>6+</sup> und Mn<sup>2+</sup>. Bei Temperaturen < 520 °C wird die Reaktion eingefroren, während sie oberhalb 600 °C im Gleichgewicht ist (innerhalb der Zeitskala dieses Experimentes). Im Temperaturbereich zwischen 530 °C und 600 °C nimmt durch eine Wärmebehandlung die Intensität der Cr<sup>6+</sup>-Bande ab, während die der Mn<sup>3+</sup>-Bande gleichzeitig mit der Zeit der Wärmebehandlung steigt. Die Relaxationszeiten sind im Bereich von 9.460 bis 2.000 s für Temperaturen von 550 und 570 °C. Das ist der erste experimentelle Nachweis für einen chemischen Redox-Relaxationsprozess in Gläsern



## Contents:

Zusammenfassung. ....	i
1. Introduction and aims of the project. ....	3
2. State of the art. ....	5
3. Theoretical Introduction. ....	16
3.1. Thermodynamics and kinetics of redox reactions in glasses. ....	16
3.1.1. Thermodynamics of redox equilibria. ....	16
3.1.2. Kinetics of redox reactions in glass melts. ....	18
3.2. Influence of temperature on transition metal complexes. ....	19
4. Experimental part. ....	26
4.1. Preparation and characterization of the samples. ....	26
4.1.1. Glass preparation. ....	26
4.1.2. General characterisation of the base glass. ....	27
4.1.3. Preparation of samples for spectroscopic investigations. ....	28
4.2. Optical absorption spectroscopy. ....	29
4.3. Equipment for the high temperature absorption spectroscopy. ....	30
4.4. Treatment of HT absorption spectra of different glasses. ....	33
4.4.1. Copper doped glasses. ....	33
4.4.2. Manganese doped glasses. ....	36
4.4.3. Chromium doped glasses. ....	38
4.4.4. Manganese and Chromium doped glasses. ....	41
4.4.5. Evaluation of errors of HT measurement. ....	44
4.5. Electron spin resonance. ....	44

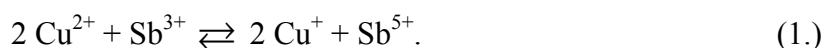
5. Results.....	46
5.1. Basic glass spectra as a function of temperature.....	46
5.2. Copper doped glasses.....	47
5.3. The mutual redox interaction between copper and tin, antimony, arsenic.....	52
5.3.1. Copper – Tin interaction.....	53
5.3.2. Copper – Antimony interaction.....	55
5.3.3. Copper – Arsenic interaction.....	56
5.4. Chromium.....	62
5.5. Manganese.....	69
5.6. Chromium - Manganese interaction.....	72
5.7. Study of the kinetics of a redox reaction in the particular case of the chromium and manganese doped glasses.....	79
6. Conclusions.....	88
6.1. Glasses doped with copper or additionally with tin, antimony, arsenic.....	88
6.2. Glasses solely doped with manganese or chromium or simultaneously with chromium and manganese.....	90
7. References.....	93

## 1. Introduction and aims of the project.<sup>+</sup>

Since the first glass was melted, the colourization and decolourization process of this important and specific materials attracts the attention of people.

Colourization of glass (in volume) is connected with the absorption of electromagnetic radiation having wavelengths in the visible range, and a certain colour arises, e.g., by adding a small amount of a polyvalent transition element. Transition metals in glasses have an effect on the macroscopic properties. Although the concentration of the transition metals is often only in the ppm range, they have, for example, a significant influence on the optical properties. This is mostly used if glass should have a specific colour shade with the application. Decolourization in turn is a mechanism which disables colouring substances. Concerning polyvalent elements, different oxidation states absorb in different ranges of the spectrum, for example absorption bands due to the chromium  $\text{Cr}^{3+}$  ion occur in the visible region, whereas those of the  $\text{Cr}^{6+}$  ion mainly occur in the UV region. Ions such as  $\text{Cr}^{6+}$  also possess ligand to metal charge transfer bands which occur in the UV region. Then, if the equilibrium of  $[\text{A}^{n+}]/[\text{A}^{(n-z)+}]$  is completely shifted towards the direction of one of the elements, which then absorbs the light in infrared or, mostly, ultraviolet, no colour will appear. However, in some cases, e.g., ferrous/ferric or cuprous/cupric equilibria, it is not possible to use this pattern because  $\text{Fe}^0$  or  $\text{Cu}^0$  might be produced. Hence, not only the nature of the polyvalent element has an important effect on the glass colour, but also the oxidation state and, in special cases, the microstructure influence these properties.

The redox equilibrium can be influenced by the melting conditions (oxidising or reducing atmosphere) and/or by introducing another polyvalent element. In the latter case, their valences change and form redox pairs in a redox system. An example is the reaction of copper with antimony:



As a result, the position of the equilibrium between these two ions greatly affects the absorption spectrum and hence the colour of the host glass.

---

<sup>+</sup> všetko dôležité, čo sme sa mali naučiť v škole, sme sa naučili v prvej triede: čítať, písať a počítať! ;o) ... posadili nás na drevenné stoličky a zakázali nám rozprávať ... zvláštná to "1<sup>st</sup> class".

Furthermore, by introducing the second polyvalent element into a glass (Eq. (1)), the redox equilibria between  $[A^{n+}]/[A^{(n-z)+}]$  or  $[B^{n+}]/[B^{(n-z)+}]$ , have a fairly different effect. From the points mentioned above, it is important to understand the redox equilibrium in the glass system. In many studies, these problems were mostly solved either by using methods that operate with glass at room temperature or the glass was quenched from high temperature and investigated at room temperature, and extrapolation of redox equilibrium was done. In last decades, square-wave voltammetry in molten glasses has been taken an important part in describing redox behaviour in glass melts. However, there is still a large temperature gap from room up to glass softening temperature. With some modifications, an absorption spectrometer combined with a microscope heating stage can be used to bridge over this gap.

The aim of this project has been predominantly oriented to better understand redox phenomena in 16Na<sub>2</sub>O-10CaO-74SiO<sub>2</sub> (mol%) glass systems doped either solely with one polyvalent element or simultaneously with two polyvalent elements at temperatures in the range from 25 up to 800 °C. This glass was chosen as one of the most frequently used glass compositions in the glassmaking industry, and it can also be considered as an approximation of the Na<sub>2</sub>O-3SiO<sub>2</sub> basic composition.

Absorption behaviour of polyvalent elements in different glasses at room temperature was studied thoroughly and reported in many papers. By contrast, there are only a few investigations on their high temperature absorption behaviour, although, the absorption behaviour at higher temperatures is responsible for heat transfer and transport in glasses and glass melts. Furthermore, the knowledge of absorption behaviour of polyvalent elements as a function of temperature is the basis for understanding and interpretation of the optical emission spectroscopy which should be used to estimate the concentration of these polyvalent elements in glass melts.

Changes in optical absorption, caused by redox reactions by cooling or heating glass processes, should be investigated. Especially, if there is a reaction between two polyvalent elements in glass, it is interesting and important to describe direction, freezing-in temperature and other changes connected with certain redox reaction. The investigations should be done by the means of high-temperature UV-vis-NIR absorption spectroscopy as an in-situ method, which offers collecting of spectra directly from a sample at higher temperature.

## 2. State of the art.

Many properties of glass melts and, finally, also glass products are influenced by the concentration and the redox stage of polyvalent elements present. It should be mentioned, that not only the colour or the optical absorption has important meaning for cooled glasses but also for melts. The absorption of IR radiation significantly influences the heat transport during melting process and, thus, the convection in a melting tank and hence the whole melting process. The light emission of a melt strongly depends on polyvalent elements and their redox stage.

To investigate the redox equilibrium of a certain polyvalent ion in the cooled glass or melt two ways are described in the literature: at room temperature and melting temperature. In the former case, melt is equilibrated at a defined oxygen partial pressure and a certain temperature and, subsequently, the cooled (quenched) glass is investigated at room temperature [1, 2]. Analyses at ambient temperature, however, sometimes do not result in the right conclusions on the redox behaviour in the melt, since some polyvalent elements do not only occur in two redox states but can simultaneously exist in many ones. This can lead into false conclusions.

Investigations at high temperature are predominantly done by means of electrochemical methods. Here, the standard potential of a redox pair can be directly measured. If the measurements are done at different temperature, then thermodynamic parameters, such as standard enthalpy,  $\Delta H^0$ , or standard entropy,  $\Delta S^0$ , can be calculated.

Besides, there are some works, which connect both ways. For example, the redox ratio of vanadium ions in glasses equilibrated at high temperatures (temperature range of 1600 °C up to 2000 °C) was investigated using EPR and UV-vis-NIR spectroscopy and compared with the results obtained from voltammetric measurements [3]. It was shown, that only  $V^{4+}$  and  $V^{5+}$  are present in glass at room temperature, whereas during voltammetric measurements at high temperature around 12 %  $V^{3+}$  is in equilibrium with  $V^{4+}$  and  $V^{5+}$ . Based on the respective  $\Delta H^0$  and  $\Delta S^0$  values it was shown that this evident discrepancy depends on synproportional reaction during cooling. Therefore, using both ways, it is possible to find logical conclusions.

However, it is still little known what happens in glasses during the cooling process below temperatures where voltammetric methods will not work anymore. If only one polyvalent element is present and if its concentration in the reduced form is large in comparison with the

real amount of physically dissolved oxygen, the redox ratio will not change during cooling, because the diffusion of oxygen into the melt is too slow. But if the glass contains two or more polyvalent elements, a redox reaction between the two (or more) polyvalent elements is expected. In the glass melt at high temperatures ( $\gg T_g$ ), the redox reaction is in equilibrium. During cooling of the glass melt, it could be possible that the reaction is no longer in the thermodynamic equilibrium and kinetic effects play an important part. Even a complete kinetic hindrance is possible, if the temperature falls below a certain limit. In many papers it is assumed that the equilibrium can be frozen in at temperatures, normally used to melt glass. This assumption is expected to be valid also in the case if two polyvalent elements are incorporated in the melt [4, 5].

On the other side, there are theoretical works [6, 7] supported by experimental results [8] that shift the frozen-in temperature far lower, close to the transition range of a certain glass. According to Ref. [6], the enthalpy of a redox reaction is estimated and then the equilibrium state during cooling is calculated. Considering a reaction of 2<sup>nd</sup> order, the differential equation can be concluded. Furthermore, if the kinetics is diffusion-controlled then, according to the task, the diffusion coefficient can be numerically calculated. Depending on the cooling rate, the redox reaction is frozen-in in the  $T_g \pm 50$  K temperature range.

Investigations of the redox interaction of  $Fe^{2+}/Fe^{3+}$  and  $Mn^{2+}/Mn^{3+}$  in glasses in the temperature range from 25 to 680 °C have been done by means of EPR. Here, at first the temperature dependency of a glass containing only one polyvalent element was examined. From that the other measurements were adjusted. It is shown, that the redox reaction



is shifted to the left during cooling. Here, the signal intensity of the  $Fe^{3+}$  peaks increases in comparison to glass containing only iron. The redox reaction is completely frozen-in at 400 °C. In the system  $Fe^{2+}/Fe^{3+}$  and  $As^{3+}/As^{5+}$  the redox reaction is shifted to the left during cooling:



The frozen-in temperature is almost the same as for the iron-manganese system.

In literature, three different measuring principles are described which enable to determine the spectral absorption of melts, namely, the *transmission method*, the *reflection method* and the

*emission method.* Emission spectroscopy and reflection spectroscopy are preferred for wavelengths  $>3 \mu\text{m}$ , where transmission spectroscopy is not longer possible\*, since the glass becomes increasingly opaque.

Intensive research into the measurement of spectral characteristics of glass melts was initiated by the works of Genzel and Neuroth. For his measurement design, Genzel [9] used a platinum mirror ( $1 \times 3 \text{ cm}^2$ ), which was placed just below the surface of a glass melt at  $1300^\circ\text{C}$ . For the first time, an optical chopper was used to separate the thermal self-radiation of the sample from the transmitted radiation. The absorption coefficient was calculated taking into account the depth of immersion and the reflectivity of the interfaces glass/mirror, and glass/air, respectively. A hot platinum filament was used as radiation source. One potential source of error with this method is the formation of a surface meniscus that works as a dispersing lens for the light beam reflected at the platinum mirror. This problem will be discussed below again. Another possible source of errors is the position of the platinum mirror in the glass melt, since its position can change during the measurement.

Neuroth [10, 11] used the method developed by Genzel and extended the analysis to several types of glass: window glass, green glass and x-ray protection glass of the composition  $61\text{PbO}\cdot 34\text{SiO}_2\cdot 3\text{BaO}\cdot 2\text{Na}_2\text{O}$  (wt %). He observed the flattening of the  $\text{Fe}^{2+}$  absorption band at  $1.1 \mu\text{m}$  and of the OH band at  $2.8 \mu\text{m}$  with increasing temperature. He ascribed this flattening of the absorption bands to the increased damping of the ions due to their stronger movement at higher temperatures. Neuroth showed [12] that the influence of the temperature also leads to a decrease of the absorption coefficient of the Si-O oscillation in window glass and  $\text{SiO}_2$  glass at  $9 \mu\text{m}$ . Here, the shift towards longer wavelengths of the band bears close resemblance to the linear thermal expansion with the temperature.

His results led Neuroth to the conclusion that with increasing temperature the absorption decreases as long as the glass is solid. Once the glass enters into the liquid phase, the absorption starts to increase again. Recent research contradicts this statement [13]. Interpretations of the temperature dependence of the absorption coefficients can be derived from the ligand field theory for the different electron migrations.

---

\* The layer thickness would have to be extremely small ( $\mu\text{m}$ ).

The reflection method developed by Genzel and Neuroth was no longer used after 1953. Coenen [14] used the transmission method and extended the analyses of Genzel and Neuroth with his own apparatus to temperatures up to 1400°C. Both sapphire and polished silica glass are used for the sample cell. The apparatus allows measurements in reducing atmosphere. The glasses he analysed contained the colouring oxides Fe<sub>2</sub>O<sub>3</sub> (0.05 - 4 wt %), Cr<sub>2</sub>O<sub>3</sub> (0.05-0.5 wt %), CoO, MnO<sub>2</sub>, and NiO. The glasses belong to the glass system 74SiO<sub>2</sub>·16Na<sub>2</sub>O·10CaO (mol %). Coenen found that glasses with high concentrations of colouring oxides do not comply with the law of Lambert and Beer, since in this case, the absorption does not increase linearly with the concentration. Regarding the influence of the temperature on the glass structure, he states that due to the thermal oscillations of the colouring metal ions, the strengths of the bonds in the network decrease for temperatures below the glass transition temperature. Accordingly, the absorption bands become weaker and broaden. However, at temperatures above (T<sub>g</sub>), with increasing temperatures the bonds in glass break up increasingly, which leads to an increase in terminal [≡ Si-O] groups, which tend to group around the colouring metal ions. This manifests itself in an increase of the absorption coefficient, until the thermal expansion exceeds this effect and, hence, the coefficient decreases again. Coenen supports this result with a plot of the absorption coefficient of a glass that is doped with 1 wt % Fe<sub>2</sub>O<sub>3</sub> at λ = 460 nm vs. temperature. The absorption coefficient decreases up to a temperature of 500 °C, then increases up to 950°C, and decreases again for still higher temperatures. The resulting absorption coefficients are used to calculate radiation conductivity that can be applied in practice, e.g., for the so-called re-dyeing of melting tanks.

Wedding et al. [15] used an experimental set-up where two furnaces were used to measure absorption spectra at temperatures between 25°C and 1300°C. The sample is heated in one furnace while the other is used as reference radiator. The light beam of the radiation source is directed by a sector mirror alternately towards the sample and the reference furnace, and then focused on the entrance slit of the monochromator. In front of the rotating sector mirror a chopper wheel modulates the light beam of the radiation source. The measurable spectral range lies between 0.25 and 7 μm. In the sample furnace the sample is placed between two sapphire plates (2.5 cm diameter).

These works are focused on three particular spectral ranges: the ultraviolet absorption edge, the region of the water bands, and the region of the Fe<sup>2+</sup> absorption bands. The results also show a shift of the UV absorption edge with increasing temperature. In the spectral range



where the hydroxyl groups absorb, the absorption coefficient of the absorption band at 3.6  $\mu\text{m}$  decreases as well\*, while for the OH-band at around 2.8  $\mu\text{m}$  increases. This increase becomes larger with increasing ratio between  $\text{M}_2\text{O}$  ( $\text{M} = \text{Li}, \text{Na}, \text{K}$ ) and  $\text{MO}$  ( $\text{M} = \text{Ba}, \text{Ca}, \text{Mg}, \text{Pb}, \text{Sr}$ ). The decrease of the hydrogen-bridge bonds between the hydroxyl groups and the non-bridging oxygens with increasing temperatures was inferred from these results. These changes are reversible and occur smoothly.

For the  $\text{Fe}^{2+}$  absorption bands, the expected behaviour of the decrease of the absorption coefficient with the temperature was confirmed. For a glass that contains  $\text{Sn}^{2+/4+}$  ions in addition to  $\text{Fe}^{2+/3+}$  and  $\text{Sb}^{3+/5+}$  ions, the decrease of the absorption coefficient is less pronounced than for glass with the same concentration of  $\text{Fe}^{2+/3+}$  and  $\text{Sb}^{3+/5+}$  ions but that was not doped with  $\text{Sn}^{2+/4+}$  ions. The author ascribed this to an increasing transformation of  $\text{Fe}^{2+}$  into  $\text{Fe}^{3+}$ .

One method for the measurement of emission and absorption in liquid slags is described by Mausbach et al. [16]. In a high-temperature cell that can be flooded with inert gas, a glass sample is melted on a Pt70Rh30 net and heated up to 1500°C. The small mesh extension of 0.5 mm secures that the substance is held due by its surface tension and does not drop through. However, this measurement set-up is limited to the analysis of very thin layer thicknesses (up to 0.1 mm).

The analysis of slags (47 $\text{Al}_2\text{O}_3$ ·53 $\text{CaO}$  (mol %)) were doped with different amounts of  $\text{Cr}_2\text{O}_3$  and  $\text{Fe}_2\text{O}_3$ . it was found that the absorption bands become broader with increasing temperature and shift towards longer wavelengths. For the charge-transfer transition of  $\text{Fe}^{2+}$  at 280 nm a band shift of 60 nm towards longer wavelengths was detected in the temperature range between 25 °C and 1500 °C. This was attributed to a lower bonding energy within the complex that can be calculated from the band shift:  $\Delta W = \left( \frac{hc}{\lambda_1} - \frac{hc}{\lambda_2} \right) \cdot N_A$ .

By contrast, a decrease of the absorption coefficient with the temperature was not found. With an increasing degree of network (lower share of terminal  $[\equiv \text{Si-O}]^-$  groups), the charge-transfer absorption bands shift towards shorter wavelengths.

---

\* The decrease of the absorption coefficient occurs reversibly.

Okretic, Nowack and Mausbach [17] analysed the behaviour of the charge-transfer absorption bands of the  $[\text{CrO}_4]^{2-}$  anion between 25°C and 1500°C in a slag of the composition 46SiO<sub>2</sub>-55CaO (wt %). The slag was doped with 2 mass % Cr<sub>2</sub>O<sub>3</sub>. At room temperature, two charge-transfer transitions at 280 and 367 nm could be detected. At temperatures above 1000 °C, the charge-transfer absorption bands are shifted slightly (5 nm) towards longer wavelengths, which is ascribed to the thermal excitation of the lattice vibrations of the Cr-O bond (wavenumber: 900-370 cm<sup>-1</sup>). The samples, which are yellowish-green at the beginning, become colourless after an extended holding time at 1500 °C. The intensity of the charge-transfer absorption bands decreases with increasing holding time at 1500 °C; after 80 min, the Cr<sup>6+</sup> can no longer be detected in the samples. The authors ascribe this to the evaporation of CrO<sub>3</sub>.

In addition to the above mentioned authors, Tilquin et al. [18] analysed chromium containing melts at temperatures of 1000 °C and different oxygen partial pressure. The system Na<sub>2</sub>O·1.2SiO<sub>2</sub>·1.2B<sub>2</sub>O<sub>3</sub> was studied and the glasses were doped with 20 ppm Cr as Na<sub>2</sub>CrO<sub>4</sub>·4H<sub>2</sub>O. For the high temperature spectroscopic analysis double-beam spectrometer was used (Cary Model 17DH) in which a furnace could be placed with two SiO<sub>2</sub> pipes (length 1.5 m, diameter 23 mm). The light of the radiation source is, at first, directed into a monochromator and, subsequently, through a chopper, and is then split into two beams. The two beams enter the furnace through SiO<sub>2</sub> windows and pass through the two SiO<sub>2</sub> pipes. One of the SiO<sub>2</sub> pipes can be filled with the sample, while the other is used as reference. Then, both beams are targeting on a detector.

Tilquin et al. also assumed that the absorption bands at 370 nm are caused by Cr<sup>6+</sup>, which is surrounded by four oxygen ligands in the form of a tetrahedron. The only change in the absorption spectrum they found at 1000 °C in comparison to the absorption spectrum at room temperature is a broadening of the absorption band at 370 nm. With increasing oxygen partial pressure, the absorption coefficient of the charge-transfer absorption bands also increases. The authors inferred from their results that, at temperatures above 1000°C,  $[\text{CrO}_4]^{2-}$  groups occur in oxidic melts. In addition to the charge-transfer band, four d-d transfer bands of Cr<sup>3+</sup> can be detected: at 430, 625, 640 and 680 nm. At 1000 °C, they are shifted towards longer wavelengths and broaden. At higher temperatures, these bands could no longer be detected due to the increased noise in the far IR region. Hence, the authors do not have detailed results for the extent of the band shift and band broadening. With the described apparatus, Fe<sub>2</sub>O<sub>3</sub>

doped sodium silicate glasses of the composition  $67\text{SiO}_2\cdot 33\text{Na}_2\text{O}$  (mol%) were also analysed [19]. There are no significant changes in the absorption coefficient of the  $\text{Fe}^{2+}$  absorption band in the high temperature range between  $700^\circ\text{C}$  and  $1000^\circ\text{C}$ . It behaves analogously to the Cr bands of the sodium oxide-boron oxide-silica glasses doped with chromium.

In addition to Tilquin et al., Paul [20] conducted temperature-independent studies of  $\text{SiO}_2$  free, but high in boron-oxide glasses. The composition of his glasses varied between  $66.7\dots 89\text{B}_2\text{O}_3\cdot 33.3\dots 11\text{Na}_2\text{O}$  (mol %). Additionally, a sodium-silicate glass was investigated:  $70\cdot\text{SiO}_2\cdot 30\cdot\text{Na}_2\text{O}$  (mol%). The glasses were doped with 0.04 wt %  $\text{Cr}_2\text{O}_3$  as  $(\text{NH}_4)_2\text{Cr}_2\text{O}_7$  and analysed spectroscopically in a temperature range between 0 and  $400^\circ\text{C}$ . In this temperature interval, the absorption coefficients of all glasses decrease with increasing temperature. For a glass with the composition  $30\text{Na}_2\text{O}\cdot 70\text{B}_2\text{O}_3$  (mol %), the decrease of the absorption at the band maximum amounts up to 5%. For  $\text{Na}_2\text{O}$  concentrations of larger than 25 mol %, the absorption coefficient decreases less with the temperature. This was reported to be attributed to structural changes in the glass, since for rising  $\text{Na}_2\text{O}$  concentration the chromate group is increasingly favoured over the boron chromate group. This is also reflected in the change of the thermal expansion coefficient.

The shift of the peak maximum towards longer wavelengths occurs linearly and amounts to 5 nm for a  $30\text{Na}_2\text{O}\cdot 70\text{B}_2\text{O}_3$  glass. The change in the ion radius of the anion is given as a possible explanation, but there are no data which support this interrelation. Paul [20] also finds a broadening of the absorption band and a linear relation between the band halfwidth of the charge-transfer absorption band and  $T^{1/2}$ .

Endrys [13] described the set-up of a high temperature spectroscopy measuring system, where the glass samples are placed between two sapphire windows. At temperatures of about  $1400^\circ\text{C}$  the appearance of crystalline layers at the interface of sapphire and glass was observed. These crystalline layers lead to an incorrect determination of the absorption coefficient. Another source of error for the determination of the absorption coefficient of the analysed container glasses results from the reading of the analogously recorded intensities. The authors show that the change of the absorption coefficient with the temperature is reversible both for the OH-bands and for the  $\text{Fe}^{2+}$  absorption band. The reversible changes in the region of the  $\text{Fe}^{2+}$  absorption band give hints at a temperature-dependent extinction coefficient. The change of the OH-band at  $2.8\ \mu\text{m}$  is characterized by the difference of the absorption coefficients at

2.8  $\mu\text{m}$  and 2.5  $\mu\text{m}$ . At high temperatures, the band at 3.6  $\mu\text{m}$  disappears and the band at 2.8  $\mu\text{m}$  is reduced in intensity.

Goldman [21] investigated the temperature dependence of the  $\text{Fe}^{2+}$  absorption band of Ca-Al-borosilicate glasses with the composition  $56\cdot\text{SiO}_2\cdot 23\text{CaO}\cdot 15\text{Al}_2\text{O}_3\cdot 6\text{B}_2\text{O}_3$  (mol %). To explain the insertion of the  $\text{Fe}^{2+}$  ion in the glass network, the absorption spectrum of the glass is compared with the absorption spectra of three silicate minerals: orthopyroxene, aktinolithe and cordierite. In these minerals,  $\text{Fe}^{2+}$  has two absorption bands: one at 1  $\mu\text{m}$  and another one at wavelengths between 2 and 2.5  $\mu\text{m}$ . In orthopyroxene  $(\text{Mg,Fe})_2\text{Si}_2\text{O}_6$ , two positions for  $\text{Fe}^{2+}$ ,  $\text{M}_1$  and  $\text{M}_2$ , exist, where  $\text{Fe}^{2+}$  is octahedrally coordinated. With increasing bond length metal ion and oxygen, the bands are shifted towards longer wavelengths. According to the authors, this means that the band in silicate glasses at 2  $\mu\text{m}$  is not necessarily caused by tetrahedral coordinated  $\text{Fe}^{2+}$ .

If comparing the absorption spectrum at 1260°C with the absorption spectrum at room temperature, the authors did not find any modification. They ascribed the decrease of the absorption coefficient in the maximum of the  $\text{Fe}^{2+}$  absorption band at around 1  $\mu\text{m}$  that was found by other authors to an oxidation reaction of  $\text{Fe}^{2+}$ . To support this thesis, they kept the glass melt at 1260 °C for several hours. Similarly in this experiment, the absorption decreased notably at 1.67  $\mu\text{m}$  and 2.85  $\mu\text{m}$ , until after about 3 h the absorption remained constant.

Nolet [22] recorded absorption spectra of aluminosilicate glasses under reduced atmosphere ( $p(\text{O}_2) = 10^{-8}$  bar) at temperatures between 25 and 400 °C. For a glass of the composition  $49.2\text{SiO}_2\cdot 10.3\text{Al}_2\text{O}_3\cdot 10\text{FeO}\cdot 19.5\text{MgO}\cdot 10.3\text{CaO}$  (wt %), the absorption coefficient increased at 1  $\mu\text{m}$  and 1.9  $\mu\text{m}$  linearly with the temperature. The author discussed the possibility that the increasing distortion of the complex and the thermal oscillations lead to an increase in the absorption coefficient. This cannot be compared with the temperature dependent absorption spectra of orthopyroxene, that also have absorption bands at 1 and 1.9  $\mu\text{m}$ , since the band at 1.9  $\mu\text{m}$  ( $\text{M}_2$ ) decreases with temperature. By contrast, the band at 1  $\mu\text{m}$  increases with temperature. The absorption bands of  $\text{Fe}^{2+}$  in the aluminosilicate glass are, therefore, ascribed to octahedral (1  $\mu\text{m}$ ) and tetrahedral (1.9  $\mu\text{m}$ ) coordinated  $\text{Fe}^{2+}$ .

Van Nijnatten et al. modified in [23] the experimental equipment of Wedding. The authors used an  $\text{Al}_2\text{O}_3$  crucible with a sapphire window mounted in the center of the bottom. Another

Al<sub>2</sub>O<sub>3</sub> tube having a sapphire window at the end is immersed into the glass melt, creating a controllable measurement volume between the two sapphire windows. Using a system of mirrors, the radiation is reflected into an FTIR-spectrometer, which can measure both the emission of the sample and the blackbody furnace. The results from measurements obtained using clear float glass showed that the H<sub>2</sub>O evaporation is rather high if the samples are thin (0.37 cm), i.e., thicker samples were much more stable at high temperature. Besides, the use of the sapphire windows caused glass contamination by Al<sub>2</sub>O<sub>3</sub>.

In early works, Genzel and Neuroth analysed the temperature dependence of spectral absorption coefficients of glasses, some of which contained two or more polyvalent elements. In these cases, it is hard to distinguish whether the change of the absorption coefficients is due to a change of the extinction coefficient or to a redox reaction between the polyvalent elements. Especially for the spectral region of the Fe<sup>2+</sup> absorption band, a band separation is required for the high temperature and room temperature absorption spectra in order to specify the influence of the temperature at the band halfwidth of the electron transition. In the literature, there is only a limited number of works that performed a band separation for the high temperature spectra of Fe<sub>2</sub>O<sub>3</sub> doped glasses [24, 25].

Considering the experimental set-ups described in the literature, it becomes clear that in most cases sapphire instead of SiO<sub>2</sub> glass was used for the transparent windows of the sample holder. Sapphire is well suited for this purpose due to its transparency in the range between 0.17 and 6.5 μm. In addition, it is suitable for high temperature spectroscopy due to its high melting point at 2040 °C. However, for wavelengths < 3 μm, SiO<sub>2</sub> glass is to be preferred over sapphire, since the transparency of SiO<sub>2</sub> glass decreases significantly only for longer wavelengths. In addition, SiO<sub>2</sub> glass is less expensive than sapphire and has a lower refraction index\*. Hence, the reflection losses at the surface are lower and the signal-noise ratio improves. The crystallisation phenomena at the interface of sapphire and glass melt that Endrys describes can occur as well if using SiO<sub>2</sub> glass.

Temperature-dependent investigations using UV-vis-NIR spectroscopy were also applied to study the growth of nano-phases in glass. There, the formation of CuX and AgX (X = Cl or Br) [26, 27] as well as CdS and CdSe nano-crystals [26] were in focus. Those experiments

---

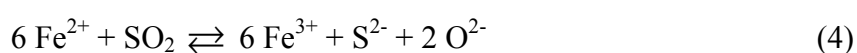
\* Refraction index of sapphire:  $n_{d \perp c} = 1.77$  compared to SiO<sub>2</sub>-glass  $n_d = 1.46$  (at 589.3 nm)

using UV-vis-NIR spectroscopy showed that the growth of particular nano-phases could be directly observed but also noteworthy to define the range of the nucleus-formation. It was found that the ultraviolet absorption edge of the glass samples without nano-crystals is shifted linearly towards higher wavelengths with increasing temperature, as assumed, until the glass transition is passed over. A deviation occurs in the temperature range below the  $T_g + 50$  K which is identified also from other measurements as the nucleus-growth range. Above  $T_g + 50$  K, the formation of CuX, AgX, CdS or CdSe nano-phases could be observed from the particular absorption bands of these semiconductor nano-phases.

If the temperature is constant, the increase of the intensity of those bands depends on, i.e.,  $Cl^- / Br^-$  ratio in the glasses, and hence also in the  $CuCl_xBr_{1-x}$  nano-crystals. That means: the higher the ratio of  $Br^- / Cl^-$ , the less soluble are the separable nano-phases in a glass matrix and the faster their growth. For CuBr nano-phases, all precipitable material is separated at 600 °C after 10 minutes, however, for CuCl nano-phases such a stadium is reached after 100 minutes. During further decrease of temperature, more material is separated as long as the  $T_g$  is reached, since the solubility of a particular phase decreases with decreasing temperature.

If the temperature is below a certain value, significant changes in the recorded spectra are observed, i.e., the intensity of characteristic absorption bands assigned to separated CuX nano-phases is decreased in a narrow temperature range, at the same time new absorption bands arise, which show the characteristic exciton absorption peaks for the CuX nano-crystals. When the samples with CuX nano-crystals are heated up again, then the described process turns back but at rather higher temperature, since the nano-crystals melt. This hysteresis of solidifying and melting behaviour is characteristic for such small phases. The smaller the nano-phases are, the larger is the difference between the melting and solidifying temperatures. The melting and solidifying temperature of the nano-crystals is up to 200 K lower than the melting point of the particular bulk material. The smaller the crystals are the higher is the difference.

Another work refers on the temperature dependency of the intensity of  $Fe^{2+}$  and  $Fe^{3+}$  in (mol %)  $16Na_2O \cdot 10CaO \cdot 74SiO_2$  glasses and also the decomposition of the chromophore in amber glass [28]. This is responsible for the brown colour of many hollow glass products. If  $Fe^{3+}$  and  $S^{2-}$  are simultaneously present in glass, then the chromophore can be described as a  $FeS_x$  structure and the redox reaction is expected:



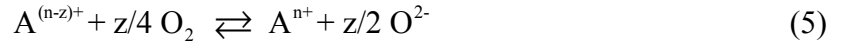
A shift of the absorption edge towards higher wavelengths with increasing temperature was found. The amount of the shift depends on the  $\text{Fe}^{3+}$  concentration. Here, the UV absorption edge may superimpose or even cover up the absorptions bands of colouring ions with increasing temperature. It was shown, that with increasing temperature, the intensity of the absorption bands of the amber chromophore decreases slowly. However, above  $T_g + 50 \text{ K}$  the decomposition of the chromophore is observed. All changes are reversible when temperature is decreased again. The relative intensity of bands assigned to this chromophore change does not change below  $T_g - 50 \text{ K}$ .

### 3. Theoretical Introduction.

#### 3.1. Thermodynamics and kinetics of redox reactions in glasses.

##### 3.1.1. Thermodynamics of redox equilibria.

First, a glass melt with only one polyvalent element A is considered. The polyvalent element A forms a redox equilibrium at high temperatures with the physically dissolved oxygen O<sub>2</sub> of the melt [29, 30, 31]:



The attributed equilibrium constant  $K'_A(T)$  can be defined as follows:

$$K'_A(T) = \frac{a_{A^{n+}} \cdot a_{O^{2-}}^{z/2}}{a_{A^{(n-z)+}} \cdot a_{O_2}^{z/4}} \quad (6)$$

with  $a_i$  = activity of the respective species.

Since the activity of oxide anions O<sup>2-</sup>, usually is much larger than the activities of the polyvalent species, and thus, is not affected by the redox reaction (see Eq. (5)), it is advantageous to define an equilibrium constant  $K_A(T) = K'_A(T)/a_{O^{2-}}^{z/2}$ . The redox ratio  $[A^{n+}]/[A^{(n-z)+}]$ , is not affected by the total concentration of A, if  $[A] < 1$  mol %, the activity coefficients if referenced to ideally diluted solutions can be considered as unity. This enables to replace the activities by the respective concentrations.

$$K_A(T) = \frac{[A^{n+}]}{[A^{(n-z)+}] \cdot a_{O_2}^{z/4}} \quad (7)$$

For another polyvalent element B equilibrated under the same conditions, the same concept is valid, although with the variables characteristic for it. The equilibrium constants  $K_A(T)$  and  $K_B(T)$  depend on temperature. Their temperature dependencies and hence  $\Delta H^0$  and  $\Delta S^0$  are usually different for different redox pairs [6, 8, 30]:

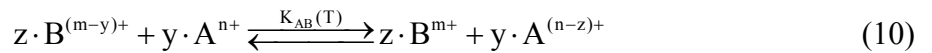
$$-RT \ln K_A(T) = \Delta G_A^0 = \Delta H_A^0 - T \Delta S_A^0 \quad (8)$$

$$-RT \ln K_B(T) = \Delta G_B^0 = \Delta H_B^0 - T \Delta S_B^0 \quad (9)$$



with  $\Delta G^0$  = standard free enthalpy,  $\Delta H^0$  = standard enthalpy and  $\Delta S^0$  = standard entropy of the assigned redox reactions.  $K_A(T)$  and  $K_B(T)$  generally decrease with increasing temperature [8, 31]. This means that with decreasing temperature the equilibrium is shifted to the oxidized species. This is observed, if cooling is carried out slowly enough to enable oxygen diffusion into the melt and to maintain the equilibrium with the surrounding atmosphere. Since oxygen diffusion is a slow process, both under laboratory conditions and during industrial melting of glass, during cooling, oxygen diffusion into the melt is usually negligible [31]. Since in technical glass melts the concentration of physically dissolved oxygen is usually much smaller than that of the polyvalent ion [31], the oxygen activity of the melt strongly decreases during cooling. Furthermore, if only one polyvalent element is present in the melt, its redox ratio  $[A^{n+}]/[A^{(n-z)+}]$  remains constant due to the lack of a reaction partner [31]. In technical glass melts this should usually be the case, while in melts used for the production of optical glasses, the concentration of polyvalent elements is usually very small and this approximation is questionable. Hence, in a technical silicate melt, in a good approximation, the redox ratio will remain constant during quenching the melt from high temperatures.

However, this situation changes, if two polyvalent elements A and B are simultaneously present in the glass-forming system. Redox reactions during cooling may play an important part [6, 30, 8]. At high temperature, a melt containing two polyvalent ions, A and B equilibrated with an atmosphere of a certain oxygen fugacity will exhibit the same redox ratios  $[A^{n+}]/[A^{(n-z)+}]$ ,  $[B^{m+}]/[B^{(m-y)+}]$  as the melts solely containing the polyvalent ion A or B, equilibrated under the same condition [6]. This can be concluded e.g. from voltammetric studies where the standard potentials, which are directly related to the equilibrium constants, do not change if a second type of polyvalent element is present. During subsequent cooling, redox reactions may take place, if they are not kinetically hindered:



The attributed equilibrium constant  $K_{AB}(T)$  and its dependency on temperature can be calculated from Eqs. (8) and (9):

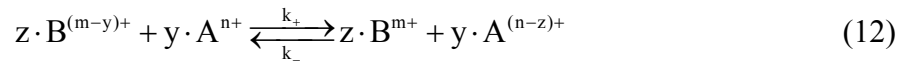
$$\begin{aligned} K_{AB}(T) &= \frac{(K_A(T))^y}{(K_B(T))^z} = \exp\left[\frac{(-y\Delta G_A^0 + z\Delta G_B^0)}{(R \cdot T)}\right] \\ &= \exp\left[\frac{(z \cdot \Delta H_B^0 - y \cdot \Delta H_A^0)}{(R \cdot T)}\right] \cdot \exp\left[\frac{(y \cdot \Delta S_A^0 - z \cdot \Delta S_B^0)}{R}\right] \end{aligned} \quad (11)$$

Therefore, the equilibrium constant  $K_{AB}(T)$  depends on temperature, if  $z \cdot \Delta H_B^0 \neq y \cdot \Delta H_A^0$ . Then also the attributed redox ratios  $[A^{n+}]/[A^{(n-z)+}]$  and  $[B^{m+}]/[B^{(m-y)+}]$  depend on temperature, i.e. will change during cooling the melt. It should be noted that, in contrast to a melt with only one polyvalent ion, diffusion of oxygen in the melt is not necessary to change the respective redox ratios. At high temperatures and slow cooling rates, however, effects caused by the diffusion of oxygen from the gas atmosphere into the melt may play an additional part.

In contrast to the reaction with gaseous oxygen from the surrounding atmosphere, these redox reactions are fast because the diffusion path lengths are in the nanometer range. The equilibrium shifts with temperature, and below a certain temperature (usually around  $T_g$ ) it is frozen in [8, 30, 31].

### 3.1.2. Kinetics of redox reactions in glass melts.

The kinetics of a redox reaction according to Equations (10), (11) can be described by the rate constants  $k_+$  and  $k_-$  of the forward and backwards reactions, respectively.



These redox reactions were considered to be diffusion-controlled and the results were quantitatively explained by using experimentally determined activation energies for the diffusion process.

In Refs. [6, 8] showed already theoretically, the kinetics of the reaction according to Eq. (12) is given by:

$$\frac{dx}{dt} = \left( [A^{n+}]_0 + \frac{x}{z} \right)^y \left( [B^{(m-y)+}]_0 + \frac{x}{y} \right) \cdot k_+ - \left( [A^{(n-z)+}]_0 - \frac{x}{z} \right)^y \left( [B^{m+}]_0 - \frac{x}{y} \right) \cdot k_- \quad (13)$$

where  $k_+$  and  $k_-$  are the rate constants of the forward and backward reactions, respectively.  $[A^{n+}]_0$  is the initial concentration of the respective species (at  $t = 0$ ). The quotient of  $k_+$  and  $k_-$  is equal to the equilibrium constant:

$$\frac{k_+}{k_-} = K_{AB}(T) \quad (14)$$

Both,  $k_+$  and  $k_-$  depend upon temperature according to Arrhenius equation.

$$k_+ = k \cdot \exp\left(-\frac{E_+}{RT}\right) \quad (15)$$

$$k_- = k \cdot \exp\left(\frac{\Delta S_{AB}^0}{R}\right) \cdot \exp\left(-\frac{E_+ + \Delta H_{AB}^0}{RT}\right) \quad (16)$$

Furthermore, when the redox reaction is in an equilibrium and the temperature changes suddenly, the system will react till a new equilibrium is reached. This deviation can be described: after infinitely long times, i.e., after reaching the new equilibrium, the concentrations of reactants and products will have changed by  $\Delta C_0$  from the former equilibrium. At the time  $t$ , the concentrations deviate by  $\Delta C$ :

$$\Delta C = \Delta C_0 \cdot \exp(-t/\tau) \quad (17)$$

where  $\tau$  is the relaxation time which depends on the rate constant, and for reaction orders  $> 1$  on the concentrations of the reacting species. For the reaction according Eq. (12),  $\tau$  can be expressed [6] as follows:

$$\tau = \left\{ k_+ \left( \frac{1}{y} [A^{n+}] + y [B^{(m-y)+}] \right) [A^{n+}]^2 + k_- \left( \frac{1}{y} [A^{(n-z)+}] + y [B^{m+}] \right) [A^{(n-z)+}]^2 \right\}^{-1} \quad (18)$$

### 3.2. Influence of temperature on transition metal complexes.

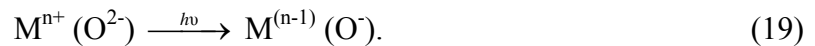
At high temperatures, redox equilibria and redox reactions in glass melts can be investigated by cyclic voltammetry, as already mentioned above. Unfortunately, this method will not work below a certain temperature since the viscosity becomes too high and diffusion processes become too slow. Thus, it is necessary to use optical spectroscopy in the UV-vis-NIR spectral region to estimate the concentrations of one or more of the different species involved in the redox reaction.

The base glass mentioned in this work is a colourless material, which only absorbs in the ultraviolet and in the IR range. The former is a result of the interaction of light with the oxygen ions of the glass. The weaker the oxygen 'ions' are bound, the more easily interaction occurs. For that reason vitreous silica with its strongly bound oxygen 'ions' has a very good UV transparency. The introduction of network modifiers (e.g. sodium and calcium oxide) results in the formation of non-bridging oxygen 'ions' which are weaker bound [32]. They can be excited more easily so that absorption takes place even with light of smaller energy,

and the absorption edge is shifted towards the region of longer wavelengths. For the glass 74SiO<sub>2</sub>·16Na<sub>2</sub>O·10CaO (mol %), absorption edge is located at 210 nm. Since the influence of the cations on the oxygen ‘ions’ becomes weaker with increasing temperature, the absorption edge is shifted towards longer wavelengths with increasing temperature. The above observations apply only for pure glasses without impurities from colouring elements.

The introduction of polyvalent elements, such as Cu<sup>2+/+</sup>, Mn<sup>3+/2+</sup>, Cr<sup>6+/3+</sup>, Fe<sup>3+/2+</sup>, into a base glass causes a stronger absorption in the near UV, the visible, and/or the NIR range and become coloured. Two different colouring mechanisms can occur: i) charge transfer transitions and ii) d-d transitions.

Charge transfer transitions are electronically allowed transitions. Therefore, they are responsible for strong absorption bands with molar absorption coefficients between 10<sup>4</sup> to 10<sup>5</sup> l·mol<sup>-1</sup>·cm<sup>-1</sup>, for example for the band around 365 nm which is attributed to Cr ions in the 6+ state in form of CrO<sub>4</sub><sup>2-</sup>. In the case of the charge-transfer absorption bands, the absorption of a photon leads to an electron transfer between the oxygen ligand and the central cation.



Charge transfer bands obviously overlap the absorption edge of the basic glass and therefore it is rather difficult to decinvolute them from it.

For the inner-shield transitions, like the d-d transitions, the ligand field theory is a good approach. Briefly, the energetic degeneration of the five d states of the metal ion M<sup>n+</sup> is cancelled due to the interaction with the nearest neighbors, which are referred as “ligands”. They are always present as negatively charged ions or oriented dipoles. Depending on the geometrical arrangement of the ligands round the central ion and due to the orientation of the d orbitals, one part of the d states is energetically stabilized whereas the other part is destabilized (with respect to the energy of the d orbitals without the ligand interaction). d-d transitions are not allowed (LAPORTE rule), therefore molar absorption coefficients are small and may vary between 5 and 500 l·mol<sup>-1</sup>·cm<sup>-1</sup> [33]. In addition, tetrahedral complexes of d-d transitions absorb, in comparison with octahedral, usually stronger [33].

Absorption spectra obtained in the form of absorbance vs. wave number usually consists of more than one single absorption band. For the analysis and the interpretation of a composed

spectrum it is necessary to separate it into single bands, based on band parameters from the literature or deduced using a physical theorem. Normally, it is assumed that the bands are described by Gaussian's. Therefore, band parameters are the intensity, the full width of the band at half maximum its intensity, FWHM, and the band position of the electron transitions.

Additionally, it is well known that for a certain (3d) ion these parameters change from glass system to glass system because of structural differences. Therefore, absorption spectra carry important information, which can be also obtained by comparing with some facts from the literature.

It is expected that with increasing temperature the bond between central atom and ligands will be weakened, leading to a reduction of the d-orbital splitting and hence to a decrease of the ligand field strength (Dq). The ligand field splitting reacts very sensitively to bond distance changes within this complex. Assuming a point charge for the charge of the ligand, the ligand field strength can be described by [33]:

$$10Dq = \frac{5q\bar{r}^4}{3R^5} \quad (20)$$

where q = charge of the ligand;  $\bar{r}^4$  = average value of the 4<sup>th</sup> force of distance d-electron vs. nucleus of the central ion; R = distance ligand vs. central ion.

According to Equation (20), an increase in the bond distance leads to a reduction of Dq. The change of the absorption coefficient with the temperature depends on the symmetry of the complex, i.e., a rising temperature can lead to an increase or decrease. The d-d-transitions are not allowed according to the Laporte's rule, since the spin number does not change in the transition. All d-orbital states have the same parity. However, the restriction of Laporte's rule can be taken out by asymmetric vibrations, and the electron transitions can still be observed at room temperature. The influence of the vibrations becomes clear when comparing the absorption spectra of crystal and aqueous  $[\text{Cr}(\text{H}_2\text{O})_6]^{3+}$ . The absorption in the solution is higher than in the crystal, since the thermal movement in the solution is stronger [34].

An increasing temperature leads to increasing vibrations of ligands around the central ion, such that in complexes with an inversion centre ( $O_h$ ), this centre can temporarily disappear. This allows electronic transitions, since they are no longer parity forbidden. Hence, with increasing temperature one expects an increase of the absorption coefficient. This case also applies to the octahedrally coordinated  $\text{Cr}^{3+}$ . The physical law was reported by Liehr and

Ballhausen [35]: the approach assumes a Boltzmann distribution of the vibration states in the basic state, observing them as harmonic oscillators. The absorption coefficient of an absorption band,  $a$ , at temperature,  $T$ , by coupling it with the energy,  $\bar{\nu}_n$ , can then be specified as:

$$\frac{a_{(T)}}{a_{(0)}} = \frac{[1 + e^{-\frac{\bar{\nu}_n}{kT}}]}{[1 - e^{-\frac{\bar{\nu}_n}{kT}}]} \quad (21)$$

where  $a(0)$  = intensity at 0 K;  $k$  = Boltzmann constant;  $\bar{\nu}_n$  = coupling energy;  $T$  = temperature in K.

Rearranging the above equation yields the following relation:

$$\coth^{-1} \left( \frac{a_{(T)}}{a_{(0)}} \right) = \frac{\bar{\nu}_n}{2kT}. \quad (22)$$

The absorption coefficient changes with the temperature depending on the mass of the ligand and the bond strength within the complex. For comparatively light ligands with a strong bond with the central ion one expects only a weak dependence on the temperature. By contrast, for heavy and weakly bonded ligands, a stronger temperature dependence can be expected. Since in the considered glass systems oxygen is the only possible ligand, bond strength is the parameter that determines the temperature dependence of the absorption coefficient in centre symmetric complexes (e.g.,  $\text{Cr}^{3+}$ ).

The charge-transfer transitions of  $\text{Fe}^{3+}$  and  $\text{Cr}^{6+}$  result from tetrahedrally coordinated complexes that do not possess any inversion centre. Here, due to the resulting weakening of the bonding, one expects a rise in the temperature to lead to a reduction of the absorption coefficient. The FWHM of the absorption band is expected to increase with the temperature. The FWHM mirrors the equilibrium distances between central ion and ligand. According to Orgel [36], it is proportional to  $\frac{d(h\nu)}{dDq}$ . The larger the band halfwidth, the larger is the difference in the gradients of the two states in the Orgel diagram. The band halfwidth is narrow if the energy levels between ground state and excited state run parallel. The minima of the potential curves of ground and excited state are at identical equilibrium distances. If, instead, the potential curve of the excited state is shifted to a larger equilibrium distance, the absorption bands get wider, since transitions to a larger number of vibration states can take

place [33]. Figure 1 shows potential curves of ground state and excited state that lead to a widening of the absorption bands.

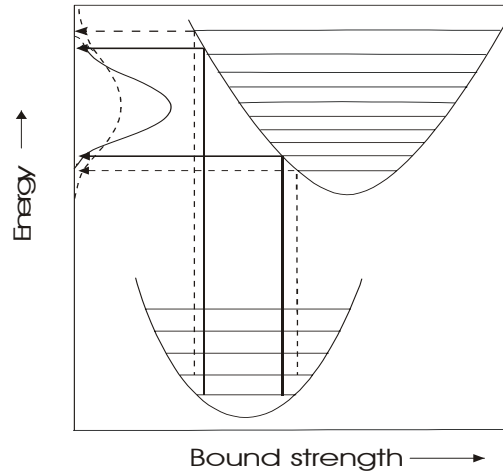


**Figure 1.** Widening of the absorption bands due to the excitement of higher vibration levels.

A higher temperature excites higher vibration levels, leading to an increased overlapping of excited vibration levels in the ground state with those in the excited state. In glass, the widening of the absorption bands with rising temperatures is also due to increasing variances in the structure. For charge-transfer absorption bands in crystals the band halfwidth follows the rule [33]:

$$\frac{FWHM_{(T)}}{FWHM_{(0)}} = \sqrt{\coth\left(\frac{\bar{\nu}_{\alpha 1g}}{2kT}\right)} \quad (23)$$

$\bar{\nu}_{\alpha 1g}$  = vibration energy of the symmetric normal vibration of the complex;  $FWHM_{(0)}$  = band width at 0 K.

Whether with increasing temperature the position of the absorption band shifts toward longer or shorter wavelength also depends on the bonding distance between ligand and central ion. If the change in the ligand field splitting with temperature is known, the size of the expected band shift can be derived from the Orgel-diagram [37]. Figure 2 shows that the shift towards larger wavelength (red shift) of the absorption band can be expected if the gradient of the excited energy levels is positive and  $Dq$  decreases with the temperature. If the gradient of the excited energy level is negative, the shift towards shorter wavelength (blue shift) of the absorption band takes place.

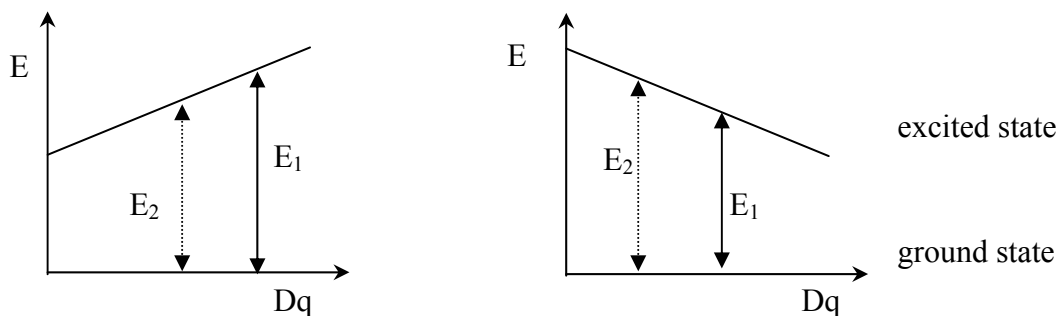


**Figure 2.** Influence of the temperature on the position of the absorption maximum (see Dunn [37]).

The mechanisms for band broadening give the same qualitative information as to the shape of the absorption band. Bands in the spectra of transition metal ions are often quite symmetrical in shape, and can be fitted to a Gaussian relation. However, the octahedral arrangements of the ligands around the transition metal ions are often distorted rather than perfect. An important phenomenon by which absorption bands are broadened and depart from symmetry is the Jahn-Teller effect. A complex, which is assumed to be octahedral, is considered to be distorted either by lengthening or shortening of the bond length along the z axis [38].

Ligand field theory can be used to predict and interpret the position of absorption bands in the spectra of transition metal ions in glasses or other solutions. The theory can also predict whether a particular band will be weak or strong but it is rather difficult to use it for obtaining an accurate value of the molar extinction coefficient [39, 40]. In the case that a transition metal can appear in only one oxidation state just its total concentration is needed to determine the molar absorptivity. However, most transition metals are polyvalent, i.e. may exist in glass in more than one oxidation state. If the element can exist in more than one redox state but can easily be either almost completely reduced or oxidized in glass only that state needs to be considered. Likewise by ferrous/ferric equilibrium, an important difficulty arises, however, if the equilibrium cannot be driven so far in either direction [41]. Then, there is a need to make the redox determination by physical methods and thus exclude the wet-analysis of the glass, by which no one can be sure whether there was no change in redox equilibrium during it. In the references [42, 40], two ways are discussed how to obtain appropriate values of extinction coefficient for the particular case of the copper containing glasses using absorption spectroscopy. The first way shows that it is possible to calculate the cupric



extinction coefficients from measurements made on glasses equilibrated at three or more different melting temperatures when only total copper concentration is known but the oxygen partial pressure,  $p(\text{O}_2)$ , stays constant. The second case is based on the constant melting temperature but different values of  $p(\text{O}_2)$ . The partial pressure should not be below about  $10^{-9}$  bar because reduction towards metallic copper may appear in typical silicate glasses. Such partial pressures may easily be obtained in a sealed furnace but at the expense of homogeneity.

## 4. Experimental part.

### 4.1. Preparation and characterization of the samples

#### 4.1.1. Glass preparation

For the investigations, glasses were prepared with the base composition 16Na<sub>2</sub>O-10CaO-74SiO<sub>2</sub> (mol %). This base glass was mostly chosen because of its common use as model glass for flat and other industrial glasses in basic research. The batches were mixed from reagent grade raw materials: SiO<sub>2</sub>, Na<sub>2</sub>CO<sub>3</sub> and CaCO<sub>3</sub>. The polyvalent elements were introduced by reagent grade raw materials in particular concentrations for copper containing glasses in Table (1) and manganese and chromium containing glasses in Table (2). The batch was calculated for either 300 or 400g of glass. Glasses were melted in a middle frequency induction furnace using a 250 ml platinum crucible. The loading of the batch into the crucible was done at temperatures between 1150 and 1250 °C. These temperatures should not be higher because then it causes a substantial volatilization of reagents. After the entire batch was pre-melted and sintered in the crucible, the temperature was increased stepwise to the melting temperature of around 1480 – 1500 °C and kept for 2 – 2½ h. During this period of time, the glass was homogenised by stirring. The lasting period is very important because:

- i. the melting temperature (also marked as the equilibrium temperature) is later taken as temperature for the thermodynamic calculations;
- ii. bubbles must be removed from the glass which could disturb the optical absorption measurements;
- iii. the glass is homogenized in the whole crucible.

After this period, the glass was cast at the same temperature into a preheated (T= 530 °C) graphite mould in a quick way in order to avoid temperature-caused inhomogeneities, and cooled in a preheated (T= 550 °C) furnace to ambient temperature using a cooling rate 30 K · h<sup>-1</sup>.

Some glasses were prepared from batches containing 1 g sugar per 100 g glass. Redox equilibrium in such glasses should be completely shifted towards the reduced form, i.e. strong reducing conditions should be expected. In that case, the melting process cannot be realized in the Pt crucible in the induction furnace but in a superkanthal furnace using a silica crucible. The temperature and time program remained the same, although, the melting conditions are rather different. The main difference and great disadvantage of the superkanthal furnace is that there a continued homogenisation during the melting process is not possible.

**Table 1.** Composition of the sample studied (mol%).

Sample	CuO	SnO	Sb <sub>2</sub> O <sub>3</sub>	As <sub>2</sub> O <sub>3</sub>
A	0.3	-	-	-
B	0.1	0.05	-	-
C	0.3	0.15	-	-
D	0.6	0.3	-	-
E	0.3	-	0.15	-
F	0.6	-	0.15	-
G	0.6	-	0.3	-
H	0.3	-	-	0.15
I	0.6	-	-	0.15

**Table 2.** Table 1. Chemical compositions of the samples and raw materials used.

Sample	[Cr <sub>2</sub> O <sub>3</sub> ] in mol %	[MnO] in mol %	Raw materials
A	0	0.68	MnCO <sub>3</sub>
B	0	0.68	MnO <sub>2</sub>
C	0.11	0	Cr <sub>2</sub> O <sub>3</sub>
D	0.23	0	Cr <sub>2</sub> O <sub>3</sub>
E	0.22	0	Na <sub>2</sub> CrO <sub>4</sub>
F	0.11	0.67	MnCO <sub>3</sub> , Cr <sub>2</sub> O <sub>3</sub>
G	0.11	0.67	MnO <sub>2</sub> , Cr <sub>2</sub> O <sub>3</sub>
H	0.23	0.67	MnCO <sub>3</sub> , Cr <sub>2</sub> O <sub>3</sub>
I	0.22	0.67	MnCO <sub>3</sub> , Na <sub>2</sub> CrO <sub>4</sub>
K	0.44	0.67	MnCO <sub>3</sub> , Na <sub>2</sub> CrO <sub>4</sub>
L	0.11	1.33	MnCO <sub>3</sub> , Cr <sub>2</sub> O <sub>3</sub>
X	0	0.68	MnCO <sub>3</sub> , sugar

**4.1.2. General characterisation of the base glass.**

Some important characteristics of the basic glass were measured and summarized in Table (3). The glass transformation point was specified by differential thermal analysis DTA (Shimadzu DTA-50), and the linear expansion coefficient ( $\alpha$ ) was measured in a temperature range from 100 to 300 °C by dilatometer (402 ES, Netzsch). Especially important for high

temperature spectroscopy investigations is the softening point of the glass, at which a glass sample begins to deform. Here, the maximum of the expansion curve was taken as the softening point. The density of the glass was measured by a Helium pycnometer (AccuPyc 1330, Micromeritics).

**Table 3.** Characteristics of basic glass (mol %): 74SiO<sub>2</sub>·16Na<sub>2</sub>O·10CaO.

T <sub>g</sub> [°C]	545 ± 5	softening point [°C]	603 ± 5
α [10 <sup>-7</sup> K <sup>-1</sup> ]	94 ± 5	density [g·cm <sup>-3</sup> ]	2.492 ± 0.0003

#### 4.1.3. Preparation of samples for spectroscopic investigations

After cooling to room temperature, some samples were taken from the glass according to the method used. Because each glass had a certain number of visible bubbles, at first an area without bubbles was chosen to drill some cylinders (φ= 6mm) for high-temperature absorption spectroscopy (HTAS). The cylinders were cut in order to get samples from the middle volume of the glass block. If one compares the optical spectra of a sample obtained from the centre and a sample from the surface part of the glass block, a slight difference can be observed. For samples prepared from the same area, this difference is not expected. This is due to the fact that during cooling in the mould, the redox reaction can still run in volume of the glass block where the temperature is higher than on the surface of the block where the redox reaction is probably frozen-in earlier.

Appropriate thickness of the samples was determined from UV-vis-NIR spectra recorded by a Shimadzu UV-3101PC spectrometer at room temperature. The intensity should lay in the range from 0.2 to 1.0 absorbance units (optimum 0.5). For glasses doped solely with chromium, or simultaneously with chromium and manganese, measurements have to be done in the visible as well as in UV region, because of the absorption of the chromium(VI) in UV. The used sample thicknesses were different (0.2 and 1.0 mm for UV and vis range, respectively). However, for high-temperature absorption spectroscopy, a thickness of more than 2.0 mm is not recommended because of the limited height of the heating-stage chamber-crucible. The weight of a 2 mm sample is ~ 0.142 g. The surface was ground and polished to optical quality.

Samples for EPR were prepared as a powder with maximum grain sizes of < 0.4 mm.

## 4.2. Optical absorption spectroscopy

Optical spectra of glasses doped with transition metal ions provide information on the structural state of the ions in glass and also reflect the structure of their environments [A-23]. Furthermore, absorption spectroscopy can also be used for quantitative (or, at least, semi-quantitative) analysis of redox species in glass.

Three spectral areas have to be distinguished corresponding to different absorption mechanisms of electromagnetic radiation. At short wavelengths (UV region), the absorption is due to electron transitions between the polyvalent ion and the surrounded ligands also known as the charge transfer phenomena. The molar absorptivity  $\epsilon$  is, in general,  $> 10^3 \text{ l}\cdot\text{mol}^{-1}\cdot\text{cm}^{-1}$ . In the visible and near infrared range, absorption is much smaller and essentially due to intra-atomic transitions ( $d \rightarrow d$  transitions), which are forbidden by selection rules. The value of  $\epsilon$  lies between  $10^{-2}$  and  $300 \text{ l}\cdot\text{mol}^{-1}\cdot\text{cm}^{-1}$ . Molecular bond transition bands are to be found at higher wavelengths. Above  $4.15 \mu\text{m}$  glasses are almost opaque [24].

Absorption spectroscopy allows to estimate the concentration of the absorbing species from the absorption bands according to the Beer-Lambert law\*:

$$\text{Absorbance} = \log \frac{I_0}{I} = \epsilon \cdot c \cdot d . \quad (24)$$

If radiation of the intensity  $I_0$  (incident beam intensity) passes through a sample of thickness  $d$ , then, the resulting intensity  $I$  (transmitted beam intensity) is decreased due to absorption processes. The absorbance,  $A$ , (in arbitrary units [a.u.]) is linear in the concentration  $c$  [ $\text{mol}\cdot\text{l}^{-1}$ ] and the thickness  $d$  [cm], with the molar absorptivity  $\epsilon$  [ $\text{l}\cdot\text{mol}^{-1}\cdot\text{cm}^{-1}$ ] as the proportional factor. However, this linearity is only valid in a certain concentration range of polyvalent elements, i.e., for less than 5000 ppm.

The term *molar absorptivity* describes the value of absorbance at the maximum of the absorption band (peak position). As it was already shown in the Theoretical Introduction, it is expected that the peak position will be shifted towards either shorter or longer wavelengths with increasing temperature.

From a practical point of view, the measured absorbance is divided by thickness of the sample (in cm) which results in the absorptivity  $\alpha$ :

$$\frac{\text{Absorbance}}{d} = \varepsilon * c = \alpha . \quad (25)$$

Using equation (25), the resulting spectra (absorbance vs. wave number) then allow a direct comparison of spectra of glasses with varying thickness and concentration and with different polyvalent elements.

Absorption spectra of glasses were measured by the UV-vis-NIR spectrometer Shimadzu UVPC 3101 (Kyoto, Japan). It is a double-beam spectrometer which allows measurements only at room temperature. The measured spectrum includes the range from  $\sim 52\,632\text{ cm}^{-1}$  (190 nm, UV) up to  $\sim 3\,125\text{ cm}^{-1}$  (3200 nm, NIR). Spectra obtain from Shimadzu UVPC 3101 spectrometer, were considered as a reference for high-temperature absorption spectroscopy HTAS.

All spectra obtained from glasses were evaluated in the following manner. The spectra were presented as absorptivity vs. wave number. Wavenumber  $\tilde{\nu}$  is defined in Eq. (26) [43] and given in  $\text{cm}^{-1}$ :

$$\tilde{\nu} = \frac{1}{\lambda} \quad (26)$$

These spectra were then deconvoluted into separate Gaussian-shaped peaks using the SYSTAT software Inc. Peakfit 4.02 package. As a starting point, parameters (peak position or center and FWHM) obtained from the literature were used.

### 4.3. Equipment for the high temperature absorption spectroscopy.

The spectra that are analysed here can be divided into two ranges: i. the ultraviolet (UV) and ii. the visible and near-infrared (vis-NIR) region. To cover such a large absorption spectrum is not in general a technical problem. However, difficulties arise if a sample is measured at temperatures significantly higher than room temperature. According to Planck's and Wien's law, any body increases its emitted intensity is increased and the emission maximum is shifted towards smaller wavelengths (higher wave numbers) with increasing temperature. Thus, the investigated sample as well as the heating-chamber crucible will emit radiation in the (N)IR and visible region during high-temperature absorption spectroscopic measurements. Therefore, thermal emission has to be taken into account. Two different arrangements of

---

\* nomenclature for absorption spectroscopy as recommended by J. Wong & C.A. Angell [46].

high-temperature equipment were used for UV and for vis-NIR spectral region. Schematic drawings both of them are showed in Figure [f-27].

For absorption measurements in the UV region, a diode-array spectrometer (INSTASpecII, L.O.T.) was used. In the region with wavelengths  $< 500$  nm and for temperatures below  $800$  °C, the intensity of thermal emission can be neglected, thus, an optical chopper is not necessary. Light source is a xenon lamp (XBO 150 W). The light was conducted by a special optical lens system and by quartz light guide ( $\sim 50$  cm) into the chamber of the heating stage (LINKAM TS1500, Waterfeld, Great Britain). The heating stage was mounted on a microscope-base. In the chamber of the heating stage, a high-temperature crucible with the glass sample is placed. To protect high temperature chamber-crucible from sticking together with the glass sample at higher temperature, a quartz disc ( $\phi= 7$ mm,  $d= 0.2 - 0.4$ mm,  $\alpha= 5 \cdot 10^{-7} \text{ K}^{-1}$ ) was used. A second quartz disc was put onto the sample to avoid its bending at higher temperature ( $> 650$  °C). The temperature expansion coefficients of the analysed glass and quartz glass differ widely (factor 20). This was the reason why the sample was usually destroyed during cooling. The light transmitted through the sample was guided by a quartz light guide ( $\sim 50$  cm) into a grating monochromator (MULTISPEC, L.O.T.). Normally, a grating with a line density  $400$  l/mm and a blaze wavelength  $500$  nm was used. The measured spectral region was  $250$  to  $750$  nm. The dispersed light was then analysed by a diode-array Si detector (1024 cells). The main advantage of the diode-array spectrometer is its short measuring time ( $< 1$ s). This is very useful for observing redox processes during heating and cooling, e.g., in glasses doped with manganese and chromium.

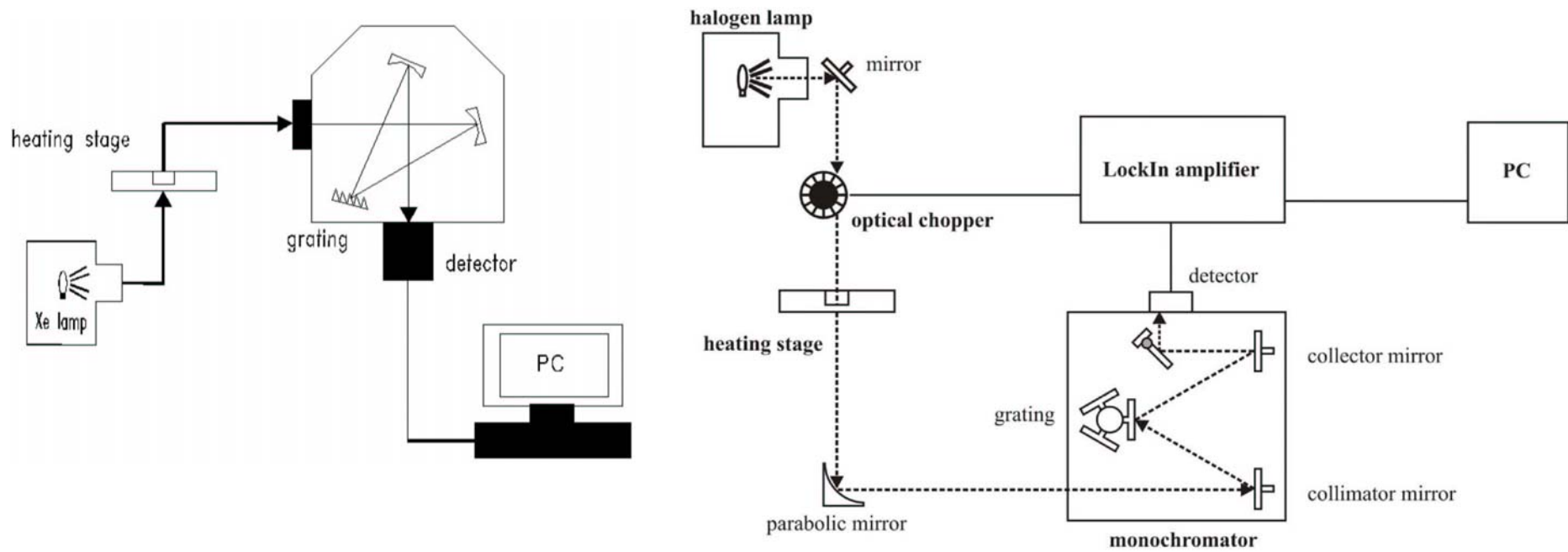


**Figure 3.** Fig. –27. Schematics of the HTAS experimental arrangement used for: UV range (left), vis-NIR range (right).



High temperature *vis-NIR spectra* were recorded by a modular spectrometer. A halogen lamp (100 W) was used as a light source. The collimated light beam was reflected by a planar mirror, passed through a chopper (chopper frequency:  $113\text{ s}^{-1}$ ) and, subsequently, the sample. The sample was placed inside the heating chamber of a microscope heating stage (TS 1500, LINCAM, Waterfield, Great Britain). Here, a quartz disc was placed between the sample and the heating-chamber crucible. The transmitted light was reflected by  $90^\circ$  using an off-axis parabolic mirror (focal distance: 19.1 cm) and focused to the entrance slit of a grating monochromator (TRIAX 320, Jobin-Yvon, Edison, NY, USA). The signals were collected by a detector (see later) evaluated by a lock-in amplifier (SR830, Stanford Research Systems, Stanford, CA, USA) adjusted to the chopper frequency. For high temperature absorption measurements, it is necessary to arrange the chopper in front of the heating chamber to eliminate the thermal radiation of the sample and the heating chamber.

Collection of a spectrum takes about 2-3 min. During this period the temperature is hold. The time depends on the breadth of the spectral range and the integration time. It is essential to shorten this time as much as possible, particularly at temperatures above  $T_g$ , when redox processes and the corresponding spectral changes take place, and the shape of the sample can be distorted. Hence, here, the quality must meet the quantity.

The heating and cooling rates in most of the experiments presented in this work were  $20\text{ K}\cdot\text{min}^{-1}$ . The upper temperature limit was  $800\text{ }^\circ\text{C}$ , because the shape of the samples is distorted at higher temperature due to the surface tension. Then the adjusted imaging conditions for spectrometers are not longer valid.

#### **4.4. Treatment of HT absorption spectra of different glasses.**

High-temperature UV-vis-NIR absorption spectra were measured using two different spectrometers. Spectra recorded at room temperature with the high temperature equipment were compared with spectra recorded with the commercial SHIMADZU UVPC 3101 spectrometer to guarantee their reliability. It was found that the spectra from the HTAS spectrometers sometimes have slightly smaller absorbance.

##### **4.4.1. Copper doped glasses.**

All HT spectra of glasses doped solely with copper, or with copper and tin, antimony or arsenic, respectively, were treated in the following manner:

After measuring spectra at room temperature, it was decided to use samples of 2 mm thickness for HT analysis. The analysed absorption range was from 380 nm to 1100 nm using the modular spectrometer with the Si-detector. The temperature range was from room temperature up to 800 °C with a heating rate of 20 K·min<sup>-1</sup>. The obtained data were visualized using SigmaPlot software (SYSTAT software Inc.). The spectra were then deconvoluted using the Peakfit 4.02 package (SYSTAT software Inc.). Starting with the spectrum obtained at room temperature, a basic line was subtracted taking into account the reflection loss at the surfaces of the sample. As already mentioned above, the Cu<sup>2+</sup> peak was fitted with just one Gaussian peak. It turned out that this is an adequate approximation, since the measured absorption range ended at 1100 nm which is already at the decreasing part of the peak. Since the measured part did not include the whole absorption band of the Cu<sup>2+</sup>, the results would be meaningless if fitting was done with three peaks. In Fig. (4), the whole spectrum is showed, although, the spectral range from 500 up to 1100 nm is used. The fit parameters (intensity and position the maximum of the peak) were plotted vs. temperature. The FWHM dependence on temperature has not been shown because those values are not accurate enough since the peak is not completed.

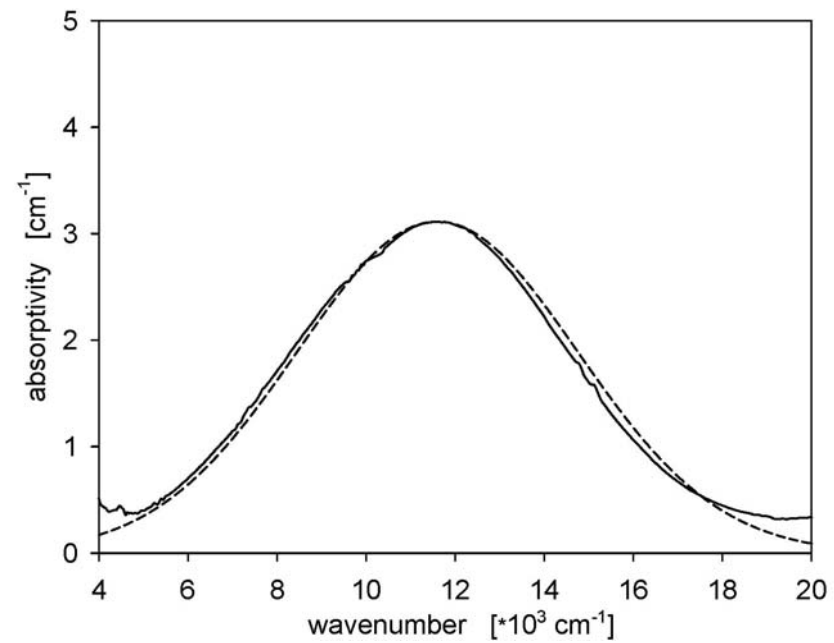
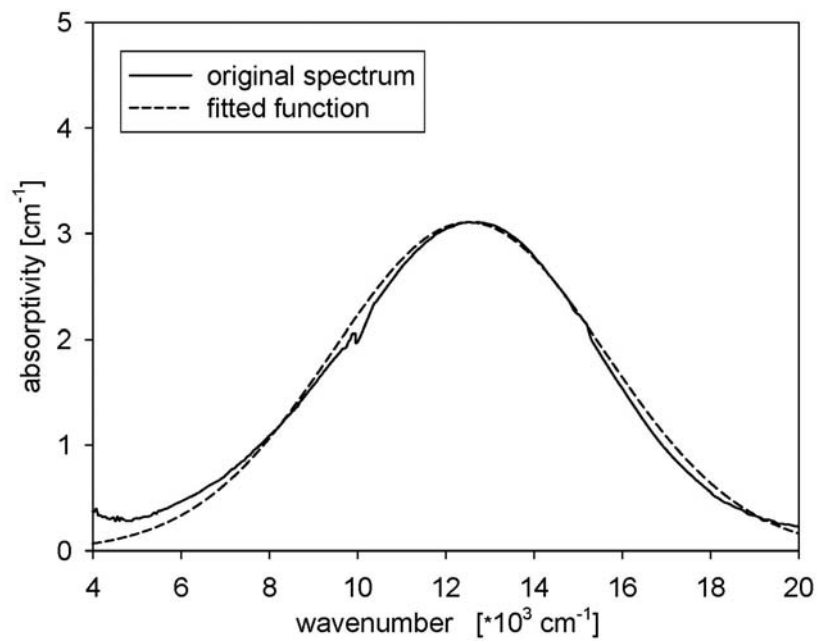


**Figure 4.** Band analysis of the absorption spectrum of the glass doped with (mol %) 0.6 CuO and 0.3 SnO: 25 °C (left) and 800 °C (right).

#### 4.4.2. Manganese doped glasses

$Mn^{3+}$ : As for copper containing glasses, the thickness of the samples was 2 mm. The analysed absorption range was from 380 up to 1100 nm using the modular spectrometer with the single Si-detector, at temperature up to 800 °C using a heating rate of 20 K·min<sup>-1</sup>. The spectra were deconvoluted in the following manner (see Fig. (5)):

Starting with the spectrum obtained at room temperature, again the base line was subtracted. The spectra were fitted with two Gaussian peaks using data from literature: the main peak (~ 20,300 cm<sup>-1</sup>) and the ‘shoulder’ peak (~ 15,100 cm<sup>-1</sup>). The band parameters (intensity, position of the maximum of the peak and FWHM) were plotted vs. temperature.

$Mn^{2+}$ : Peaks caused by Mn<sup>2+</sup> were not considered during deconvolution of the absorption spectra because of its extremely small absorptivity of less than 0.015 cm<sup>-1</sup>. They were only shown and HT spectra taken to demonstrate their presence\* .

---

\* glass doped with manganese and sugar prepared for this purpose.

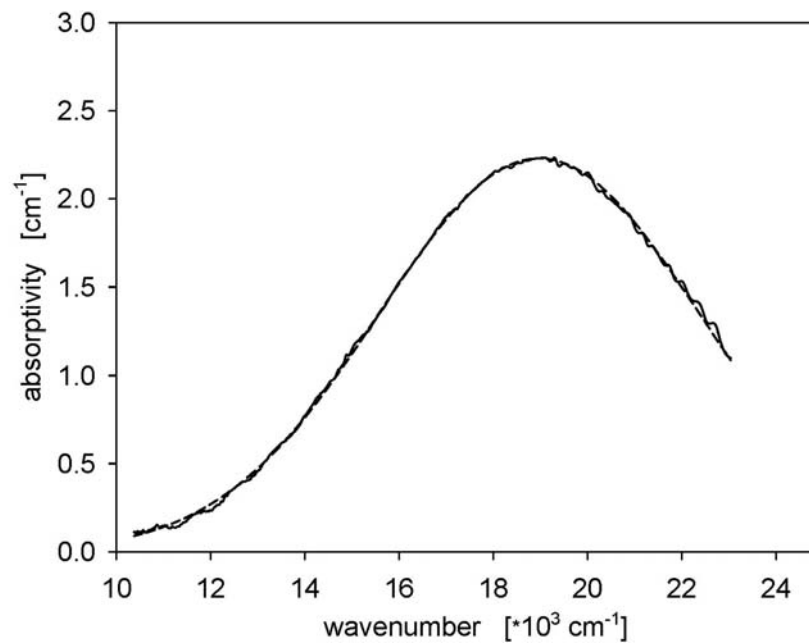
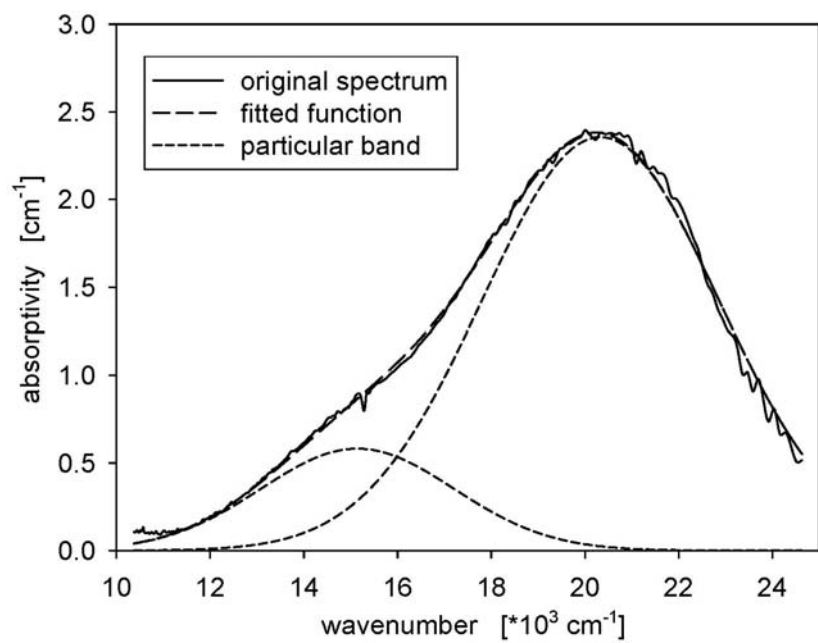


**Figure 5.** Band analysis of the absorption spectrum of the glass doped with 0.68 mol% MnO: 25 °C (left) and 800 °C (right).

### 4.4.3. Chromium doped glasses

For chromium doped glasses, recording of HT spectra is more complex than described above. The absorption range of interest includes the UV as well as the visible part of the spectrum. Hence, two different arrangements were used (see Figs. (6) and (7)):

*UV range:* The thickness of the samples was 0.2 mm. The analysed absorption range was from 250 up to 750 nm. The diode-array spectrometer was used in a temperature range of up to 800 °C with a heating rate of 20 K·min<sup>-1</sup>. These spectra were treated using the PeakFit program in the following way. All spectra were plotted as absorption versus wavenumber. Spectra were not smoothed (this procedure can significantly increase the deviation from original spectrum). Starting with the spectrum collected at room temperature, the basic line was subtracted.

Using band parameters obtained from the literature, the spectrum was fitted with two main Gaussian peaks: at ~ 27,500 cm<sup>-1</sup> (attributed to Cr<sup>6+</sup>) and ~ 22,600 cm<sup>-1</sup> (Cr<sup>3+</sup>). The other two peaks were used as assistant ones. The band parameters (intensity, peak position and FWHM) were plotted vs. temperature.

*vis range:* The thickness of the samples was 1.0 mm, the absorption range from 380 up to 1100 nm. The a modular spectrometer was used in a temperature range up to 800 °C with heating rate of 20 K·min<sup>-1</sup>. All spectra were plotted using SigmaPlot. Starting with the spectrum taken at room temperature, the basic line was subtracted.

Using band parameters obtained from the literature (see above), the spectrum was fitted with one main gaussian peak at ~ 15,200 cm<sup>-1</sup> (attributed to Cr<sup>3+</sup>), which covers all three Cr<sup>3+</sup> peaks. This was chosen to simplify the whole fitting procedure. The assistant peak represented the UV region. The band parameters were plotted vs. temperature.

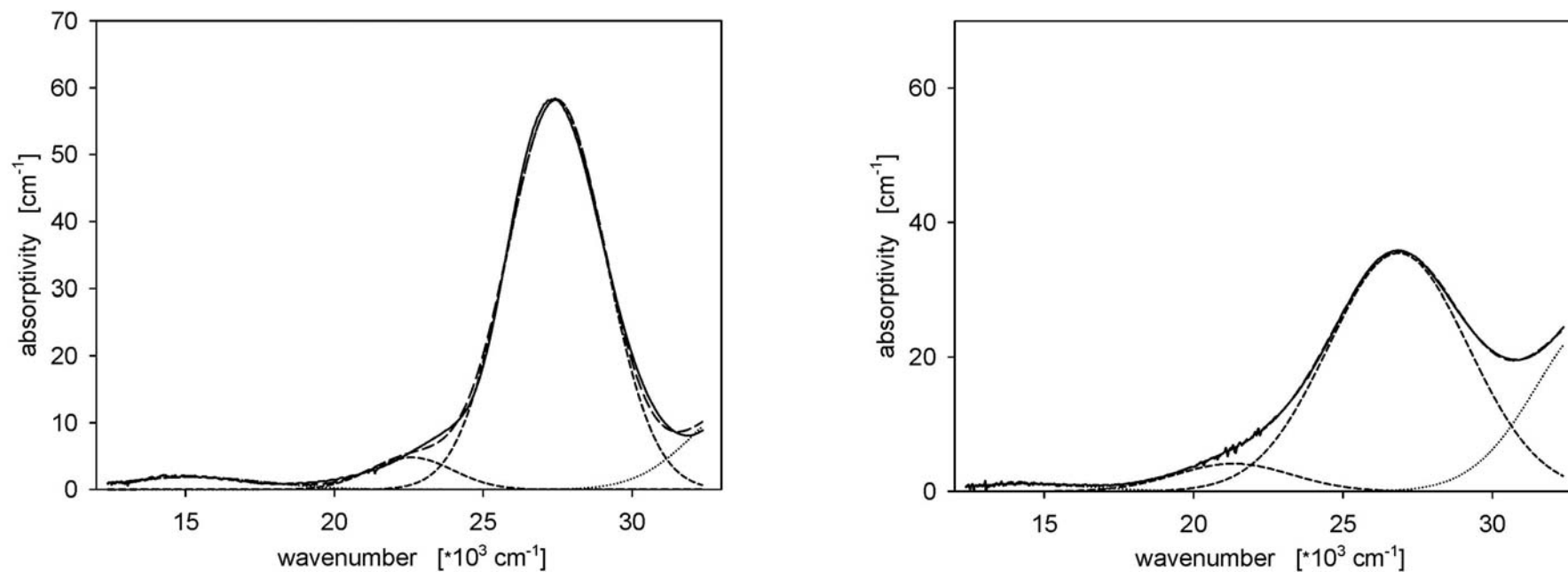


**Figure 6.** Band analysis of the absorption spectrum of the glass doped with 0.11 mol% Cr<sub>2</sub>O<sub>3</sub>: UV region, 25 °C (left) and 800 °C (right).

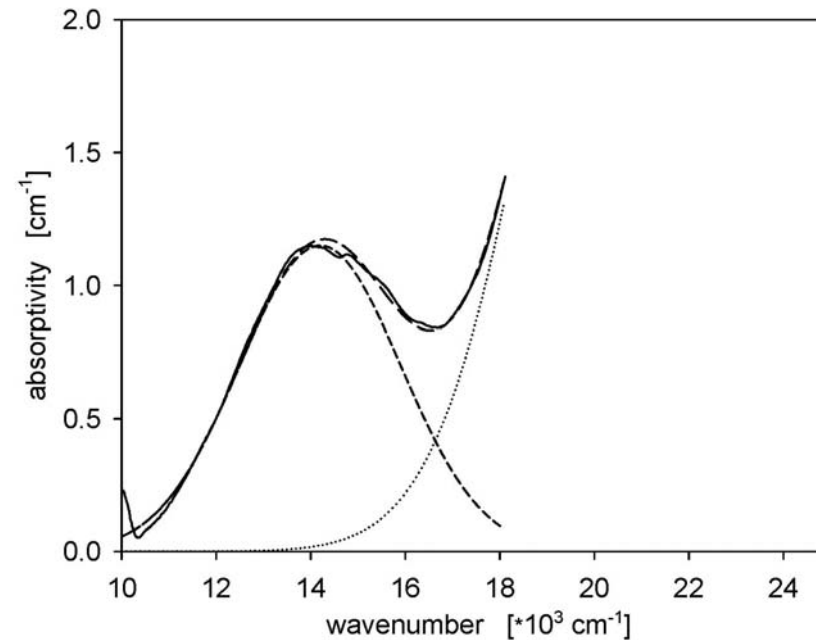
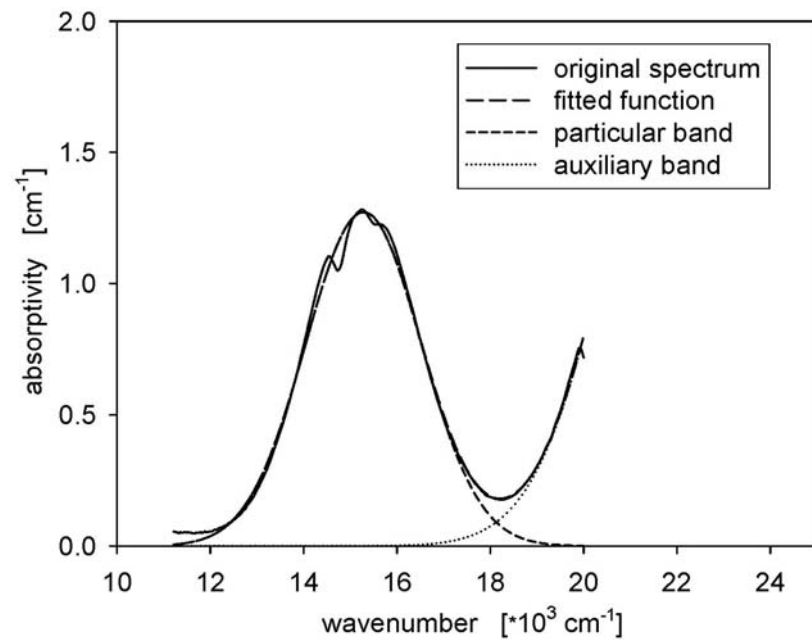


**Figure 7.** Band analysis of the absorption spectrum of the glass doped with 0.11 mol% Cr<sub>2</sub>O<sub>3</sub>: vis region, 25 °C (left) and 800 °C (right).



#### 4.4.4. Manganese and Chromium doped glasses.

Although these glasses have been doped with manganese and chromium, the treatment of HT spectra was done in a similar way as for chromium doped glasses. The whole process is showed in Figs. (8) and (9).

*UV range:* The thickness of samples was 0.2 mm; the investigated absorption range was from 250 to 750 nm, the diode-array spectrometer was used in temperature range up to 800 or 700 °C with heating rates of 1, 5 and 20 K·min<sup>-1</sup>. Using PeakFit software, the spectra were similarly treated as described for the chromium-doped glasses. However, one has to concern two polyvalent elements: chromium (Cr<sup>3+/6+</sup>) and manganese (Mn<sup>3+/2+</sup>). Thus, a spectrum was fitted with three main Gaussian peaks: at ~ 27,500 cm<sup>-1</sup> (Cr<sup>6+</sup>), ~ 22,600 cm<sup>-1</sup> (Cr<sup>3+</sup>) and ~ 20,300 cm<sup>-1</sup> (Mn<sup>3+</sup>). However in this case, the Cr<sup>3+</sup> peak and the non-symmetrical Mn<sup>2+</sup> peak (~ 23,700 cm<sup>-1</sup>) are superimposed. The two assistant peaks represent the UV absorption edge and the Mn<sup>3+</sup> shoulder peak (~ 15,100 cm<sup>-1</sup>) and the Cr<sup>3+</sup> peak (15,200 cm<sup>-1</sup>). The band parameters were plotted vs. temperature. In this manner, spectra at higher temperature were also deconvoluted.

*vis range:* The thickness of samples was 1.0 mm, the absorption range from 380 to 1100 nm. The modular spectrometer at temperatures up to 800 °C with only one heating rate 20 K·min<sup>-1</sup> was used. Using PeakFit software, spectra were similarly treated as chromium doped glasses regarding the Mn<sup>3+</sup> peaks. Hence, a spectrum was fitted with three main Gaussian peaks: at ~ 22,600 cm<sup>-1</sup> (Cr<sup>3+/Mn<sup>2+</sup></sup>), ~ 20,300 cm<sup>-1</sup> (Mn<sup>3+</sup>), and ~ 15,200 cm<sup>-1</sup> (Cr<sup>3+</sup>) plus ~ 15,100 cm<sup>-1</sup> (Mn<sup>3+</sup>). The assistant peaks represent the UV absorption edge. The band parameters were plotted vs. temperature. In this manner also spectra obtained at higher temperature were deconvoluted.

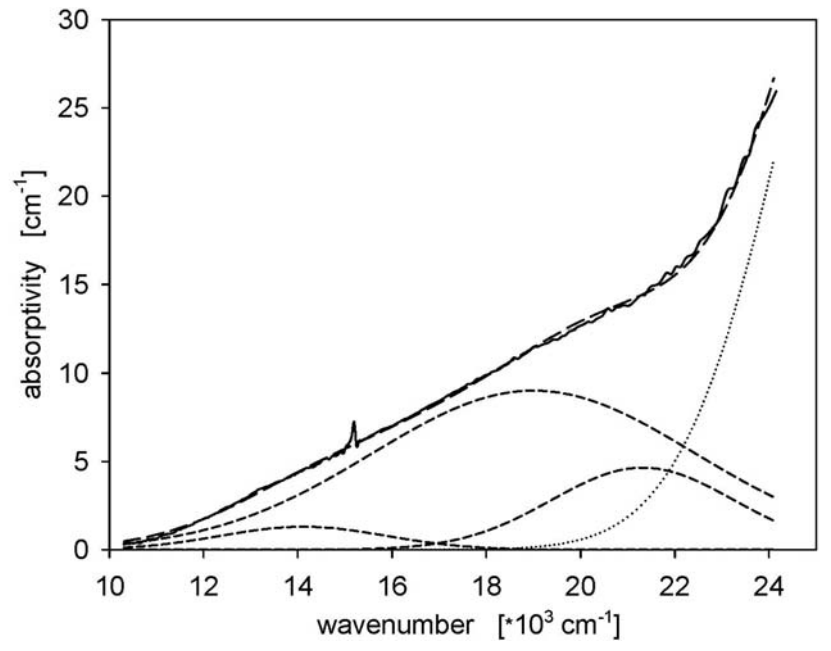
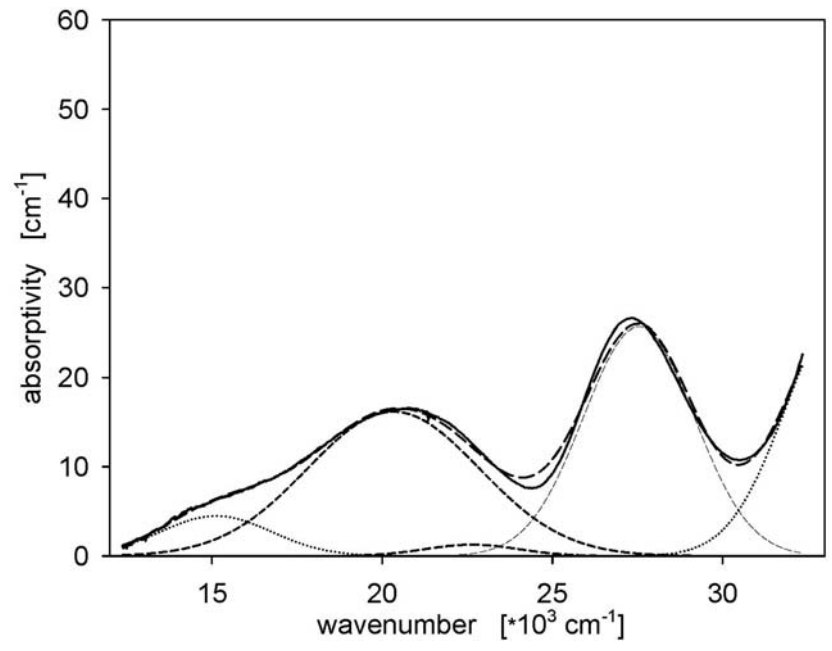


**Figure 8.** Band analysis of the absorption spectrum of the glass doped with (mol %) 0.67 MnO and 0.22 Cr<sub>2</sub>O<sub>3</sub>: UV region, 25 °C (left) and 800 °C (right).

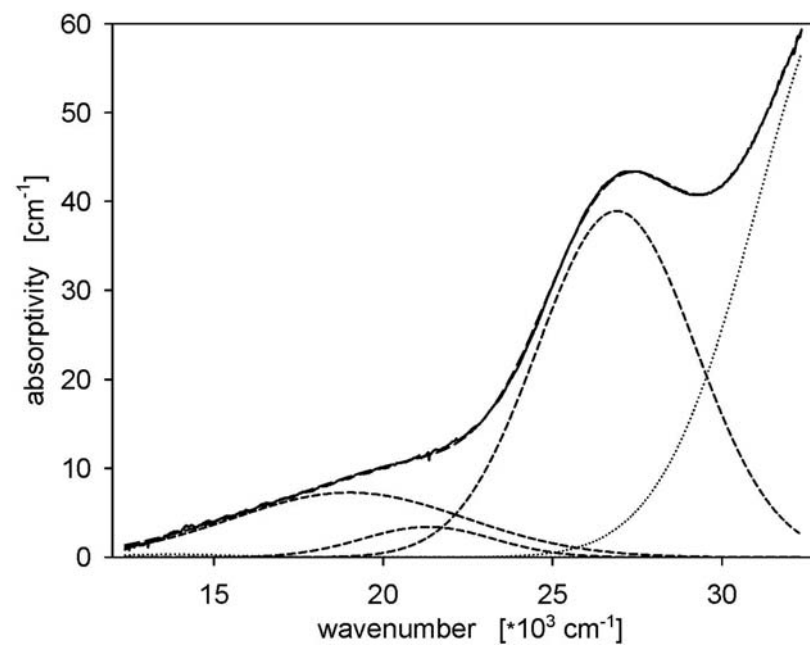
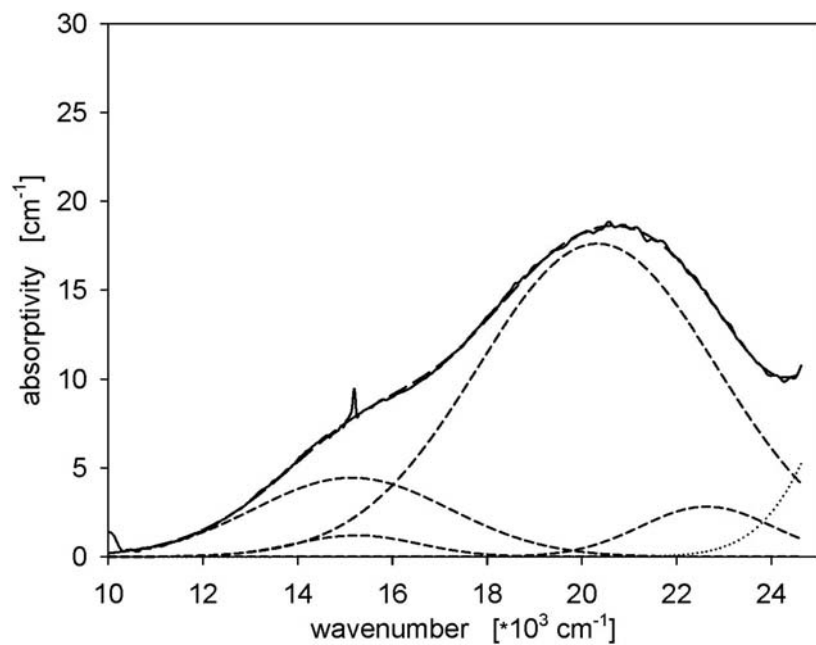


**Figure 9.** Band analysis of the absorption spectrum of the glass doped with (mol %) 0.67 MnO and 0.22 Cr<sub>2</sub>O<sub>3</sub>: vis region, 25 °C (left) and 800 °C (right).

#### 4.4.5. Evaluation of errors of HT measurement

Since the HT equipment is an absorption spectroscopy system connected with a high temperature heating stage, two main fields of errors can arise concerning optical parts (predominantly the detector) and measuring the real temperature of the sample.

In the former case, the error of measurement is not constant within the spectral range, though, an error minimum exists at a certain absorption  $A(\lambda_1) = \log I_0(\lambda_1) - \log I(\lambda_1)$  and at a certain wavelength  $\lambda_1$ . At high absorbance the transmitted radiation intensity is rather low and thus also the relative error [43]. Therefore, by choosing the proper thickness of a sample, the error can be lowered. It is expected that the error should reach a minimum in the middle of the measured absorption region. If one compares (by intensity and peak position) a spectrum of a sample taken by the SHIMADZU spectrometer (as a reference spectrum) with one taken by the HT apparatus at room temperature, one can estimate the intensity error.

#### 4.5. Electron spin resonance

Electron spin resonance (EPR or ESR) can detect unpaired electrons in paramagnetic species (ions, molecules, radicals). In the external magnetic field  $H$ , the splitting will take place in two spin states, so-called Zeeman levels. The energy difference between the two splitted states is:

$$\Delta E = g\beta H. \quad (27)$$

If a radio frequency field with a frequency  $\nu$  is now applied in the direction perpendicular to the external magnetic field  $H$ , the system will induce resonance transition between the two Zeeman energy levels at a specific magnetic field  $H_r$ . This happens when it absorbed a photon with an energy  $h\nu$  from the radio frequency field, and it meets the relation

$$h\nu = g\beta H_r, \quad (28)$$

where  $\nu$  is the frequency of  $H_r$  in Tesla [1T],  $\beta$  is the Bohr magneton. The variable magnetic field flux at constant frequency was measured. The resulting spectrum is obviously interpreted as a 1<sup>st</sup> derivation of the microwave absorption depending on induction,  $B$ . From EPR spectra one can obtain information on the structure and surrounding (ligand symmetry) of the investigated species. Hence, from EPR spectra, a  $g$ -factor and a superfine interaction tensor,  $A$ , are derived [44]:

$$g = \frac{h\nu}{\mu_B B}. \quad (29)$$

EPR spectroscopy is also appropriate for the evaluation of the relative concentration of polyvalent ions. For that, a number of unpaired electrons  $N$  in the sample will be estimated. The concentration evaluation is done by comparative measurements of the sample with a known spin number.  $\text{CuSO}_4 \cdot 5\text{H}_2\text{O}$  was taken as standard. The error of the method is rather large ( $\sim 20\%$ ), and it was mainly used for copper containing samples.

One of the errors from estimating the parameters for the calculation of concentrations is a large signal width, which lowers even more the sufficient accuracy.

Because in this work, glass is investigated in a fairly large temperature range, which exceeds the  $T_g$  region, some species (e.g.,  $\text{Mn}^{2+}$ ) might appear in glass in octahedral and tetrahedral coordination, respectively, depending on the temperature. Therefore, samples were prepared in the following way. From a glass block a slide of glass was cut out and halved [part X and Y]. One part [Y] was thermally treated up to  $1000\text{ }^\circ\text{C}$  and quenched by quenching into a water bath ( $t = \sim 25\text{ }^\circ\text{C}$ ). This process might freeze the structure. From both parts [X, Y] separately, powder was prepared. If three conditions are kept during EPR measurements:

- i. the amount of sample is nearly constant (about  $0.2 \pm 0.002\text{g}$ );
- ii. received gain (amplification) is known;
- iii. any other condition stay constant,

then it is possible to compare EPR spectra of these samples whether there are differences between room and high temperature sample.

EPR spectra of glasses were measured by ESP 300E (Bruker, X-band [9-10 GHz]). All EPR spectra are presented as a function of magnetic flux density (in Tesla) versus intensity (in arbitrary units). In the case of the samples X and Y, spectra are recalculated on constant receive gain which makes it possible to compare these two measurements.

## 5. Results.

In the next sections, the results of the spectroscopic investigation of glasses doped solely with one polyvalent element A and B, respectively, or with both of them simultaneously are presented. The former case allows to study the effect of only one polyvalent element from some significant points of view. At first, an absorption spectrum recorded at room temperature gives information on the equilibrium between the oxidized and the reduce state of the polyvalent element in the glass,  $[A^{n+}]/[A^{(n-z)+}]$ , and also on the structural incorporation of the different states in the glass, which is compared with results from other methods. Secondly, observation of the trends of the absorption bands of  $A^{n+}$  and  $A^{(n-z)+}$  with increasing (and decreasing) temperature helps to interpret what is happened if a second polyvalent element is in the glass. Finally, the Gaussian parameters for the absorption bands can only be obtained from high-temperature absorption spectra (HTAS) of glasses solely doped with one polyvalent element. These parameters are later used to decompose spectra from glass doped with two polyvalent elements into the bands of the two polyvalent elements.

### 5.1. Basic glass spectra as a function of temperature.

In figure (10), UV-vis-NIR absorption spectra of the basic glass at different temperatures are shown.

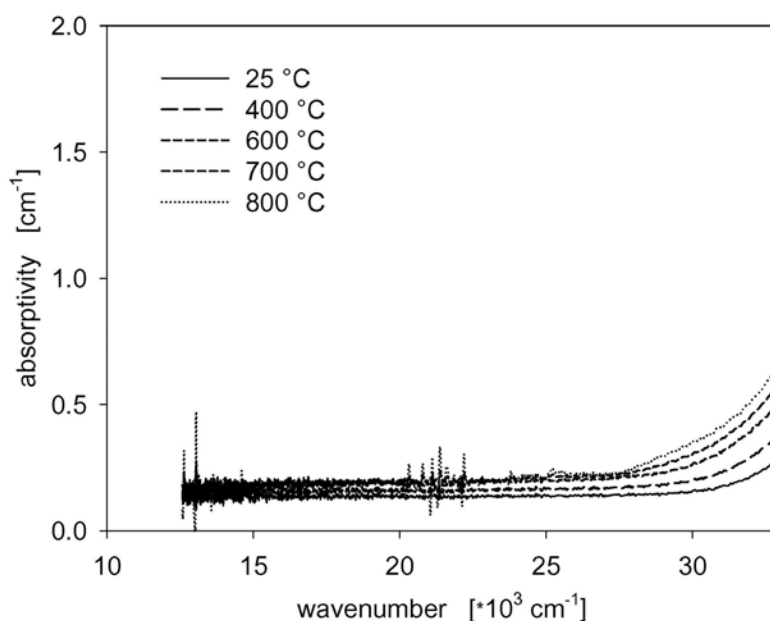


**Figure 10.** UV-vis-NIR absorption spectra of basic glass at different temperatures

It can be seen that with increasing temperature the UV absorption edge shifts towards higher wavelength (smaller wavenumbers) but the absorption minimum remains on the same level (in limits of errors of measurements) over the whole spectral range. Thus, the basic glass shows the expected and predicted behaviour.

## 5.2. Copper doped glasses.

Copper may exist in silicate glasses as cupric ( $\text{Cu}^{2+}$ ) and/or cuprous ( $\text{Cu}^+$ ) ions and/or metallic copper ( $\text{Cu}^0$ ), each of which has different optical absorption characteristics.  $\text{Cu}^+$  ions have a  $d^{10}$  configuration and, hence, do not show a ligand field splitting. No absorption occurs either in the visible or near infrared range, but samples may fluoresce during UV irradiation. The well-known deep red copper ruby colour is due to colloidal metallic copper or cuprous oxide [45].

$\text{Cu}^{2+}$  ions in silicate glasses results in blue to green colour, depending on glass composition. The configuration is  $d^9$  and, thus,  $\text{Cu}^{2+}$  is paramagnetic. Figure (11) shows an intense and characteristic EPR line of  $\text{Cu}^{2+}$ . The two sets of four-line hyperfine structure originates from the isotopy of  $^{63}\text{Cu}$  and  $^{65}\text{Cu}$  with the same nuclear spin  $I = 3/2$  and are respectively designated as parallel and perpendicular hyperfine peaks, since they arise from the resonance of these centres having their symmetry axes parallel and perpendicular to the static field [44]. Principal values of g factor are  $g_{\parallel} \sim 2.3$ ,  $g_{\perp} \sim 2.08$ .

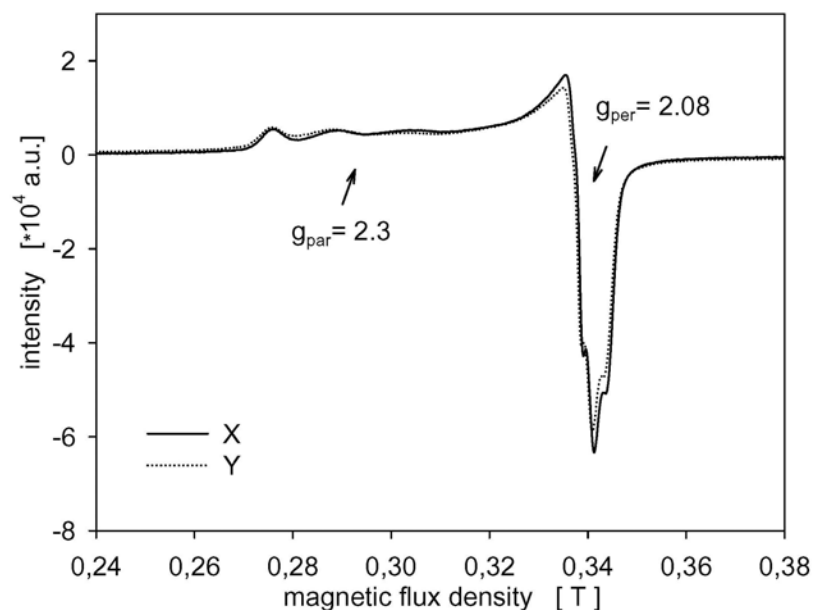


**Figure 11.** EPR spectra of copper-doped glass.

Analysis according to Sands showed that the  $\text{Cu}^{2+}$  ions occupy modifying-cation positions and are octahedrally coordinated with oxygen. The free ion state of  $\text{Cu}^{2+}$  is  ${}^2\text{D}_{5/2}$ . In an octahedral field, it splits into a low-energy  $e_g$  doublet and a higher energy  $t_{2g}$  triplet [46].

The spectrum of a quenched sample at 1000 °C (Y), is similar, i.e., the structure of the  $\text{Cu}^{2+}$  stays octahedral, at least, up to of 1000 °C.

The optical absorption of the  $\text{Cu}^{2+}$  ion in an octahedral field should consist of a single band corresponding to the value of  $10 Dq$ , and arising from the  ${}^2\text{E} \rightarrow {}^2\text{T}_2$  transition. The value of  $10 Dq$  derived from the band at  $\sim 780$  nm in the glasses is  $\sim 12,660 \text{ cm}^{-1}$ . However, the ground state of the cupric ion in the octahedral field is  ${}^2\text{D}$ , therefore, Jahn-Teller splitting will arise and more than one transition is then possible. This splitting is the origin of the broadness of the  $\text{Cu}^{2+}$  absorption band and attempts have been made to resolve it into its components (Gaussian bands) [47, 48, 38]. Using this analysis, a number of bands are recommended by several authors, depending on distortion. In this case, the kind of host glass must be taken into account. The  $\text{Cu}^{2+}$  spectra in phosphate containing glasses consist of three Gaussian bands in vis-NIR absorption region, which are situated at 14,400, 12,500 (main band) and  $10,800 \text{ cm}^{-1}$  [49]. For sodium disilicate glasses, the distortion is also observed but according to most authors there is no need to use more than one  $\text{Cu}^{2+}$  absorption band centred around  $12,500 \text{ cm}^{-1}$  [48, 42, 50] to describe the spectra. However, the position of the band maximum depends on glass composition [50]. Since in this work the composition of the basic glass is constant, it is not necessary to elaborate the composition effect.

Figure (12) presents absorption spectra of glasses also solely doped with copper in different concentration. A strong ultraviolet absorption edge is observed, which is a superposition of the absorption edge of the basic glass and of  $\text{Cu}^{2+}$  and  $\text{Cu}^+$  absorption bands in the UV region. The  $\text{Cu}^+$  ion has an absorption band in the UV region arising from the  $3d^{10} > 3d^9 4s$  transition but this is usually covered by the UV cut-off of silicate and borate glasses. However, it can be resolved from the UV cut-off of phosphate glasses [50]. Under normal circumstances, the spectra of the  $\text{Cu}^{2+}$  are studied when  $\text{Cu}^+$  is also present in the glass. This does not result in difficulties in the visible and near infrared regions where the  $\text{Cu}^+$  has no absorption band.



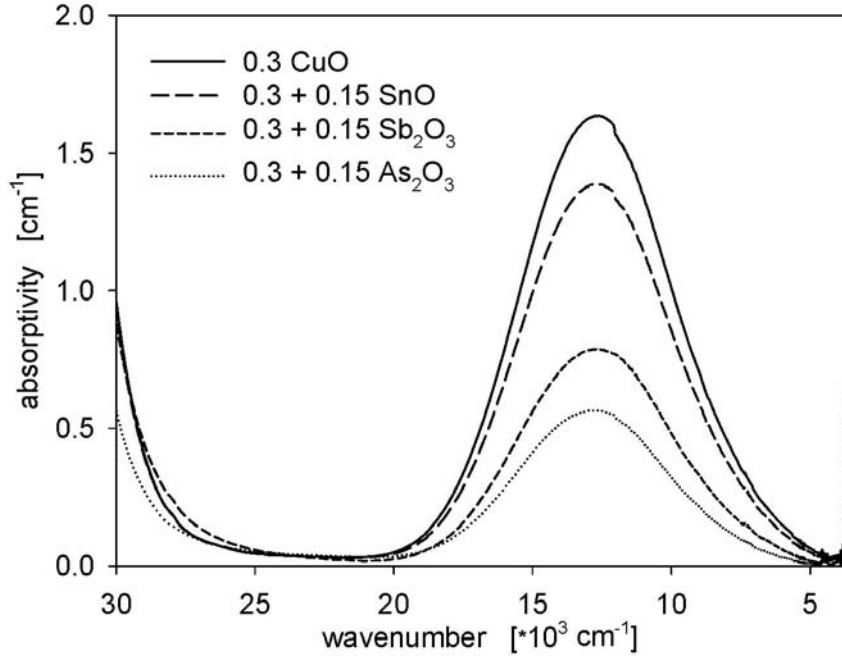
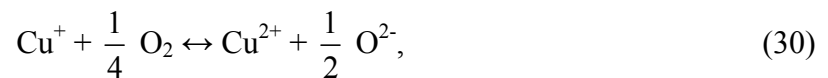


**Figure 12.** Optical spectra of copper containing glasses (in mol %).

The similarity between the  $\text{Cu}^{2+}$  absorption bands in glasses and in aqueous solutions has prompted the suggestion that the  $\text{Cu}^{2+}$  ion in glasses is octahedrally coordinated but with strong tetragonal distortion [51, 52].

The proportion of copper, present in each of the two possible states discussed above, will be determined by glass composition and melting conditions [42]. The work of Johnston & Chelko on sodium disilicate glasses [53] has shown that the equilibrium in can be described over a wide range of oxygen partial pressure by



and may be strongly dependent on both temperature and glass composition as well as oxygen partial pressure,  $p(\text{O}_2)$ . They showed, further, that the reduction of cuprous to metallic copper required  $p(\text{O}_2) < 10^{-4}$  Pa in sodium disilicate at 1085 °C. Most oxide glasses equilibrated with air may thus be assumed to contain copper only as  $\text{Cu}^{2+}$  and  $\text{Cu}^+$  ions.

As already discussed in the theoretical part, studies showed that the  $[\text{A}^{n+}]/[\text{A}^{(n-z)+}]$  ratio does not change as a function of the total concentration of A. In the particular case of copper, this assumption is supported by Cable & Xiang, at least over the range from 0.1 to 1.2 mol% CuO [42, 54]. They also found that melts could be brought to equilibrium much more quickly by

stirring them than by using very long melting times with nominally static melts. The fact that stirring considerably accelerated equilibrium supports another assumption, namely that diffusion of oxygen within the melt controls the rate of equilibration.

Figure (13) shows spectra from a glass doped with 0.3 mol % CuO recorded in the temperature range from 25 to 800 °C. All spectra exhibit a distinct maximum which appears at wave numbers from 12,700 to 11,500  $\text{cm}^{-1}$ . The position of the maximum of the absorption band is continuously shifted to smaller wave numbers with increasing temperature, as is shown in Fig (14). This effect is derived from Orgel diagram for  $d^9$  configuration with transition  ${}^2E \rightarrow {}^2T_2$ . Furthermore, Fig. (15) shows, the absorption band becomes broader with increasing temperature. The height of the maximum of the absorption band (denoted as absorptivity) is also affected by temperature and is slightly decreased with increasing temperature. This effect is small. Within the range from 25 to 800 °C, the absorbance decreases from 1.68 to 1.56  $\text{cm}^{-1}$ , i.e. by less than 10 %, as also shown in Fig. (16).

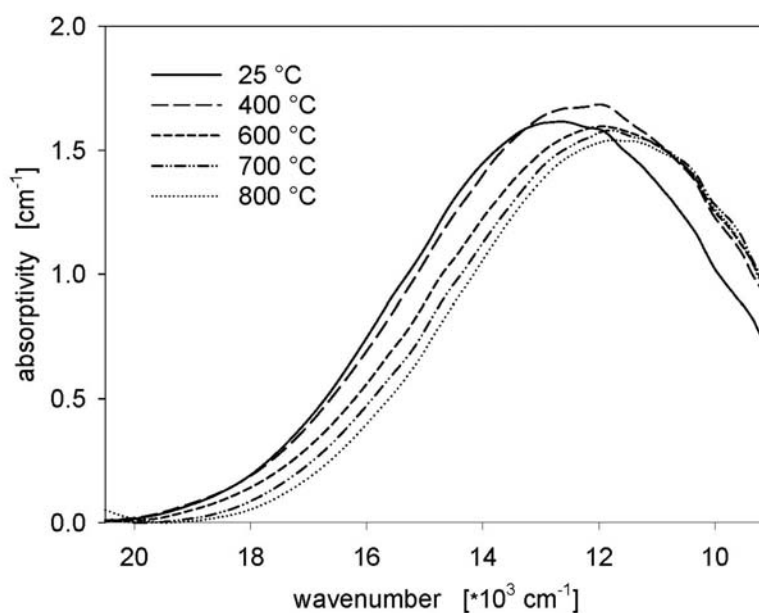


**Figure 13.** Absorption spectra collected from a glass doped with 0.3 mol % CuO at different temperatures.

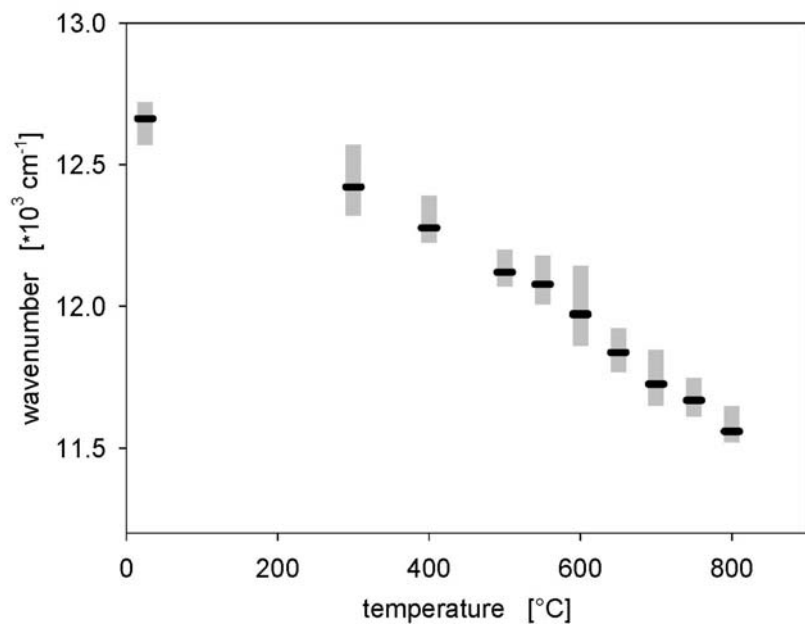


**Figure 14.** Wavenumber attributed to the absorptivity maxima as a function of the temperature.

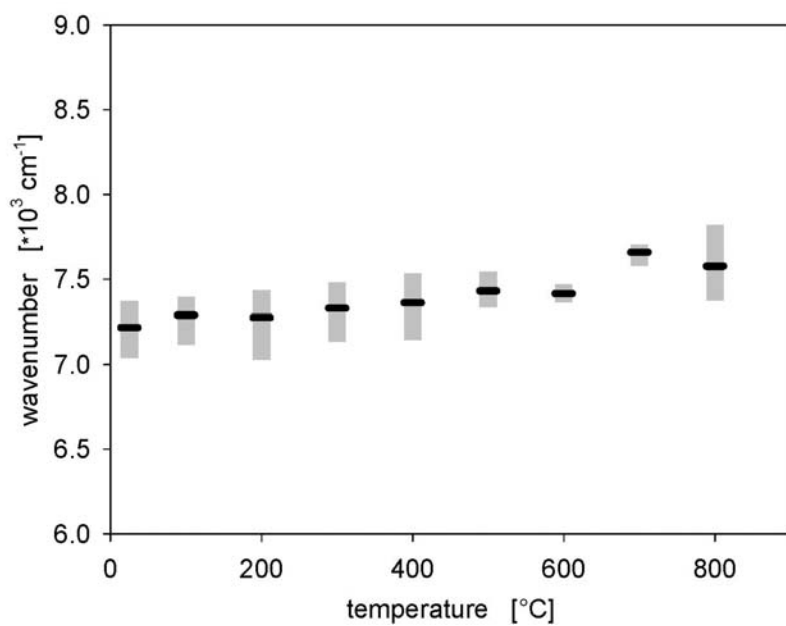


**Figure 15.** Wavenumber attributed to the FWHM as a function of the temperature.

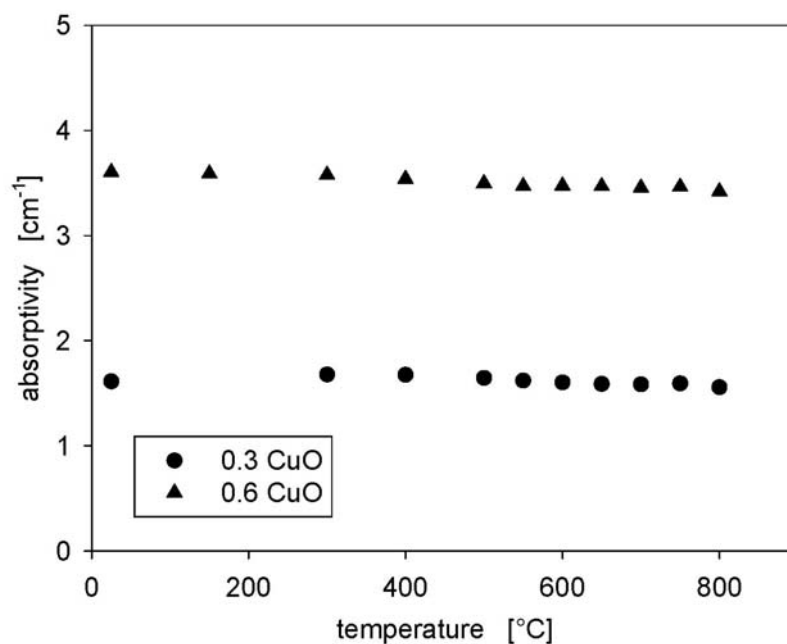


**Figure 16.** Maximum absorptivity in copper-doped glasses (mol %) as a function of the temperature.

**Table 4.** Summary of  $\text{Cu}^{2+}$  absorption band parameters at room temperature.

Transition	$k$ [ $\text{cm}^{-1}$ ]	FWHM [ $\text{cm}^{-1}$ ]	Coordination
${}^2\text{E} \rightarrow {}^2\text{T}_2$	$12,663 \pm 0.19$	$7,218 \pm 0.17$	octahedral

### 5.3. The mutual redox interaction between copper and tin, antimony, arsenic

Antimony and arsenic oxides are used in the manufacture of glass as an aid for the refining process (refining agents) [32]. A side-effect is that sometimes the glasses are also decolourised during this interaction (clarifying agents). The second effect is due to the fact that clarifying agents in glass can exist in two valence states and thus form a redox system. Oxidising or reducing agents may then have an important influence on the equilibrium of the colouring ions. In glass-making, tin(II)-oxide is often used as a reducing agent.

In  $16\text{Na}_2\text{O}-10\text{CaO}-74\text{SiO}_2$  glasses, the possible oxidation states of tin are  $\text{Sn}^{2+}$  and  $\text{Sn}^{4+}$ , of arsenic  $\text{As}^{3+}$  and  $\text{As}^{5+}$ , and of antimony  $\text{Sb}^{3+}$  and  $\text{Sb}^{5+}$ . Neither of these ions absorb in the visible and near infrared where the cupric ion has its absorption band. They absorb in the ultraviolet but this does not affect the cupric spectra. Therefore, any change in absorption at the cupric peak relative to glasses, which contained only Cu could be considered to be caused by physical or chemical interactions between copper and tin ions. This is supported by EPR

spectra (Figure (17)) of glasses doped with copper and tin, antimony, arsenic, respectively. The hyperfine structure arranged in two sets is readable for all chosen glasses. The values of  $g_{\parallel} \sim 2.3$ ,  $g_{\perp} \sim 2.08$ . They are similar for glasses doped with both copper and the second polyvalent element as for glasses only doped with copper.

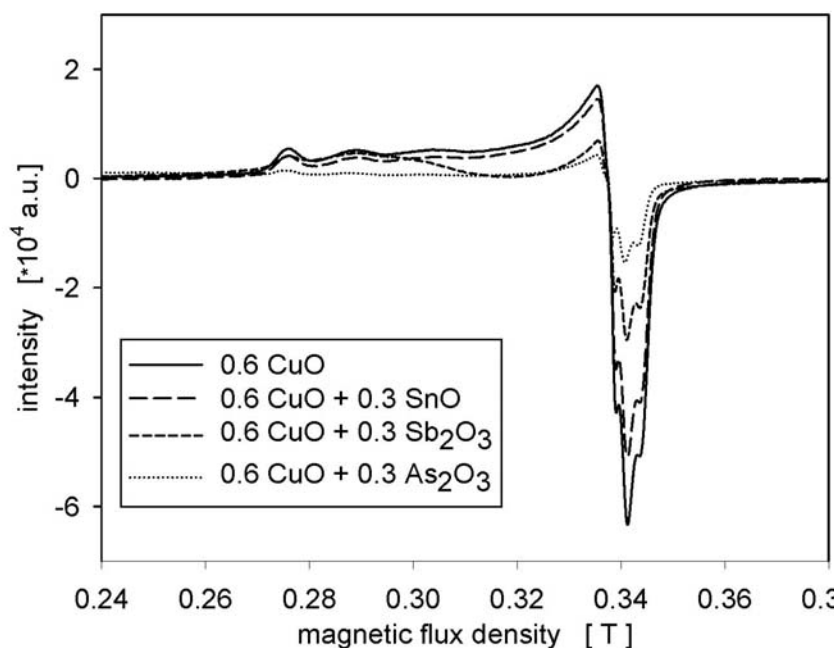


**Figure 17.** EPR spectra of glass doped with Cu and Sn, Sb or As, respectively.

This indicates that the presence of the tin ions does not affect the symmetry of the cupric coordination and the physicochemical properties of the ligands, which form the cupric complex in the glass, i.e. dipole-dipole interaction between two copper ligands are much more stronger than between copper and another dopant ligands [54, 55].

### 5.3.1. Copper – Tin interaction.

In Fig. (18), the points at room temperature represent the effect of increasing tin on the absorption spectra of the cupric ion in the visible and near infrared regions. The band position remains the same as for the glass without tin (see Fig. (12)). It can therefore be assumed that the molar extinction coefficient of the cupric ion does not change with the addition of the tin ions. Thus, the observed decrease in the cupric absorption in the glasses containing tin suggests that the cuprous-cupric equilibrium is slightly shifted to the cuprous side by introducing tin to the glasses.

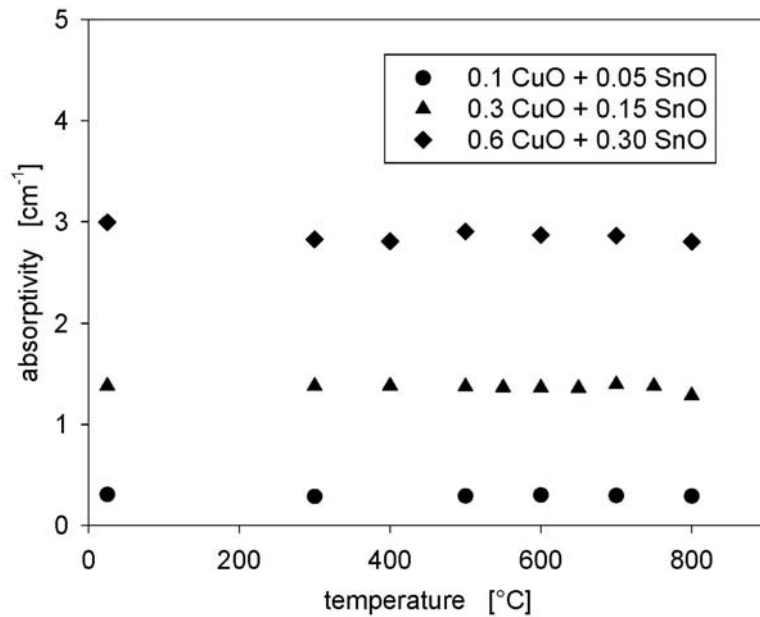


**Figure 18.** Maximum absorptivity in glasses doped with copper and tin (in mol %).

In Fig. (19) absorption spectra of a glass doped with both CuO (0.3 mol %) and SnO (0.15 mol %) are shown. Also here, a dependence of temperature of the wavenumber of the absorptivity maximum is observed, which is in the same range as shown in Figs. (14) and (15). By analogy to Fig. (13), also the absorptivity slightly decreases with increasing temperature. Hence, both effects are similar to those observed in Fig. (19).

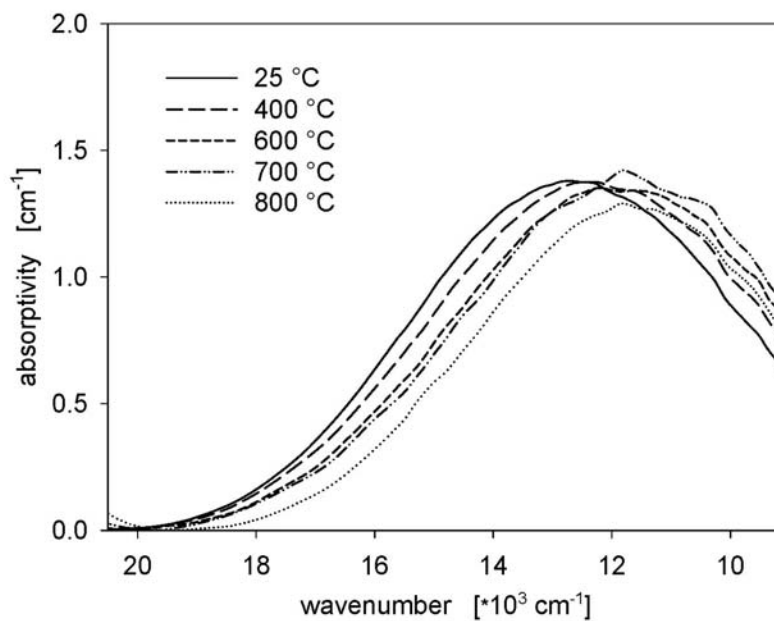


**Figure 19.** Absorption spectra collected from a glass doped with both 0.3 mol % CuO and 0.15 mol % SnO at different temperatures.

In summary, the glasses doped solely with CuO show approximately the same behaviour as those doped with both, CuO and SnO. The effect of temperature on the absorbance is shown in Fig. (18) for three different glass compositions, all containing both CuO and SnO. The absorptivity increases with the copper concentration. At room temperature, the absorbance is 3.0, 1.38 and 0.35  $\text{cm}^{-1}$  for the copper concentrations 0.6, 0.3 and 0.1 mol %, respectively. In comparison to the glass doped solely with copper, the absorbance of the glass containing 0.3 mol % CuO is around 10 % smaller, when 0.15 mol % SnO is added.

### 5.3.2. Copper – Antimony interaction.

The possible stable oxidation states of antimony in oxide glasses are  $\text{Sb}^{3+}$  and  $\text{Sb}^{5+}$  [54]. However, its absorption does not affect the cupric spectra. The band position of the cupric ion remains the same as for the glass without antimony. Decreases in absorbances are therefore a result of shifting the cuprous-cupric equilibrium to the cuprous side by introducing antimony in the glasses. Figure (20) shows the effect of adding antimony on the cupric absorption in the glasses. It can be seen that its effects are similar to those of tin but with more powerful reducing effect.

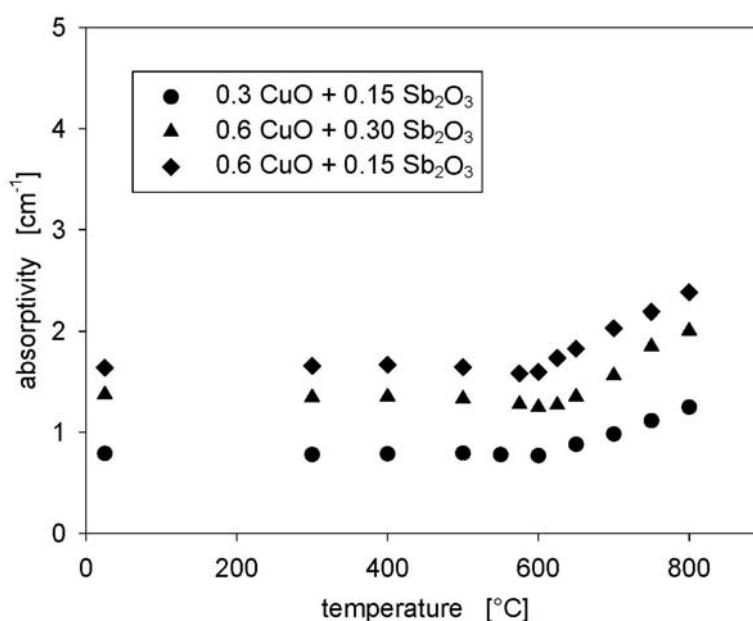


**Figure 20.** Maximum absorptivity in glasses doped with copper and antimony.

Figure (21) shows absorption spectra of a glass doped with 0.3 mol % CuO and 0.15 mol %  $\text{Sb}_2\text{O}_3$ . The absorbance maximum is again shifted to larger wavelengths with increasing temperature. At first, the absorbance decreases slightly with increasing temperature. At

temperatures above 600 °C, however, a drastic increase in the absorbance is observed. From 600 to 800 °C, the absorbance attributed to the band maximum increases from around 0.8 to 1.25  $\text{cm}^{-1}$ .

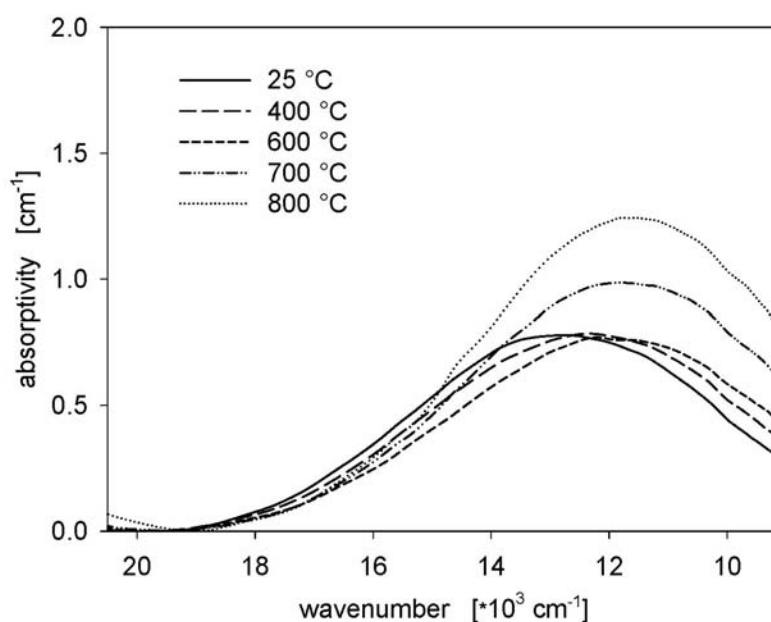


**Figure 21.** Absorption spectra collected from a glass doped with both 0.3 mol % CuO and 0.15 mol %  $\text{Sb}_2\text{O}_3$  at different temperatures.

In Fig. (20), the dependence of the maximum absorbance on the temperature is shown for three different glass compositions all containing both CuO and  $\text{Sb}_2\text{O}_3$ . At room temperature, the glass with 0.3 mol % CuO and 0.15 mol %  $\text{Sb}_2\text{O}_3$  exhibits an absorptivity of 0.8 which is clearly smaller than those observed in the glass with 0.3 mol % CuO (see Fig. (16)), as well as in that with 0.3 mol % CuO and 0.15 mol % SnO (see Fig. (18)). The glass with 0.6 mol % CuO and 0.3 mol %  $\text{Sb}_2\text{O}_3$  shows a maximum absorbance of around 1.7  $\text{cm}^{-1}$  while the maximum absorbance is 1.4  $\text{cm}^{-1}$  in the glass doped with 0.6 mol % CuO and 0.15 mol %  $\text{Sb}_2\text{O}_3$ . Obviously the presence of  $\text{Sb}_2\text{O}_3$  in the melt leads to smaller absorbance maxima. This effect is more pronounced at a larger  $\text{Sb}_2\text{O}_3$  concentration.

### 5.3.3. Copper – Arsenic interaction.

The possible stable oxidation states of arsenic in glasses are  $\text{As}^{3+}$  and  $\text{As}^{5+}$  neither of which absorbs in the visible and near infrared regions [54]. Figure (22) shows the effect of arsenic oxide on the cupric absorption in the investigated glasses. Again, the effect is similar to those observed for tin or antimony. However, the reducing effect of arsenic on cuprous-cupric equilibrium is larger than those of tin or antimony.



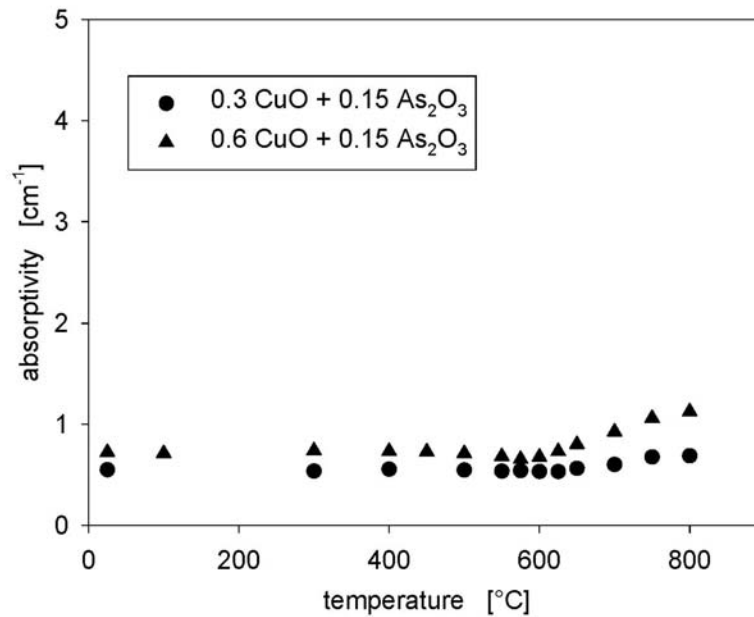


**Figure 22.** Maximum absorptivity in glasses doped with copper and arsenic.

Figure (23) shows absorption spectra of a glass doped with 0.3 mol % CuO and 0.15 mol % As<sub>2</sub>O<sub>3</sub>. As before, the absorbance maximum is again shifted to larger wavelengths with increasing temperature. At first, the absorbance decreases slightly with increasing temperature. Like in glasses doped with both CuO and Sb<sub>2</sub>O<sub>3</sub>, the absorbance apparently increases at temperatures above 600 °C. However, here the increase is smaller and less steep. From 600 to 800 °C, the absorbance attributed to the maximum increases from around 0.55 to 0.69 cm<sup>-1</sup>. Fig. (22) shows the dependence of the maximum absorbance on the temperature for two different glass compositions all containing both CuO and As<sub>2</sub>O<sub>3</sub>. At room temperature, the glass with 0.3 mol % CuO and 0.15 mol % As<sub>2</sub>O<sub>3</sub> exhibits an absorptivity of 0.55 cm<sup>-1</sup> which is clearly smaller than those observed in the glass solely doped with 0.3 mol % CuO (see Fig. (16)). The glass with 0.6 mol % CuO and 0.15 mol % As<sub>2</sub>O<sub>3</sub> shows a maximum absorbance of around 0.73 cm<sup>-1</sup>. As already mentioned in the case of SnO or Sb<sub>2</sub>O<sub>3</sub>, the presence of As<sub>2</sub>O<sub>3</sub> in the melt leads to smaller absorptivity maxima of Cu<sup>2+</sup> band.

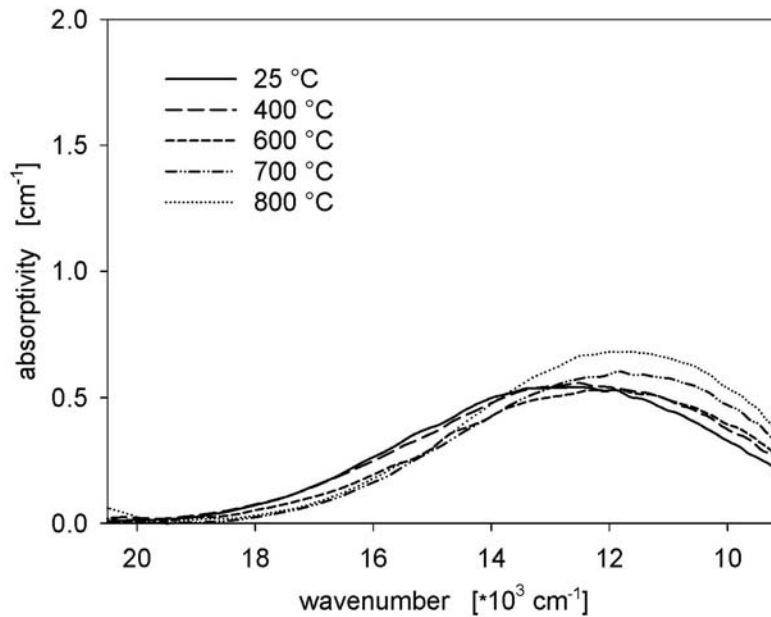


**Figure 23.** Absorption spectra collected from a glass doped with both 0.3 mol % CuO and 0.15 mol % As<sub>2</sub>O<sub>3</sub> at different temperatures.

Using the absorption of the cupric band centred at 12,660 cm<sup>-1</sup> to determine its concentration requires that the value of the molar extinction coefficient,  $\epsilon_{\text{Cu}^{2+}}$  (at room temperature), remains constant upon adding oxides of a second multivalent element in a glass of fixed composition. Xiang & Cable [54] showed that the two factors that affect its value are glass basicity and type of positive ions in the secondary coordination sphere of the cupric ion. In the glasses of a particular system such as Na<sub>2</sub>O-CaO-SiO<sub>2</sub> [42], the peak position of the cupric band may be affected little by composition,  $\epsilon_{\text{Cu}^{2+}}$ , increases with basicity. However, changing the positive ions by replacing Na<sup>+</sup> by Li<sup>+</sup> or K<sup>+</sup> affects both the band position and the extinction coefficient [52, 50].

In this study, since the concentrations of the oxides of the second polyvalent elements added are too low to affect glass basicity significantly (below 0.6 mol%), and, more importantly, since the peak position of the cupric band at certain wavelength is not affected by adding these components, it can be concluded that  $\epsilon_{\text{Cu}^{2+}}$  remains unaffected. The position of the Cu<sup>2+</sup> band is shifted towards higher wavelengths with increasing temperature. Here, the dependence of the wavelength's shift on temperature is the same as the shift of the absorptivity maxima with the temperature showed in Figures (14) and (15). However, if it is considered that  $\epsilon_{\text{Cu}^{2+}}$  is more or less constant, no structural change can occur with increasing temperature, in this case from octahedral to tetrahedral coordination. To exclude this, one

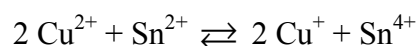
conclusion can be that the shape of the spectra is rather the same in whole studied temperature range. The other one comes from EPR experiment comparing two samples: X and Y\* (see Figs (11) and also (17)). Between the “room temperature” sample X and the “high temperature” Y is no significant difference in the shape of the EPR spectra. Furthermore, also from the literature generally is no evidence to deduce copper in silicate glasses in tetrahedral coordination even at higher temperature, at least up to 1000 °C [8].

The cupric band was deconvoluted based on these considerations. A further implication of this observation may be that the added second multivalent element is not present in the secondary coordination sphere of the cupric ion.

It can be seen that the ions of Sn, Sb and As all have considerable effect on the cuprous-cupric equilibrium. They destabilise the cupric state and favour the formation of the cuprous, and hence are reducing agents towards copper. However, as expected, the abilities of these elements to reduce the cupric ions are significantly different. Antimony appears to be the strongest and tin is the weakest reducing agent towards the cuprous-cupric equilibrium. Thus, among the elements studied the ability to reduce the cupric is in the following order: As>Sb>Sn.

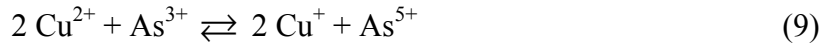
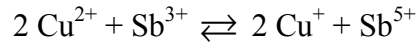
As shown in Fig. (20), the Cu<sup>2+</sup>-concentrations changes during heating at temperatures > 600 °C. Although, measurements above 800 °C were not carried out, in the following, it is assumed that further changes in the Cu<sup>2+</sup>-concentrations occur at higher temperatures (800 °C < T < 1600 °C). Furthermore, it is assumed that at T > 600 °C the Cu<sup>2+</sup>-concentration is only due to the thermodynamics of the respective redox pair, because diffusion of oxygen in or out of the melt does not take place, and hence, is the same during heating and cooling.

According to Eq.(11), the equilibrium should be shifted with temperature if  $y \cdot \Delta H_A^0 \neq z \cdot \Delta H_B^0$ . The thermodynamic data of the redox equilibrium (see Eq. (5))  $\Delta H^0 (\text{Cu}^+/\text{Cu}^{2+}) = 92 \text{ kJ}\cdot\text{mol}^{-1}$   $\text{kJ}\cdot\text{mol}^{-1}$  [56],  $\Delta H^0 (\text{Sn}^{2+}/\text{Sn}^{4+}) = 192 \text{ kJ}\cdot\text{mol}^{-1}$  [57],  $\Delta H^0 (\text{Sb}^{3+}/\text{Sb}^{5+}) = 286 \text{ kJ}\cdot\text{mol}^{-1}$  [56] and  $\Delta H^0 (\text{As}^{3+}/\text{As}^{5+}) = 230 \text{ kJ}\cdot\text{mol}^{-1}$  [30] are known from voltammetric studies at high temperatures. From those data  $\Delta H_{AB}^0$  (see Eq. 9), i.e.  $\Delta H_{\text{Cu/Sb}}^0 = 102 \text{ kJ}\cdot\text{mol}^{-1}$ ,  $\Delta H_{\text{Cu/Sn}}^0 = 8 \text{ kJ}\cdot\text{mol}^{-1}$  and  $\Delta H_{\text{Cu/As}}^0 = 46 \text{ kJ}\cdot\text{mol}^{-1}$  can be calculated.




---

\* About the way of preparing those sample is written in Cap. 4.5.



Including  $\Delta S^0$  -values reported in the literature  $\Delta S^0 (\text{Cu}^+/\text{Cu}^{2+}) = 32 \text{ J} \cdot \text{K}^{-1} \cdot \text{mol}^{-1}$  [56],  $\Delta S^0 (\text{Sn}^{2+}/\text{Sn}^{4+}) = 118 \text{ J} \cdot \text{K}^{-1} \cdot \text{mol}^{-1}$  [57],  $\Delta S^0 (\text{Sb}^{3+}/\text{Sb}^{5+}) = 206 \text{ J} \cdot \text{K}^{-1} \cdot \text{mol}^{-1}$  [56],  $\Delta S^0 (\text{As}^{3+}/\text{As}^{5+}) = 138 \text{ J} \cdot \text{K}^{-1} \cdot \text{mol}^{-1}$  [30], the respective concentrations of the redox species can be calculated. In the following, the respective melts were assumed to be in equilibrium with air at 1600 °C. This results in a  $[\text{Cu}^{2+}]/[\text{Cu}^+]$ -ratio of 1.8. In the melt doped solely with copper, the  $\text{Cu}^{2+}$ -concentration remains the same during cooling.

In the melt additionally doped with antimony, the  $\text{Cu}^{2+}$ -concentration decreases during cooling. At initial  $\text{CuO}$ - and  $\text{Sb}_2\text{O}_3$ -concentrations of 0.3 and 0.15 mol %, respectively, the  $\text{Cu}^{2+}$ -concentration is 0.193 at 1600 °C. During cooling, a  $\text{Cu}^{2+}$ -concentration of 0.1 mol % is reached at 550 °C. If the  $\text{Sb}_2\text{O}_3$ -concentration is kept constant and the  $\text{CuO}$ -concentration is increased to 0.6 mol %, the  $\text{Cu}^{2+}$ -concentration decreases from 0.386 to 0.262 mol % during cooling. In the melt doped with 0.3 mol %  $\text{CuO}$  and 0.15 mol %  $\text{SnO}$ , the  $\text{Cu}^{2+}$ -concentration decreases from 0.193 to 0.182 mol % at 550 °C.

Other concentrations calculated from the thermodynamic data and the concentrations of the respective samples are summarized in Table (5). Figure (24) shows a plot of the maximum absorptivity and the  $\text{Cu}^{2+}$ -concentration calculated from the thermodynamic data. A linear correlation between the measured and calculated values is seen.

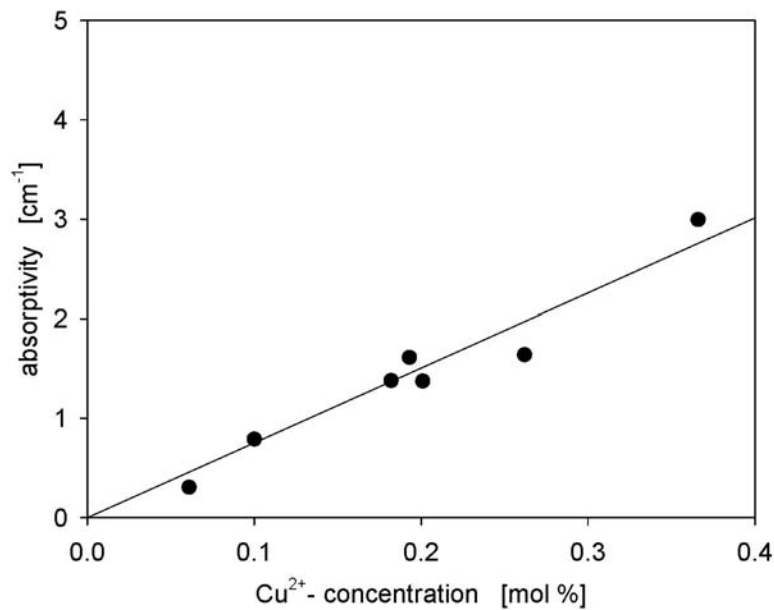


**Figure 24.** Maximum absorptivities at room temperature and  $\text{Cu}^{2+}$ -concentrations calculated from thermodynamic data.

The shift in the  $\text{Cu}^{2+}$ -concentration during cooling as calculated is readily seen in the absorption spectra. It should be noted for these calculations that  $\Delta H_{\text{AB}}^0$  has to be considered as independent of temperature over the whole temperature range (i.e. down to 550 °C), although they were measured only at temperatures between 800 and 1300 °C (in the case of  $\text{Cu}^+/\text{Cu}^{2+}$  even in a narrower temperature range). Taking this into account, the agreement of measured and calculated values is very good.

In the case of the antimony doped melts, the redox equilibrium is significantly shifted with temperature due to the large value  $\Delta H_{\text{Cu/Sb}}^0 = 102 \text{ kJ}\cdot\text{mol}^{-1}$ . The redox equilibrium of the arsenic and copper melts is shifted somewhat less, the value of the standard reaction enthalpy  $\Delta H_{\text{Cu/As}}^0$  is equal to  $46 \text{ kJ}\cdot\text{mol}^{-1}$ . By contrast, in the case of the tin doped melt,  $\Delta H_{\text{Cu/Sn}}^0$  is as low as  $8 \text{ kJ}\cdot\text{mol}^{-1}$ . Hence, the shift is small.

In Ref. [50], equilibration experiments for melts doped solely with copper and melts doped with copper and additionally with tin or antimony were reported. Also in that study, the  $\text{Cu}^{2+}$ -concentration in glasses doped with  $\text{CuO}$  and  $\text{SnO}$  was only slightly smaller than in the glass doped solely with copper. By contrast, melts doped with copper and antimony showed a much smaller  $\text{Cu}^{2+}$ -concentration than those doped solely with copper. According to Eqs. (8) to (11), the redox ratio of a polyvalent ion in a melt in equilibrium with the surrounding atmosphere at a constant temperature is not affected by the presence of another polyvalent ion. This is only valid under isothermal conditions, and at concentrations which are too small to affect the melt basicity significantly. This is also supported by numerous experimental observations: from studies on the effect of glass composition on redox equilibria (see e.g. [58]), it is known that the addition of small concentrations of non-polyvalent elements does not affect the redox equilibria noticeable. It should also be noted that in voltammetric studies carried out at high temperatures, it has been shown that the presence of another polyvalent element does not affect the peak potentials and hence, the redox equilibria at these temperatures [59, 60].

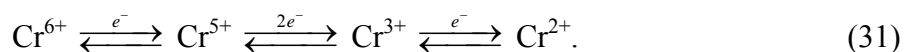
In the present study, not only the shift in the redox equilibrium has been explained by a redox reaction during cooling, but also, the change in the  $\text{Cu}^{2+}$ -concentration, in the case of the melts additionally doped with antimony directly has been measured in the temperature range from 600 to 800 °C.

**Table 5.** Concentration of redox species calculated from Eq. (11) using thermodynamic data  $\Delta H^0$  and  $\Delta S^0$  of the respective redox species (for 550 °C, mol%).

Sample <sup>§</sup>	[Cu <sup>2+</sup> ]	[Cu <sup>+</sup> ]	[Sn <sup>4+</sup> ]	[Sn <sup>2+</sup> ]	[Sb <sup>5+</sup> ]	[Sb <sup>3+</sup> ]
A	0.193	0.107	-	-	-	-
B	0.061	0.039	0.012	0.038	-	-
C	0.182	0.118	0.037	0.113	-	-
D	0.366	0.234	0.073	0.227	-	-
E	0.100	0.200	-	-	0.050	0.100
F	0.262	0.338	-	-	0.065	0.085
G	0.201	0.399	-	-	0.100	0.200

#### 5.4. Chromium.

Chromium doped glasses are widely manufactured in the glass industry and used as container glass. Another important application is that as green float glass. Chromium, in principle, may occur in glasses as Cr<sup>6+</sup>, Cr<sup>5+</sup>, Cr<sup>3+</sup> and Cr<sup>2+</sup>. All these valence states are possible to detect by absorption spectroscopy but only the Cr<sup>6+</sup> and Cr<sup>3+</sup> can clearly be distinguished in soda-lime-silica glasses. The species Cr<sup>3+</sup> and Cr<sup>5+</sup> are paramagnetic and may be determined by EPR spectroscopy. At high temperatures, voltammetric studies give evidence of the occurrence of three redox states: Cr<sup>6+</sup>, Cr<sup>3+</sup> and Cr<sup>2+</sup>. However, they do not give any hint at the redox state Cr<sup>5+</sup>. The existence of Cr<sup>2+</sup> depends strongly on the glass system and is provable only in strong reduced glasses [61]. Depending on the batch composition, the concentrations of the respective redox species may notably vary.



Equation (31) gives an overview of all redox species occurring at room temperature. Redox equilibria are generally affected by the temperature and are usually shifted to the reduced species while increasing the temperature [62].

Spectra recorded at room temperature (25) from glasses solely doped with chromium could be fitted with absorption bands of Gaussian shape. Since in glass doped with 0.23 mol % Cr<sub>2</sub>O<sub>3</sub>, prepared with reducing agent (1g sugar per 100g glass), the peaks at around 265 and 365 nm

<sup>§</sup> see Table (1)

do not appear in the spectra, it can be concluded that these peaks are caused by chromium in a higher valency state. As already described in the literature, these are attributed to the  $\text{Cr}^{6+}$  charge-transfer absorption bands and have been assigned to  ${}^2\text{T}_2(\sigma) \rightarrow {}^3\text{T}_2(\pi^*)$  and  $(\text{T}_1(\pi) \rightarrow {}^3\text{T}_2(\pi^*))$ , respectively. The  $\text{Cr}^{6+}$  is in present glasses in a tetrahedral coordination surrounded with four oxygen-ligands with relatively strong  $\sigma$ - and  $\pi$ -bonds to the  $\text{Cr}^{6+}$ , likewise in  $[\text{SO}_4]^{2-}$  molecule [17, 63]. This oxidation state is favoured by increasing basicity of the glass [32]. However, also under strong oxidation conditions it is not possible to shift the  $\text{Cr}^{6+}/\text{Cr}^{3+}$  equilibrium completely towards  $\text{Cr}^{6+}$  [64]. The reaction between  $\text{Cr}^{3+}$  and  $\text{Cr}^{6+}$  could be written as:

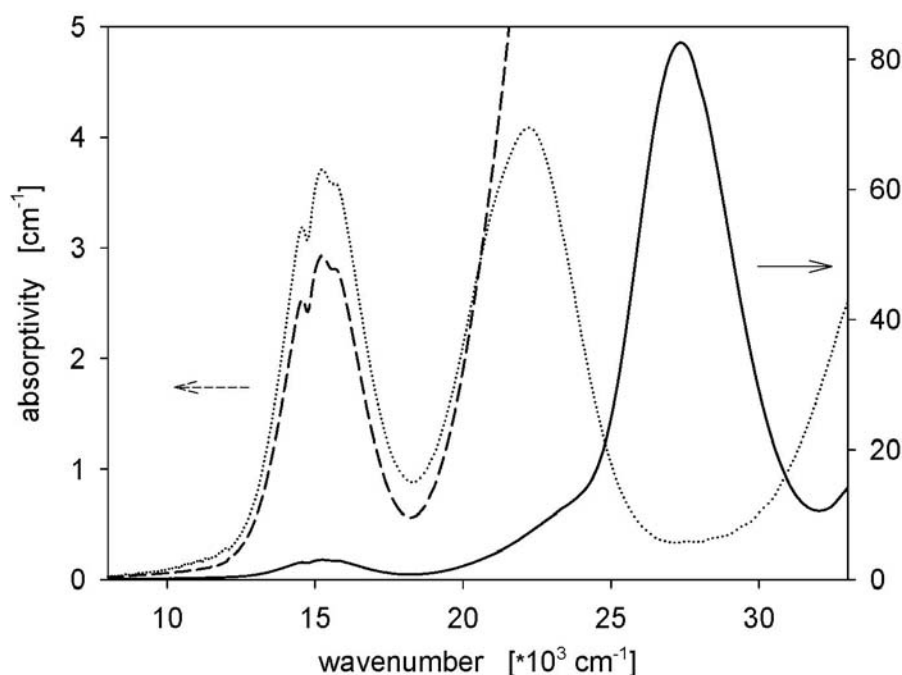
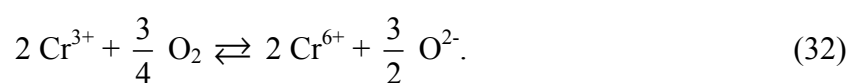


**Figure 25.** Absorption spectra of glasses doped with 0.23 mol %  $\text{Cr}_2\text{O}_3$ :  $\cdots$  sample with sugar;  $---$  vis,  $—$  UV range of the sample melt under standard redox conditions.

The  $\text{Cr}^{5+}$  is a  $d^1$  ion, which in [65, 66] is described to occur in octahedral coordination. According to Ref. [65], deconvolution of absorption spectra recorded from soda-lime-silica glass led to the conclusion that minor quantities of  $\text{Cr}^{5+}$  occur and give rise to an absorption at 462 nm. This band was attributed to the spin-allowed  ${}^2\text{T}_2 \rightarrow {}^2\text{E}$  transition which has a molar absorptivity of  $140 \text{ l}\cdot\text{mol}^{-1}\cdot\text{cm}^{-1}$ , i.e., in the same order as the absorption band caused by  $\text{Cr}^{3+}$ . In  $\text{SiO}_2$  glasses, prepared by a sol-gel procedure, absorptions are observed at around 350 nm

and 440 nm. Since both bands occur at wavelengths similar to peaks caused by Cr<sup>6+</sup> and Cr<sup>3+</sup>, respectively, it is not surprising that small quantities of Cr<sup>5+</sup> (~ 1.2 percent of whole the Cr concentration) [62] are not detected in the absorption spectra of soda-lime-silica glass doped with chromium.

The spectrum of a glass doped with 0.23 mol % Cr<sub>2</sub>O<sub>3</sub> (sample D<sup>\*\*</sup>) is shown in Fig. (25). Altogether three absorption bands can be distinguished: one band at 27,500 cm<sup>-1</sup> due to already described Cr<sup>6+</sup> absorption and two bands at 22,600 and 15,200 cm<sup>-1</sup> caused by Cr<sup>3+</sup>.

The later absorption is actually split into three different distinct absorption lines, from which two of them are spin-forbidden bands, so-called intermixed bands, with small values of a halfwidth (around 300 cm<sup>-1</sup>) and a molar extinction coefficient than the other Cr<sup>3+</sup> bands. However, the composed band at 15,200 cm<sup>-1</sup> is rather difficult to separate into three individual bands, therefore, it is taken as only one band.

The transition  $\nu_6$  is predicted from the ligand field theory ( $\lambda_{\max}$  at around 470 nm), however, it cannot be experimentally indicated in absorption spectrum. The electron transitions are assigned according to the literature [38, 18] and are summarised in Table (6). It is known that Cr<sup>3+</sup> is surrounded by six oxygen atoms and, thus, octahedrally coordinated.

**Table 6.** Assignment of the Cr<sup>3+</sup> electron transitions in soda-lime-silica glass.

Label	spin allowed	$\lambda$ [nm]	Label	spin forbidden	$\lambda$ [nm]
$\nu_1$	${}^4A_2 \rightarrow {}^4T_2$	635	$\nu_4$	${}^4A_2 \rightarrow {}^2E_2$	680
$\nu_2$	$\rightarrow {}^4T_1(F)$	450	$\nu_5$	$\rightarrow {}^2T_1$	650
$\nu_3$	$\rightarrow {}^4T_1(P)$	300	$\nu_6$	$\rightarrow {}^2T_2$	470 <sup>**</sup>

The spectrum of sample E, although melted from Na<sub>2</sub>CrO<sub>4</sub> as raw material, exhibited approximately the same extinction as sample C. The chromium Cr<sup>3+</sup> and also Cr<sup>5+</sup> have an unpaired electron and thus are both paramagnetic. Fig. (26) presents EPR spectra obtained from the glass (sample D) for a thermally non-treated, X, and a quenched sample at 1000 °C, Y<sup>+</sup>. The line X shows three prominent EPR signals. The broad peak at  $g = 5$  belongs to Cr<sup>3+</sup>

<sup>\*\*</sup> see Table (2)

<sup>\*\*</sup> not observed

<sup>+</sup> see capture 4.5.



as well as the signal at  $g_{\text{eff}} = 2$  (<sup>#</sup>), intensity of which depends on concentration [44, 67]. Further, asymmetry of the EPR line shape for  $\text{Cr}^{5+}$  in these glasses is typical for centers with anisotropic g-factors. From line analysis,  $g_{\parallel}$  and  $g_{\perp}$  can be evaluated to be 1.91 and 1.98, respectively.

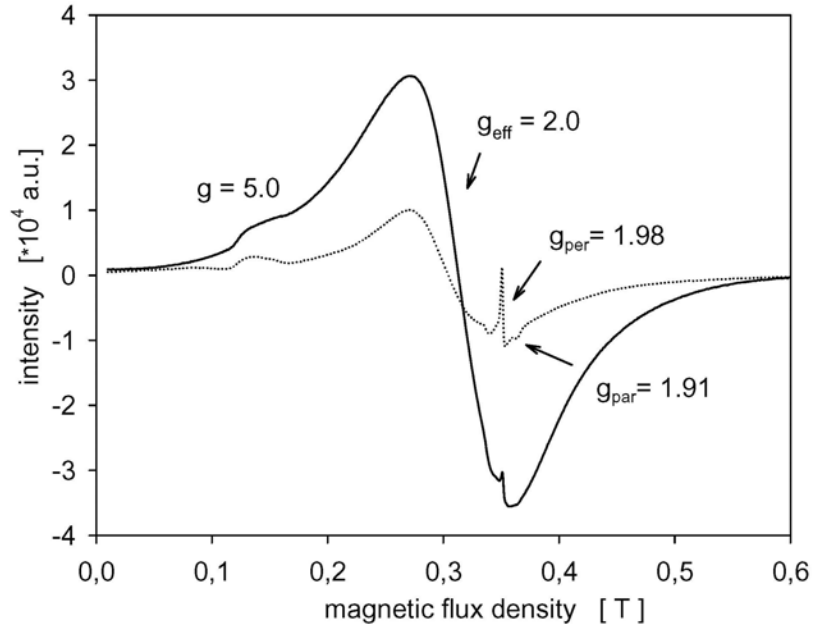


**Figure 26.** EPR spectra of chromium doped glass (sample D): — X sample; ··· Y sample.

The intensity of the  $\text{Cr}^{5+}$  line also depends on concentration [46]. Both lines, X and Y, principally describe the same components in the EPR spectrum of the chromium-doped glass. However, as is readily to see, the concentration depending peaks of the  $\text{Cr}^{3+}$  and  $\text{Cr}^{5+}$  have other intensity from the sample X to the Y. The intensity of the  $\text{Cr}^{3+}$  assigned peak at  $g_{\text{eff}} = 2$  in spectrum X is significantly higher than in Y, i.e., the  $\text{Cr}^{5+}$  concentration in the sample Y is rather higher than in the X. This can be explained by the synproportional reaction of  $\text{Cr}^{3+}$  and  $\text{Cr}^{6+}$  towards  $\text{Cr}^{5+}$  [62]:



Concluded from EPR and absorption spectroscopy, a chromium-doped glass contains  $\text{Cr}^{3+}$ ,  $\text{Cr}^{5+}$  and  $\text{Cr}^{6+}$  simultaneously at room temperature. From HTAS data, Fig. (28), is clearly to see, if the glass is heated and the temperature crosses a limit of about 600 °C a rapid descent in the  $\text{Cr}^{6+}$  intensity is caused. While the intensity of the  $\text{Cr}^{3+}$  band at around 15,200  $\text{cm}^{-1}$  is

<sup>#</sup>  $g_{\text{eff}}$  – effective value of the g is for the parallel and perpendicular component equal.

rather constant over the temperature range, the intensity of the  $\text{Cr}^{3+}$  band at around  $22,300 \text{ cm}^{-1}$  readily increases above  $600 \text{ }^\circ\text{C}$ . As mentioned above, this band has similar absorption parameters to the  $\text{Cr}^{5+}$  absorption band, which was not decomposed separately from the absorption spectrum, i.e., the  $\text{Cr}^{5+}$  can be considered as a part of the  $\text{Cr}^{3+}$  band at around  $22,300 \text{ cm}^{-1}$ . Further, if the temperature increases the ascent in the  $\text{Cr}^{5+}$  concentration is more noticeable.

Figure (27) presents the temperature dependency of the absorption spectra of the glass solely doped with chromium. The measurements were carried out at temperatures in the range from  $25$  to  $800 \text{ }^\circ\text{C}$ . The peak attributed to  $\text{Cr}^{6+}$  at around  $27,500 \text{ cm}^{-1}$  slowly decreases in intensity.

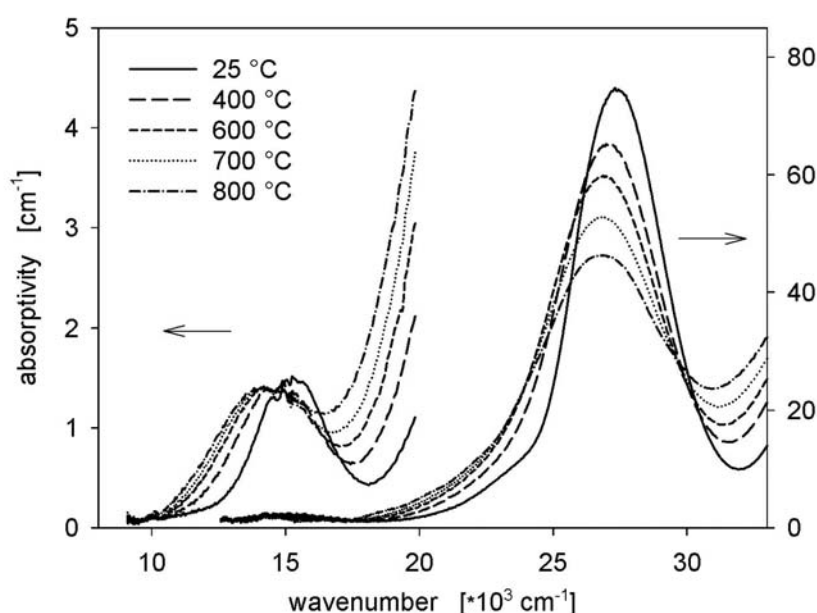


**Figure 27.** Absorption spectra of a glass doped with  $0.23 \text{ mol } \%$   $\text{Na}_2\text{CrO}_3$  recorded at different temperatures.

According to [64], the linear slow descent in the intensity of the  $\text{Cr}^{6+}$  band up to  $600 \text{ }^\circ\text{C}$  could be explained by temperature-dependent transition into  $\text{Cr}^{3+}$  and/or by thermal dissociation of complexes of  $\text{Cr}^{6+}$ . With increasing temperature, it is assumed that the tetrahedral distributed oxygen atoms become more and more statistically distributed. In the case if the oxygen atoms were only statistically distributed around the central atom of  $\text{Cr}^{6+}$ , there would not be expected any absorption band, since the bonds between the oxygen atoms and  $\text{Cr}^{6+}$  would be removed. The total  $\text{Cr}^{6+}$ -concentration stays constant and is described as a sum of  $\text{Cr}^{6+}$  in complex and dissociated  $\text{Cr}^{6+}$ :

$$C_{\text{total}} (\text{Cr}^{6+}) = C_{\text{complex}} (\text{Cr}^{6+}) + C_{\text{dissociated}} (\text{Cr}^{6+}). \quad (34)$$

Above 600 °C the Cr<sup>6+</sup>-intensity decrease even stronger. Here, the effect is amplified by synproportional reaction Eq. (33), which directly lowers the concentration of Cr<sup>6+</sup> in glass. During the whole heating period, the peak gets broader and is shifted to smaller wave numbers with increasing temperature. The shift of the charge-transfer absorption band towards longer wavelengths correlates with the increase of the bond strength between the central ion and the ligands with increasing temperature (see Cap. 3.2.).

With increasing temperature, the peaks at 22,600 and 15,200 cm<sup>-1</sup> get broader and are shifted to smaller wavenumbers. The peak at 15,200 cm<sup>-1</sup> has two spin-forbidden and one spin-allowed bands. From Orgel-diagram for d<sup>3</sup> coordination [38] is clearly seen that the two transitions run parallel with the ground energy and thus they would not show any temperature dependency. Figures (28) to (30) summarize the maximum absorptions, the attributed wavenumbers and the full width at half maxima of the peaks, respectively. In Tab. (7), these band parameters are numerically present at room temperature.

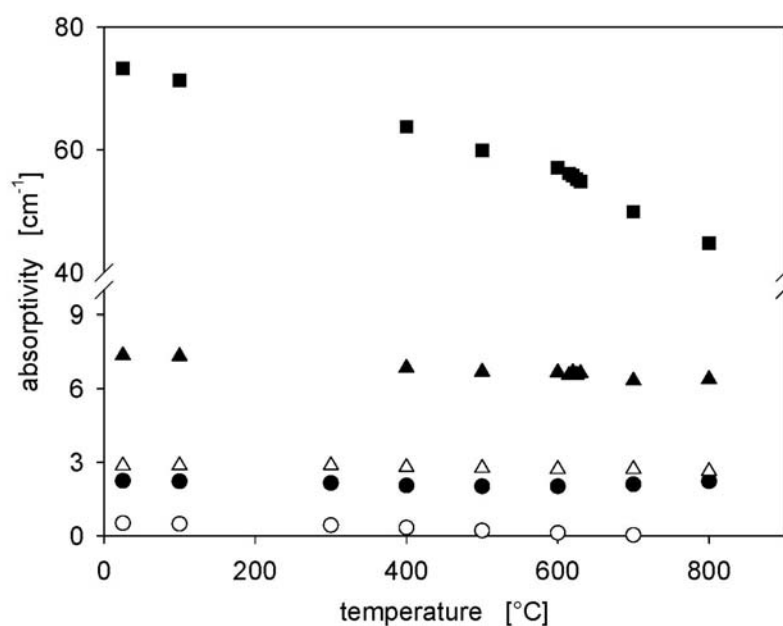


**Figure 28.** Maximum absorptivity as a function of temperature of a glass doped with 0.68 mol % MnO, ○: peak at 15,100 cm<sup>-1</sup>, ●: peak at 20,300 cm<sup>-1</sup>, and of a glass doped with 0.23 mol % Cr<sub>2</sub>O<sub>3</sub>, ■: peak at 27,500 cm<sup>-1</sup> (Cr<sup>6+</sup>), ▲: peak at 22,600 cm<sup>-1</sup> (Cr<sup>3+</sup>) and △: peak at 15,200 cm<sup>-1</sup> (Cr<sup>3+</sup>).

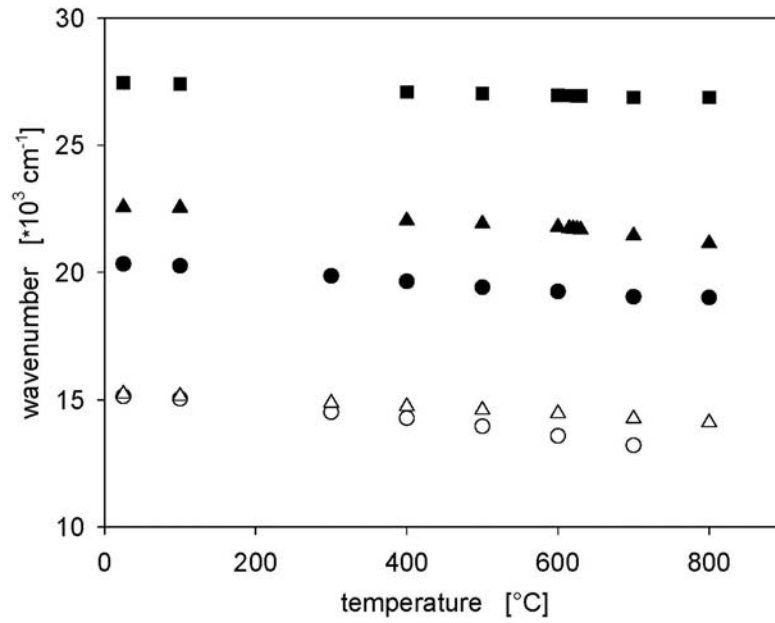


**Figure 29.** Wave number of the maximum absorption as a function of temperature of glasses either doped with manganese or chromium (independent on concentration) (symbols see Fig. (28)).

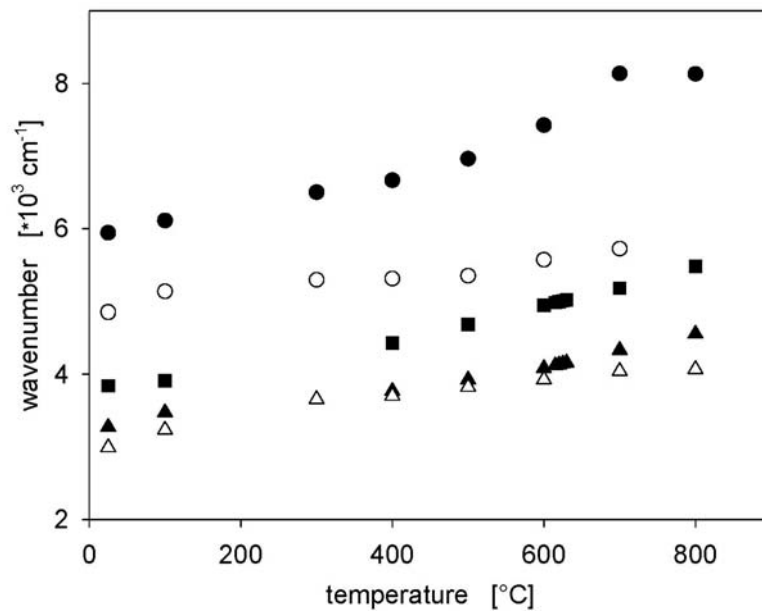


**Figure 30.** Full width at half maximum as a function of the temperature of glasses either doped with manganese or chromium (independent on concentration) (symbols see Fig. (28)).

**Table 7.** Summary of Cr<sup>3+/6+</sup> absorption bands parameters at room temperature.

Transition	k [cm <sup>-1</sup> ] (±1%)	FWHM [cm <sup>-1</sup> ] (±1%)	Coordination
T <sub>1</sub> (π) → <sup>3</sup> T <sub>2</sub> (π*)	27,459	3,841	Tetrahedral
ν <sub>2</sub>	22,561	3,273	Octahedral
ν <sub>1</sub> + ν <sub>4</sub> + ν <sub>5</sub>	15,242	2,993	-

### 5.5. Manganese.

Manganese, besides being a colouring agent, also played an important role as decolouriser because it oxidises the iron (II). It also by its own colour compensates for the green shade, which the iron produces in glass [45]. Manganese can be present in the glasses as divalent or trivalent ions.

Divalent manganese ions have a d<sup>5</sup> configuration. The energy levels of such a configuration apply to both octahedral and tetrahedral symmetry, although, in silicate glasses Mn<sup>2+</sup> is tetrahedrally coordinated. Figure (31) presents absorption spectra of manganese doped glasses and also manganese glass melted with strong reducing agent (1g sugar per 100g glass).

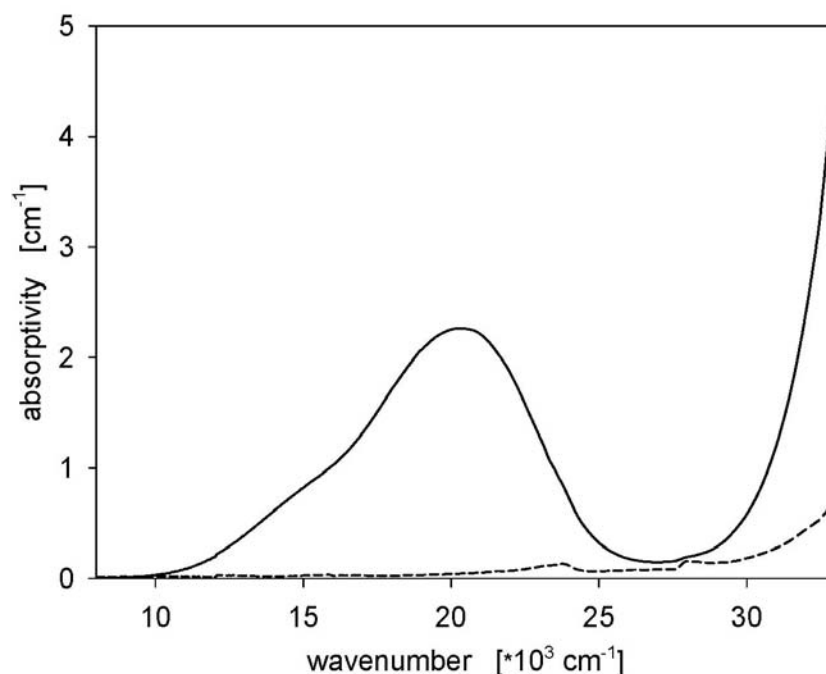


**Figure 31.** Absorption spectra of glasses doped with 0.68 mol % manganese: ---- sample with sugar; — sample melt under standard redox conditions.

Comparing that spectrum with spectra already published [68, 69], it can be seen that many expected bands are not observed or are fused together and the spectrum only consists of a weak band at 422 nm ( ${}^6A_1 \rightarrow {}^4E(G)$ ) and a small shoulder at 352 nm ( ${}^6A_1 \rightarrow {}^4E(D)$ ).

Another property of the  $Mn^{2+}$  oxidation stage is the paramagnetism. In Fig (32), EPR spectral lines of a manganese-doped glass are present of the sample X and Y. According to the literature, only the Y case is well described. Principally, for  $d^5$  configuration, g-values of 2.0, 3.3 and 4.3, respectively, are always typical [44]. In these glasses, the  $Mn^{2+}$  appears in the six lined hyperfine structure centred around  $g = 2.0$ . The spectrum is inhomogenously broadened by magnetic dipole-dipole interaction. Due to this reason, the hyperfine structure is not clearly resolved [46].

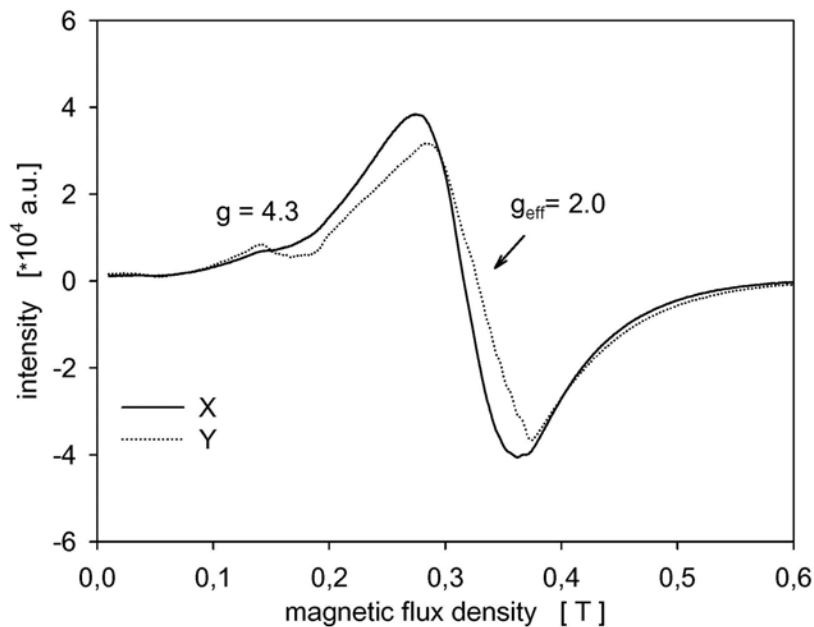


**Figure 32.** EPR spectra of manganese doped glass (sample A).

The absorption coefficient of the  $Mn^{3+}$  is about three (!) orders of magnitude higher than that of  $Mn^{2+}$ . Figure (31) presents an absorption spectrum of a glass doped with 0.68 mol %  $MnO$  (sample A) at room temperature. Deconvolution of the asymmetrical spectrum shows two Gaussian absorptions peaks. The  $Mn^{3+}$  main broad absorption band with a maximum at around  $20,300\text{ cm}^{-1}$  originates from  ${}^5E \rightarrow {}^5T_2$  transition. The other band hidden under this main absorption band at around  $15,100\text{ cm}^{-1}$  is probably due to the splitting of the ground state due to Jahn-Teller distortion [38]. Sample B melted with  $MnO_2$  as raw material exhibited approximately the same spectrum, the extinctions were the same within the error limits.

The temperature dependencies of absorption spectra of glasses solely doped with 0.68 mol % MnO (sample A) is shown in Fig. (33). The measurements were carried out in the temperature range from 25 to 800 °C. In the manganese doped glass the main peak at around 20,300 cm<sup>-1</sup> is continuously shifted to smaller wave numbers with increasing temperatures. The absorption increases slightly up to a temperature of 800 °C and gets significantly broader. The shoulder of the band at around 15,100 cm<sup>-1</sup> behaves similarly with temperature as the main band up to 700 °C, but has no more influence on the shape of the spectrum at higher temperature. That means that the spectrum becomes symmetrical and can be described with only one Gaussian band assigned for main peak.

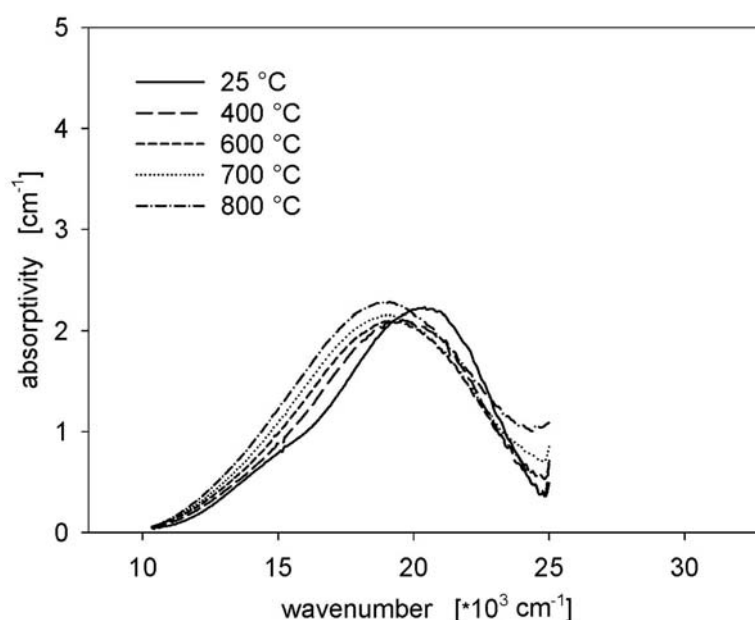


**Figure 33.** Absorption spectra of a glass doped with 0.68 mol % MnO recorded at different temperatures.

From the deconvolution, it is shown that the absorbance at around 15,100 cm<sup>-1</sup> decreases from 0.52 at 25 °C to 0.038 cm<sup>-1</sup> at 700 °C, i.e. much stronger than that of the peak at around 20,300 cm<sup>-1</sup>. Also, this peak gets broader and is shifted to smaller wave numbers with increasing temperature. Samples A and B exhibit approximately the same dependency of the absorption peaks on the temperature. The Mn<sup>3+</sup> absorption was proportional to the MnO-concentration and did not depend on the type of raw material used (MnCO<sub>3</sub> or MnO<sub>2</sub>). All temperature dependencies of those glasses are already showed in Figs. (28) to (30).

**Table 8.** Summary of Mn<sup>3+</sup> absorption band parameters at room temperature.

Transition	k [cm <sup>-1</sup> ] (± 1 %)	FWHM [cm <sup>-1</sup> ] (± 1 %)	Coordination
<sup>5</sup> E → <sup>5</sup> T <sub>2</sub>	20,331	5,941	octahedral
Jahn-Teller	15,143	4,852	-

### 5.6. Chromium - Manganese interaction.

Like as in glasses doped with copper and tin, antimony, or arsenic, also in glass doped with chromium and manganese two polyvalent elements are involved. In the former systems, only the Cu<sup>2+</sup> ion is responsible for absorption in the analysed optical range. In sodium silicate glasses solely doped with chromium or manganese, Cr<sup>3+</sup>, Cr<sup>5+</sup> and Cr<sup>6+</sup> or Mn<sup>2+</sup> and Mn<sup>3+</sup> can absorb, in principle, i.e., in a glass doped with both Mn and Cr, the absorption spectrum is a superposition of the spectra of all different oxidation state.

Some absorption spectra of glasses doped simultaneously with manganese and chromium, presented in Fig. (34), clearly show the peaks around 20,300 and 27,500 cm<sup>-1</sup> as well as a overlapping of bands at about 15,100 cm<sup>-1</sup>. It should be noted that the absorption of Mn<sup>3+</sup> overlaps with those of Cr<sup>3+</sup> and Cr<sup>6+</sup>, especially with respect to the peaks at around 15,000 cm<sup>-1</sup>.

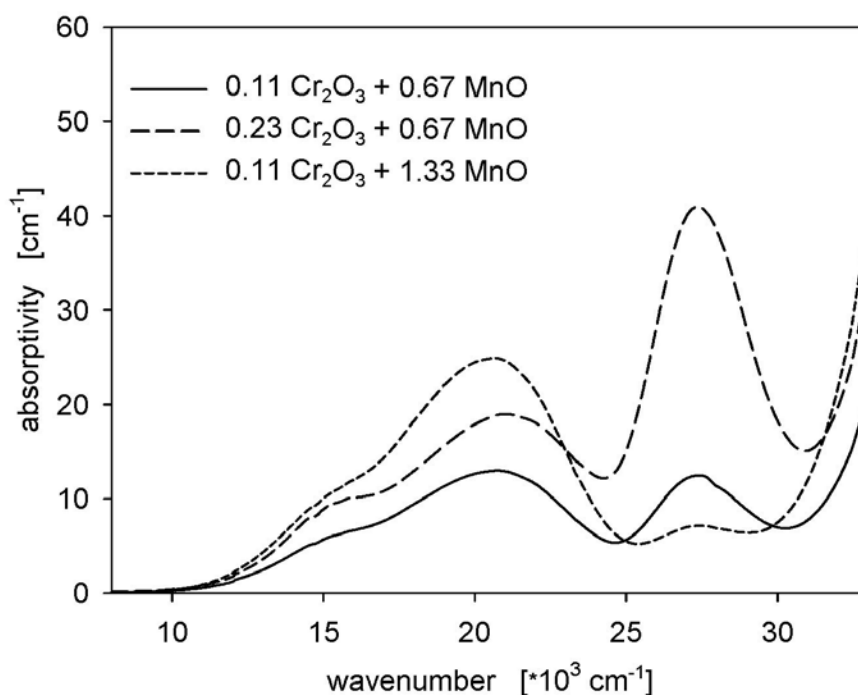


**Figure 34.** Absorption spectra of glasses doped with manganese and chromium.



As shown in previous works [50, 54], the characteristics of a certain band are influenced by the host composition, especially by its basicity. In glasses with the same composition, the polyvalent element is not expected to affect significantly the glass basicity since its concentration is too low (<1 mol %). Hence, in a glass doped with two polyvalent elements whose absorption bands overlap, it is possible to use the band characteristics obtained from glass of the same composition doped solely with manganese or chromium. Spectral analyses of an absorption spectrum based on those assumptions were already shown in Captures 4.4.3 and 4.4.4.

In glasses doped with both chromium and manganese, the same absorption bands are observed as in glasses either doped with chromium or manganese up to a temperature of 600 °C. However, at room temperature, absorption bands attributed to  $\text{Cr}^{6+}$  are smaller than those in glasses doped with the same chromium concentrations but without manganese, while absorptivities of  $\text{Mn}^{3+}$  are larger than in glasses solely doped with manganese. This is a notably difference and a hint on a shift in the redox ratios occurring during cooling the melt to room temperature. This effect will be discussed later. At larger temperatures, the band at  $27,500 \text{ cm}^{-1}$  due to  $\text{Cr}^{6+}$  increases again, while the absorption band at  $20,300 \text{ cm}^{-1}$  caused by  $\text{Mn}^{3+}$  decreases more strongly than in glasses solely doped with manganese. Figure (35) presents absorption spectra of a glass doped with both 0.67 mol % MnO and 0.11 mol %  $\text{Cr}_2\text{O}_3$  (sample F) as a function of the temperature.

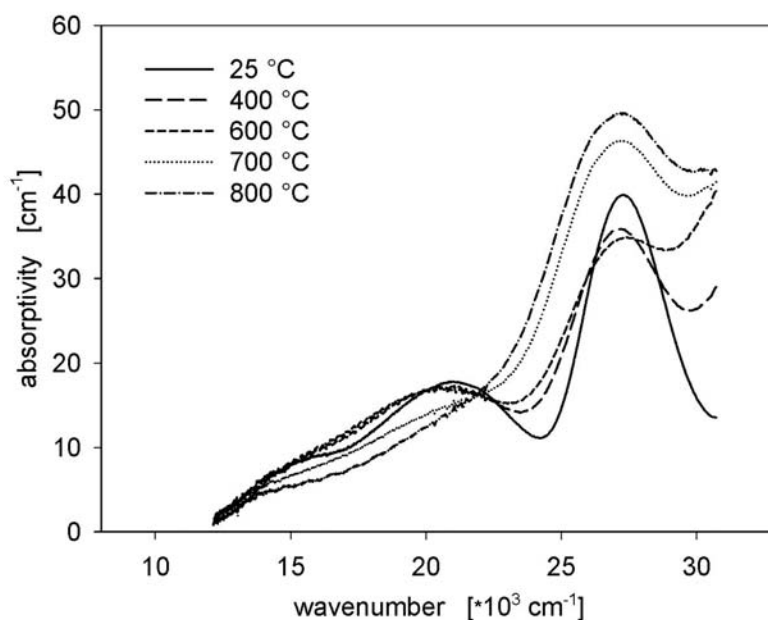


**Figure 35.** Absorption spectra of a glass, doped with 0.67 mol % MnO and 0.11 mol %  $\text{Cr}_2\text{O}_3$  recorded at different temperatures.

Increasing the temperature from 25 to 400 °C results in decreasing absorption maxima of  $\text{Cr}^{6+}$ . A further increase in the temperature, however, leads to a re-increase of the absorption peak at  $27,500 \text{ cm}^{-1}$  ( $\text{Cr}^{6+}$ ) while the peak at  $20,300 \text{ cm}^{-1}$  ( $\text{Mn}^{3+}$ ) further decreases. In Fig. (36) absorption spectra of a glass doped with 1.33 mol % MnO and 0.11 mol %  $\text{Cr}_2\text{O}_3$  (sample L) are shown. Here, the peak at  $27,500 \text{ cm}^{-1}$  is less intense than in Fig. (35), while the peak at  $20,300 \text{ cm}^{-1}$  has approximately the same shape as in Fig. (36). Increasing the temperature to 600 °C results in a continuous decrease of the absorption maximum at  $27,500 \text{ cm}^{-1}$ , while further increasing of temperature results in a re-increase of that peak. The peak at around  $22,600 \text{ cm}^{-1}$  continuously decreases with temperature.

The spectra shown in Figs. (35) and (36) and spectra recorded at other temperatures as well as those recorded from samples F to L were carefully deconvoluted especially with respect to the peaks at  $20,300$  ( $\text{Mn}^{3+}$ ) and  $27,500$  ( $\text{Cr}^{6+}$ )  $\text{cm}^{-1}$ . The peaks at  $15,100$  ( $\text{Mn}^{3+}$ ) and  $15,200$  ( $\text{Cr}^{3+}$ ) overlap too strongly to be suitable for the determination of  $\text{Cr}^{3+}$  and  $\text{Mn}^{3+}$  concentrations.

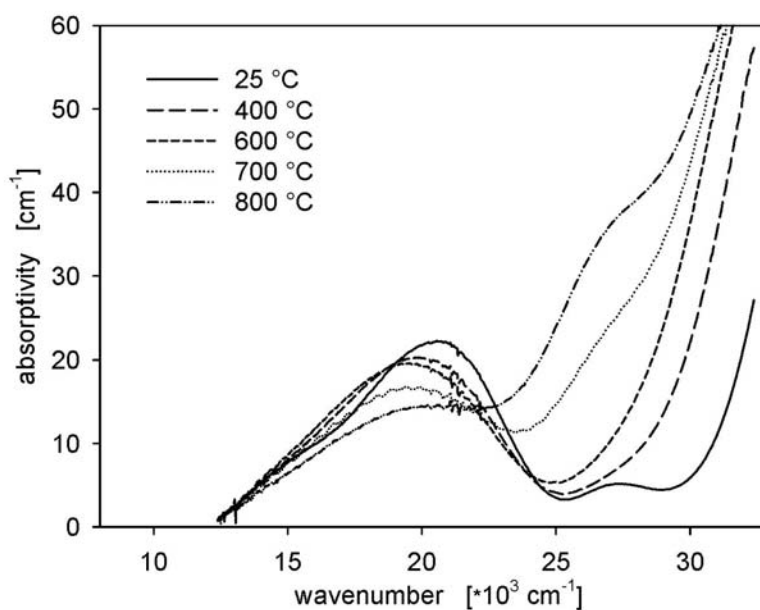


**Figure 36.** Absorption spectra of a glass, doped with 1.33 mol % MnO and 0.11 mol %  $\text{Cr}_2\text{O}_3$  recorded at different temperatures.

In Fig. (37), the dependencies of the absorption maxima at around  $20,300 \text{ cm}^{-1}$  of sample F, H, K and L are shown as a function of the temperature. In the range from 25 to 600 °C, a steady decrease in the absorptions is seen. At temperatures  $> 600$  °C, the absorption maxima at around  $20,300 \text{ cm}^{-1}$  decreases notably in all studied sample.

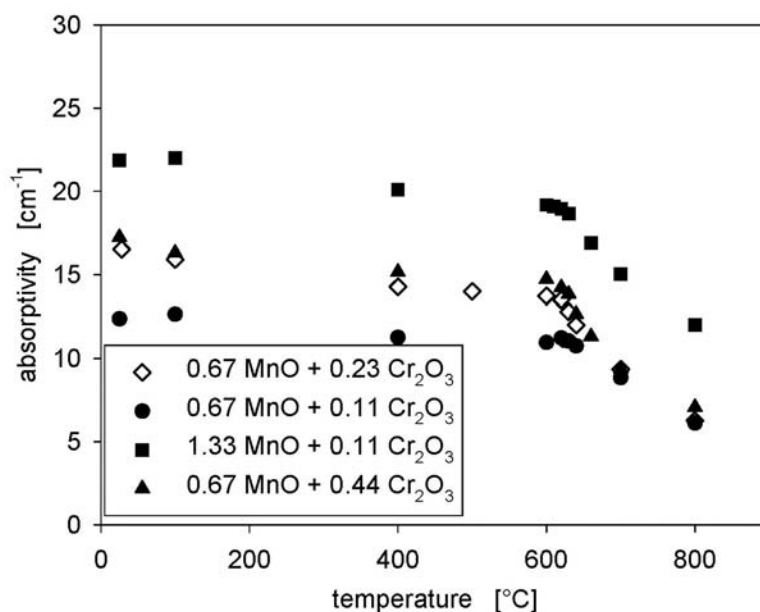


**Figure 37.** Absorptivity maxima of the peak at  $27,500\text{ cm}^{-1}$  ( $\text{Cr}^{6+}$ ) for particular concentrations (in mol %)

In Figs. (38), the temperature dependencies of the absorption maxima at  $20,300\text{ cm}^{-1}$  for samples F, K and L are respectively shown. First, the absorptions decrease up to temperature of  $600\text{ }^\circ\text{C}$ . At higher temperatures, the  $\text{Cr}^{6+}$  absorption increases in all studied samples.

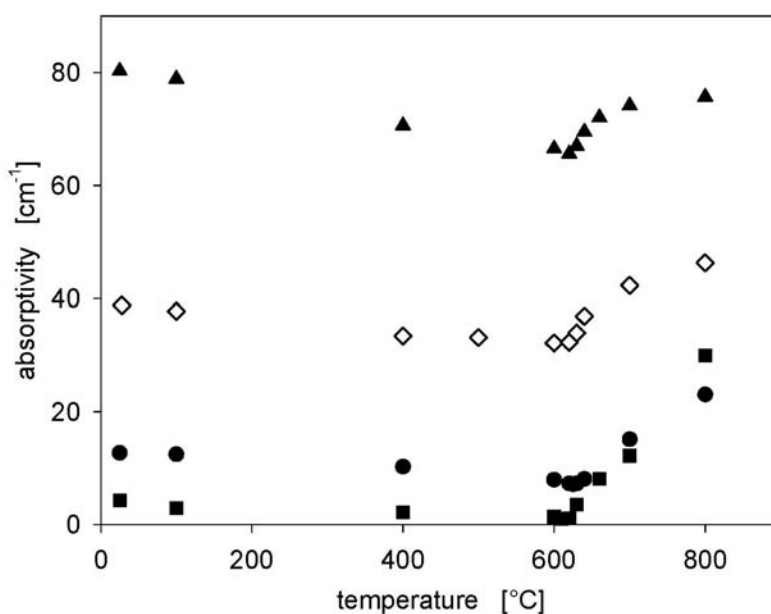
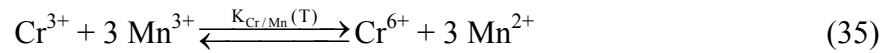


**Figure 38.** Absorptivity maxima of the peaks at  $20,300\text{ cm}^{-1}$  ( $\text{Mn}^{3+}$ ) for particular concentrations (symbols see Fig. (38)).

In summary, the dependencies of the absorptivity upon temperature are qualitatively the same as for glasses doped with either chromium or manganese up to a temperature of 600 °C, but are different for higher temperature.

As was already showed, room temperature absorptions attributed to Cr<sup>6+</sup> are smaller than those in glasses without manganese and doped with the same chromium concentrations, while absorptions of Mn<sup>3+</sup> are larger than in glasses solely doped with manganese. Furthermore, at temperatures > 600 °C, the absorptions of the Cr<sup>6+</sup> band at 27,500 cm<sup>-1</sup> significantly increase while those of the Mn<sup>3+</sup> band at 20,300 cm<sup>-1</sup> decrease more strongly as in glasses only doped with manganese. This behaviour can be explained by a shift in the redox ratio caused by a redox reaction taking place at temperatures > 600 °C:



During heating, the equilibrium is shifted to the left at temperatures > 600 °C. Hence, the Cr<sup>6+</sup> concentration increases while that of Mn<sup>3+</sup> decreases.

The attributed equilibrium constant  $K_{\text{Cr/Mn}}$  can be written as:

$$K_{\text{Cr/Mn}}(T) = \frac{[\text{Cr}^{3+}] \cdot [\text{Mn}^{3+}]^3}{[\text{Cr}^{6+}] \cdot [\text{Mn}^{2+}]^3} \quad (36)$$

It can be calculated from the equilibration constants  $K_{\text{Cr}}$  and  $K_{\text{Mn}}$  (see Eqs. (6) and (7)).

$$K_{\text{Cr/Mn}}(T) = \frac{K_{\text{Cr}}(T)}{K_{\text{Mn}}^3(T)} = \exp\left[\frac{(3 \cdot \Delta H_{\text{Mn}}^0 - \Delta H_{\text{Cr}}^0)}{(R \cdot T)}\right] \cdot \exp\left[\frac{(\Delta S_{\text{Cr}}^0 - 3 \cdot \Delta S_{\text{Mn}}^0)}{R}\right] \quad (37)$$

Both oxidized states Mn<sup>3+</sup> and Cr<sup>6+</sup> always occur as minor components (Mn<sup>3+</sup> << Mn<sup>2+</sup>, Cr<sup>6+</sup> << Cr<sup>3+</sup>). Hence, in a first approximation, the Mn<sup>2+</sup>- and the Cr<sup>3+</sup>-concentrations are equal to the respective total concentrations of the respective polyvalent ion. Using this approximation, Eq. (38) can be rewritten as:

$$K_{\text{Cr/Mn}}(T) = \frac{[\text{Cr}_{\text{total}}] \cdot [\text{Mn}^{3+}]^3}{[\text{Cr}^{6+}] \cdot [\text{Mn}_{\text{total}}]^3} \quad (38)$$

Since, as seen from Figs. (37) and (38), the equilibrium is continuously shifted with temperature until it is frozen in below 600 °C, the room temperature state is given by:

$$\frac{[\text{Cr}^{6+}]}{[\text{Mn}^{3+}]^3} = \frac{1}{K_{\text{Cr/Mn}}(600^\circ\text{C})} \cdot \frac{[\text{Cr}_{\text{total}}]}{[\text{Mn}_{\text{total}}]^3} \quad (39)$$

According to Lambert Beer's law, the following is valid for the extinctions measured:

$$\frac{(E_{\text{Cr}^{6+}}/d)}{(E_{\text{Mn}^{3+}}/d)^3} = C \cdot \frac{[\text{Cr}_{\text{total}}]}{[\text{Mn}_{\text{total}}]^3} \quad (40)$$

with  $C = \varepsilon_{\text{Cr}^{6+}} / (\varepsilon_{\text{Mn}^{3+}}^3 \cdot K_{\text{Cr/Mn}}(600^\circ\text{C}))$ ,  $\varepsilon_i$  = respective extinction coefficients,  $d$  = sample thickness.

Figure (39) shows a plot of  $\alpha_{\text{Cr}^{6+}} / \alpha_{\text{Mn}^{3+}}^3$  versus  $[\text{Cr}_{\text{total}}] / [\text{Mn}_{\text{total}}]^3$ . The line drawn is a regression line through the origin. With respect to the approximations made, the proportionality observed is fairly good.

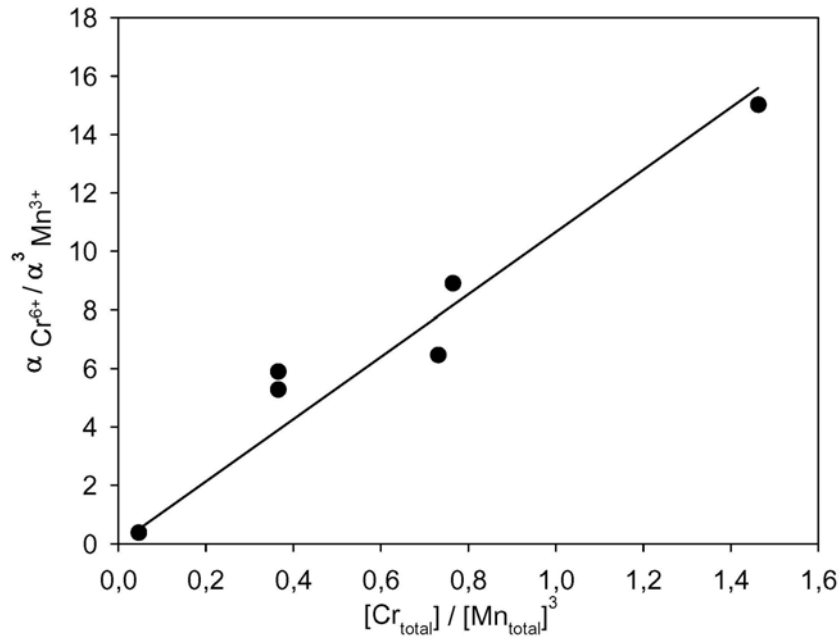


**Figure 39.** Ratio of absorption maxima as a function of the respective concentration ratio.

In the literature, thermodynamic data ( $\Delta H^0$ ,  $\Delta S^0$ ) are available from voltammetric measurements [56] for the redox couple  $\text{Cr}^{3+}/\text{Cr}^{6+}$  ( $\Delta H_{\text{Cr}^{3+}/\text{Cr}^{6+}}^0 = 76 \text{ kJ}\cdot\text{mol}^{-1}$ ,  $\Delta S_{\text{Cr}^{3+}/\text{Cr}^{6+}}^0 = 54 \text{ J}\cdot\text{K}^{-1}\cdot\text{mol}^{-1}$ ). At temperatures  $> 800^\circ\text{C}$ , in a manganese doped melt predominantly  $\text{Mn}^{2+}$  occurs. Hence, in voltammetric measurements, the attributed standard potential is positive and hence outside the accessible potential range. Also from equilibration experiments, thermodynamic data for manganese are not given in the literature.

Assuming equilibration with air at the maximum melting temperature of  $1480^\circ\text{C}$ , a  $[\text{Cr}^{6+}]/[\text{Cr}_{\text{total}}]$ -ratio of  $6.66 \cdot 10^{-3}$  can be calculated using Eq. (7). The spectrum of the glass

doped with  $[\text{Cr}_{\text{total}}] = 0.22 \text{ mol } \%$  (sample F) possess a  $\text{Cr}^{6+}$  absorptivity maximum of  $82.5 \text{ cm}^{-1}$ , from which an molar extinction coefficient of  $56 \cdot 10^3 \text{ l} \cdot \text{cm}^{-1} \cdot \text{mol}^{-1}$  can be calculated.

Assuming also the samples with  $0.68 \text{ mol } \%$  MnO (sample A) and with  $0.67 \text{ mol } \%$  MnO and  $0.23 \text{ mol } \%$   $\text{Cr}_2\text{O}_3$  (sample H) in equilibrium with air at the maximum melting temperature of  $1480 \text{ }^\circ\text{C}$ , the absorbance of  $\text{Mn}^{3+}$  is increased from  $2.3$  to  $16.4 \text{ cm}^{-1}$  and that of  $\text{Cr}^{6+}$  is decreased from  $82.5$  to  $39.6 \text{ cm}^{-1}$  during cooling. From the molar extinction coefficient of  $\text{Cr}^{6+}$  it can be calculated that the decrease in the  $\text{Cr}^{6+}$  absorption of  $42.9 \text{ cm}^{-1}$  is equal to a  $\text{Cr}^{6+}$  concentration of  $7.62 \cdot 10^{-4} \text{ mol } \%$ . According to the stoichiometry of Eq. (35) the corresponding  $\text{Mn}^{3+}$ -concentration, which was formed during cooling is  $2.28 \cdot 10^{-3} \text{ mol } \%$ . This is attributed to an increase in the  $\text{Mn}^{3+}$  absorption of  $14.1 \text{ cm}^{-1}$ , corresponding to a molar extinction coefficient of  $6.18 \cdot 10^3 \text{ l} \cdot \text{cm}^{-1} \cdot \text{mol}^{-1}$ . In the melt solely containing  $0.68 \text{ mol } \%$  MnO, the  $\text{Mn}^{3+}$ -concentration is thus  $5.52 \cdot 10^{-4} \text{ mol } \%$ . This results in a  $[\text{Mn}^{3+}]/[\text{Mn}_{\text{total}}]$ -ratio of  $8.2 \cdot 10^{-4}$ , attributed to  $\Delta G_{\text{Mn}^{2+}/\text{Mn}^{3+}}^0 = -103.6 \text{ kJ} \cdot \text{mol}^{-1}$ .

Since with decreasing temperature, the equilibrium according to Eq. (35) is shifted to the right, the equilibrium constant  $K_{\text{Cr/Mn}}(T)$  gets larger. Therefore,  $3\Delta H_{\text{Mn}}^0 - \Delta H_{\text{Cr}}^0$  must be positive, i.e.  $\Delta H_{\text{Mn}}^0 > 1/3\Delta H_{\text{Cr}}^0$ . Best fit to the experimental data was obtained for  $\Delta H_{\text{Mn}}^0 = 106.8 \text{ kJ} \cdot \text{mol}^{-1}$ , assuming the redox reaction to be in equilibrium at  $T > 600 \text{ }^\circ\text{C}$  and frozen in at lower temperatures. From the respective equilibrium concentrations, the absorptions were calculated using the molar extinction coefficient given above. Figure (40) shows the results of this calculation for both the  $\text{Mn}^{3+}$  and the  $\text{Cr}^{3+}$ -absorptivities of the respective samples.

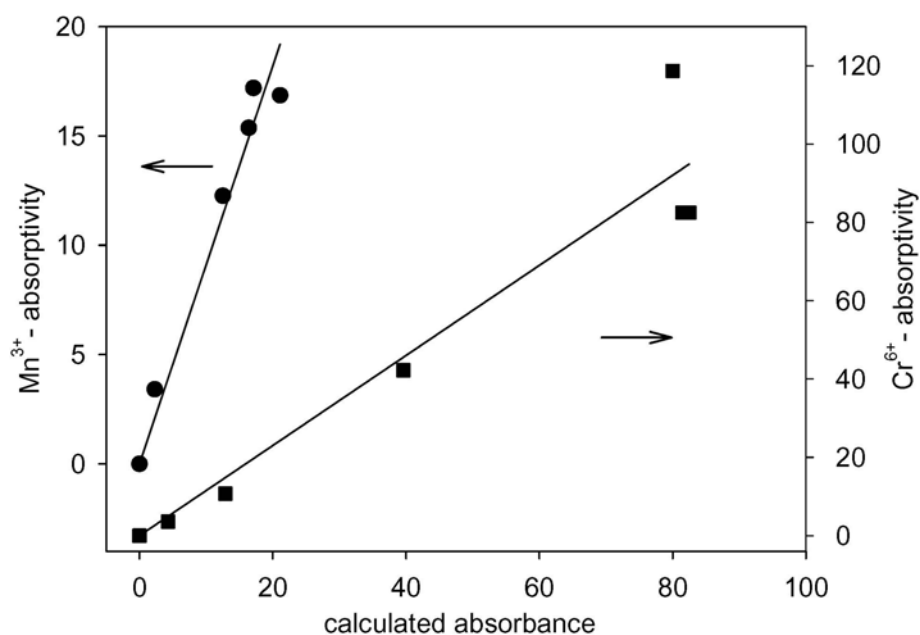


**Figure 40.** Calculated and measured absorptions. ●: Mn<sup>3+</sup>, ■: Cr<sup>6+</sup>.

### 5.7. Study of the kinetics of a redox reaction in the particular case of the chromium and manganese doped glasses.

In the previous section the high temperature spectroscopy experiments were chiefly done in temperature range from 25 up to 800 °C, applying a heating rate of 20 K·min<sup>-1</sup>. The temperatures were chosen with the object to determine the fictive temperature in which the redox reaction is started or frozen-in during heating or cooling, respectively. A set of points around the fictive temperature showed that the redox reaction, represented by maxima of Cr<sup>6+</sup> and Mn<sup>3+</sup>, describes redox relaxation behaviour. To investigate this phenomenon, a glass doped with 0.67 MnO and 0.11 Cr<sub>2</sub>O<sub>3</sub> (sample F) was taken. Absorption spectra as a function of temperature during heating (heating rate of 20 K·min<sup>-1</sup>) are already present in Fig. (35).

Figures (41a) and (41b) also show absorptivities obtained from the same glass composition, however, the spectra were recorded using heating rates of 1 and 5 K·min<sup>-1</sup>. The absorptivities up to a temperature of 530 °C are approximately the same and do not significantly depend upon the heating rate. In analogy, also the absorptivities above 650 °C are not affected by the heating rate. However, in the range between 530 and 650 °C, the absorptivities depend upon heating rates. At a heating rate of 20 K·min<sup>-1</sup>, the absorptivities of Cr<sup>6+</sup> gets only slightly smaller than those extrapolated from the temperature dependence in the range from 25 to 500 °C. The minimum occurs at a temperature of 620 °C. The re-increase in absorptivity is

observed above 625 °C. At a heating rate of 5 K·min<sup>-1</sup>, the minimum is observed at 610 °C and is attributed to smaller absorptivities. At a heating rate of 1 K·min<sup>-1</sup>, the absorptivity decreases strongly at temperatures above 550 °C, reaches the minimum at 600 °C and then increases again. In the temperature range from 530 to 650 °C at all three heating rates the absorptivities of Mn<sup>3+</sup> show the opposite behaviour. When the Cr<sup>6+</sup> absorptivity increases, the Mn<sup>3+</sup> absorption decreases, and vice versa.

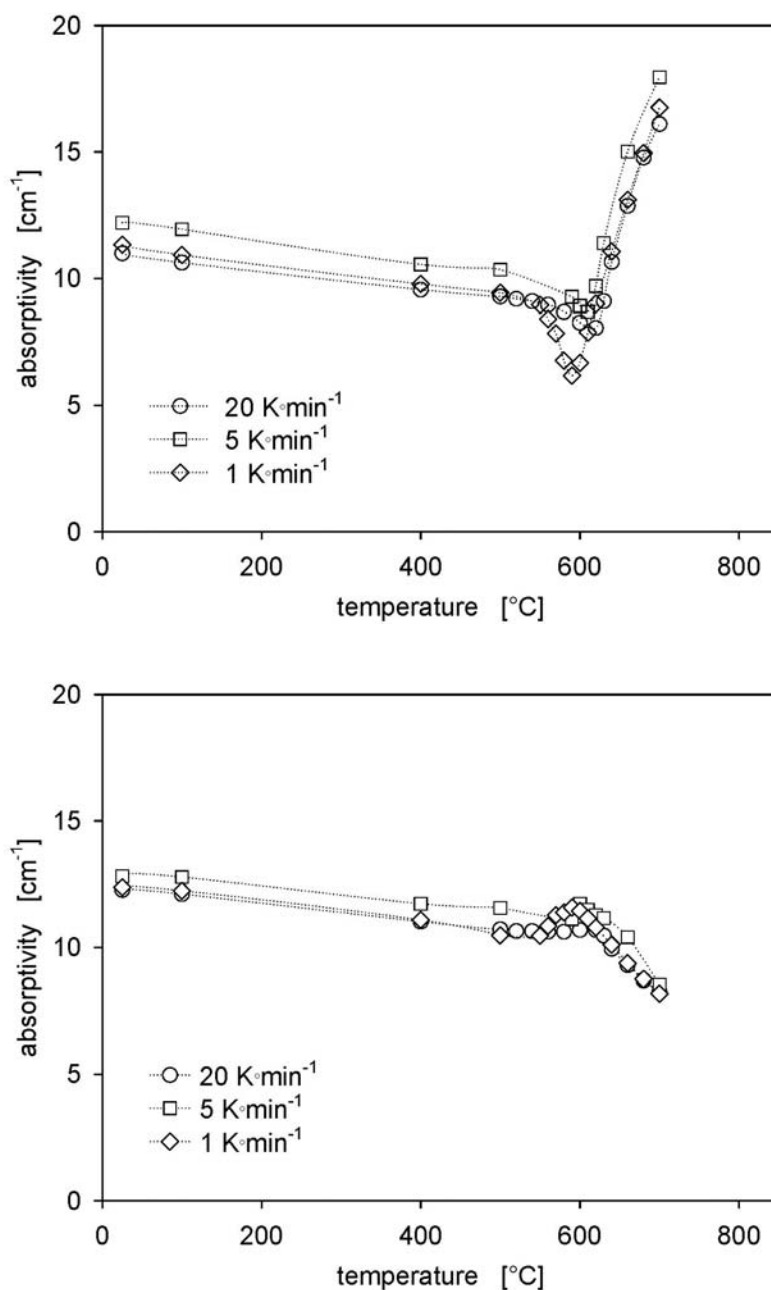


**Figure 41.** Absorption maxima of the peaks at: **a.** 27,500 cm<sup>-1</sup> (Cr<sup>6+</sup>) and **b.** 20,300 cm<sup>-1</sup> measured in a glass doped with 0.67 mol % MnO and 0.11 mol % Cr<sub>2</sub>O<sub>3</sub> during heating  $\diamond$ : 1 K·min<sup>-1</sup>,  $\square$ : 5 K·min<sup>-1</sup> and  $\circ$ : 20 K·min<sup>-1</sup>.



In Fig. (42), results of a little different experiment are shown. The sample was heated with a rate of  $20 \text{ K}\cdot\text{min}^{-1}$  up to a temperature of  $550 \text{ }^\circ\text{C}$  and then kept for 1 h. Subsequently, the sample was further heated with a rate of  $1 \text{ K}\cdot\text{min}^{-1}$ . The absorptivities below  $550$  and above  $595 \text{ }^\circ\text{C}$  are the same as those shown in Figs. (41) for a heating rate of  $1 \text{ K}\cdot\text{min}^{-1}$ . During keeping the sample at  $550 \text{ }^\circ\text{C}$ , the absorptivity of  $\text{Cr}^{6+}$  decreases continuously with time from  $9.4$  to  $7.25 \text{ cm}^{-1}$ .

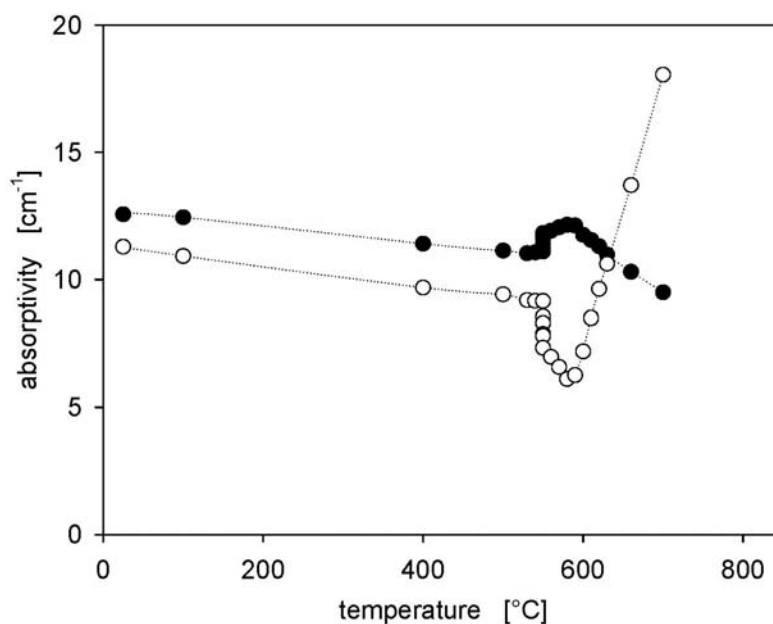


**Figure 42.** Absorption maxima of the peaks at ●:  $20,300 \text{ cm}^{-1}$  ( $\text{Mn}^{3+}$ ) and ○:  $27,500 \text{ cm}^{-1}$  ( $\text{Cr}^{6+}$ ) measured in a glass doped with 0.67 mol %  $\text{MnO}$  and 0.11 mol %  $\text{Cr}_2\text{O}_3$ . The glass was heated to  $550 \text{ }^\circ\text{C}$  with a heating rate of  $20 \text{ K}\cdot\text{min}^{-1}$ , kept for 1 h at this temperature and then further heated with  $1 \text{ K}\cdot\text{min}^{-1}$

In Fig. (43), the decrease in the  $\text{Cr}^{6+}$  and the increase in the  $\text{Mn}^{3+}$  absorption during keeping the sample at  $550 \text{ }^\circ\text{C}$  is shown as a function of time. In Figs. (44) and (45) absorptivities of  $\text{Cr}^{6+}$  and  $\text{Mn}^{3+}$  are shown as a function of the time. Here the samples were heated with a rate of  $20 \text{ K}\cdot\text{min}^{-1}$  and then kept at  $560$  and  $570 \text{ }^\circ\text{C}$  for 5 and 3 h, respectively. At both temperatures, the  $\text{Cr}^{6+}$  absorption decreases and the  $\text{Mn}^{3+}$  absorption increases with time. At temperatures of  $560$  and  $570 \text{ }^\circ\text{C}$ , constant absorptivities are reached after keeping the samples for around 4 and 2 h, respectively.

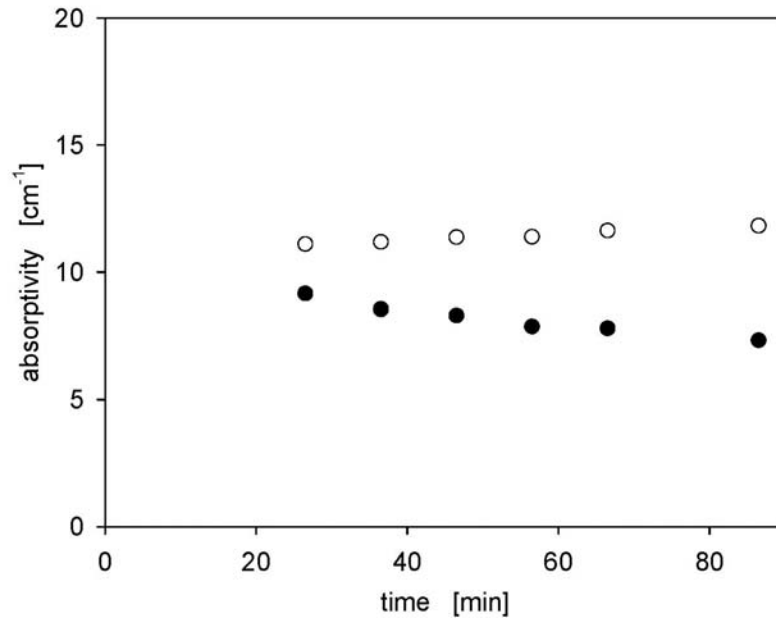


**Figure 43.** Absorption maxima of the peaks at  $20,300\text{ cm}^{-1}$  ( $\text{Mn}^{3+}$ , hollow symbols) and  $27,500\text{ cm}^{-1}$  ( $\text{Cr}^{6+}$ , full symbols) measured in a glass doped with 0.67 mol % MnO and 0.11 mol %  $\text{Cr}_2\text{O}_3$  as a function of time during thermal treatment at  $550\text{ }^\circ\text{C}$ .

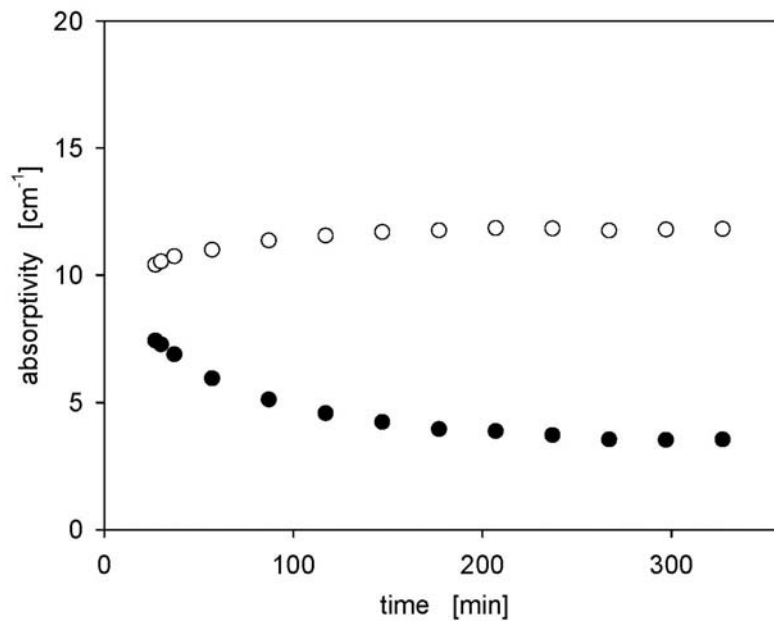


**Figure 44.** Absorption maxima of the peaks at  $20,300\text{ cm}^{-1}$  ( $\text{Mn}^{3+}$ , hollow symbols) and  $27,500\text{ cm}^{-1}$  ( $\text{Cr}^{6+}$ , full symbols) measured in a glass doped with 0.67 mol % MnO and 0.11 mol %  $\text{Cr}_2\text{O}_3$  as a function of time during thermal treatment at  $560\text{ }^\circ\text{C}$ .

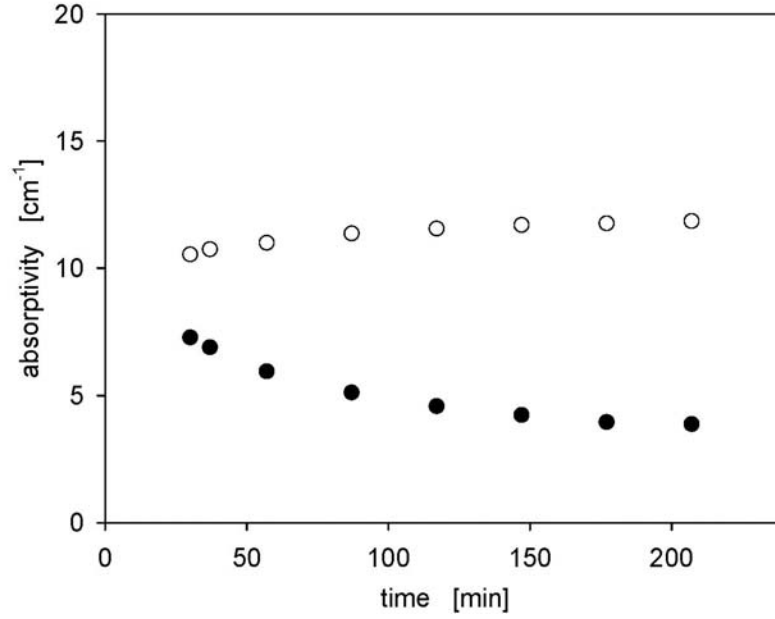


**Figure 45.** Absorption maxima of the peaks at  $20,300\text{ cm}^{-1}$  ( $\text{Mn}^{3+}$ , hollow symbols) and  $27,500\text{ cm}^{-1}$  ( $\text{Cr}^{6+}$ , full symbols) measured in a glass doped with 0.67 mol % MnO and 0.11 mol %  $\text{Cr}_2\text{O}_3$  as a function of time during thermal treatment at  $570\text{ }^\circ\text{C}$ .

Since  $\Delta H_{\text{Cr}}^0 \neq 3\Delta H_{\text{Mn}}^0$ , the equilibrium depends on temperature. The kinetics of the reaction according to Eq. (35) is given by:

$$\frac{dx}{dt} = \left([\text{Mn}^{3+}]_0 + x\right)^3 \left([\text{Cr}^{3+}]_0 + x/3\right) \cdot k_+ - \left([\text{Mn}^{2+}]_0 - x\right)^3 \left([\text{Cr}^{6+}]_0 - x/3\right) \cdot k_- \quad (41)$$

where  $k_+$  and  $k_-$  are the rate constants of the forward and backward reactions, respectively.  $[A]_0$  is the initial concentration of the respective species (at  $t = 0$ ). The quotient of  $k_+$  and  $k_-$  is equal to the equilibrium constant:

$$\frac{k_+}{k_-} = K_{\text{Cr/Mn}}(T) \quad (42)$$

Both,  $k_+$  and  $k_-$  depend upon temperature according to Arrhenius equation.

$$k_+ = k_{+(0)} \cdot \exp\left(-\frac{E_+}{RT}\right) \quad (43)$$

$$k_- = k_{+(0)} \cdot \exp\left(\frac{\Delta S_{\text{Cr/Mn}}^0}{R}\right) \cdot \exp\left(-\frac{E_+ + \Delta H_{\text{Cr/Mn}}^0}{RT}\right) \quad (44)$$

For small deviations from an equilibrium,  $\Delta C_0$ , the system will relax according to

$$\Delta C = \Delta C_0 \cdot \exp(-t/\tau) \quad (45)$$

where  $\tau$  is the relaxation time which depends on the rate constant, and for reaction orders  $> 1$  on the concentrations of the reacting species. For the reaction according to Eq. (35),  $\tau$  is given by:

$$\tau = \left\{ k_+ \left( \frac{1}{3} [\text{Mn}^{3+}] + 3 [\text{Cr}^{3+}] \right) [\text{Mn}^{3+}]^2 + k_- \left( \frac{1}{3} [\text{Mn}^{2+}] + 3 [\text{Cr}^{6+}] \right) [\text{Mn}^{2+}]^2 \right\}^{-1} \quad (46)$$

In the system studied, the redox equilibrium is shifted during changing the temperature. At temperatures  $> 650$  °C, the redox ratio does not depend on the heating rate. So the redox reaction can be considered to be in equilibrium within the time scale of the measurements performed. At temperatures  $< 520$  °C, the absorption does not depend on the heating rate and is constant at a given temperature.

As shown in Figs. (43) to (45), the absorptivities and hence the redox ratios  $\text{Mn}^{3+}/\text{Mn}^{2+}$  and  $\text{Cr}^{6+}/\text{Cr}^{3+}$  change with time at temperatures in the range from 550 to 570 °C. In Fig. (46), the  $\text{Cr}^{6+}$  absorptivities are shown. At 560 and 570 °C, within the limits of error, constant values are obtained after 4 and 2 h, respectively. The solid lines drawn were fitted to an exponential decay, i.e. to  $y = a + b \exp(-t/\tau)$ , with a, b: constants.

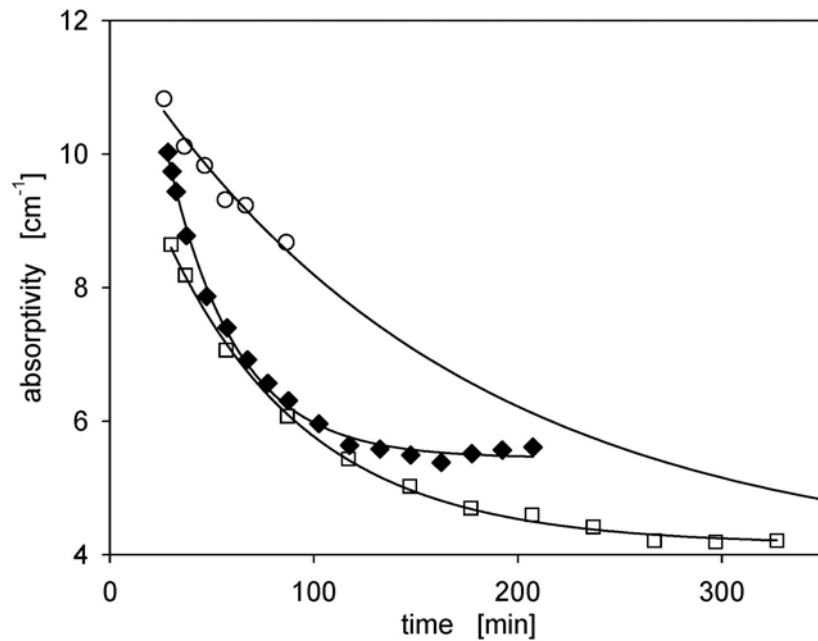


**Figure 46.** Absorption of  $\text{Cr}^{6+}$  as a function of time for  $\circ$ : 550 °C,  $\square$ : 560 °C and  $\blacklozenge$ : 570 °C.

The fit parameter  $\tau$  has the physical meaning of a relaxation time. At a temperature of 550 °C, a limiting value, attributed to the redox equilibrium is not reached within the time scale of the measurement. However, from the thermodynamic data given above, and the molar extinction coefficient of  $\text{Cr}^{6+}$  ( $56,000 \text{ l} \cdot \text{cm}^{-1} \cdot \text{mol}^{-1}$ ), the absorbance at equilibrium conditions can be calculated ( $\alpha_{\text{Cr}^{6+}} = 5.07 \text{ cm}^{-1}$ ). Assuming this value to be reached at infinitely long times, an exponential decay can also be fitted in this case (see also solid line in Fig. (46)). The relaxation times obtained were 9,460, 4,150 and 2,000 s for 550, 560 and 570 °C, respectively.

From relaxation times and the respective equilibrium concentrations of the redox species, the rate constants  $k_+$  and  $k_-$  can be calculated using Eq. (46). The respective concentrations, as well as the equilibrium constant  $K_{\text{Mn/Cr}}$  were calculated from the thermodynamics. This results in  $k_+$ -values of  $0.7 \cdot 10^{-2}$ ,  $1.86 \cdot 10^{-2}$  and  $4.47 \cdot 10^{-2} \text{ s}^{-1} \cdot \text{mol}^{-3}$  for 550, 560 and 570 °C, respectively. Figure (47) shows an Arrhenius plot of the rate constant  $k_+$ . A linear correlation is observed from which an activation energy of  $534.8 \text{ kJ} \cdot \text{mol}^{-1}$  and a pre-exponential factor of  $62.3 \cdot 10^{30} \text{ s}^{-1} \cdot \text{mol}^{-3}$  is obtained. The rate constant and equilibrium constant and their temperature dependencies enable to solve Eq. (41) numerically.

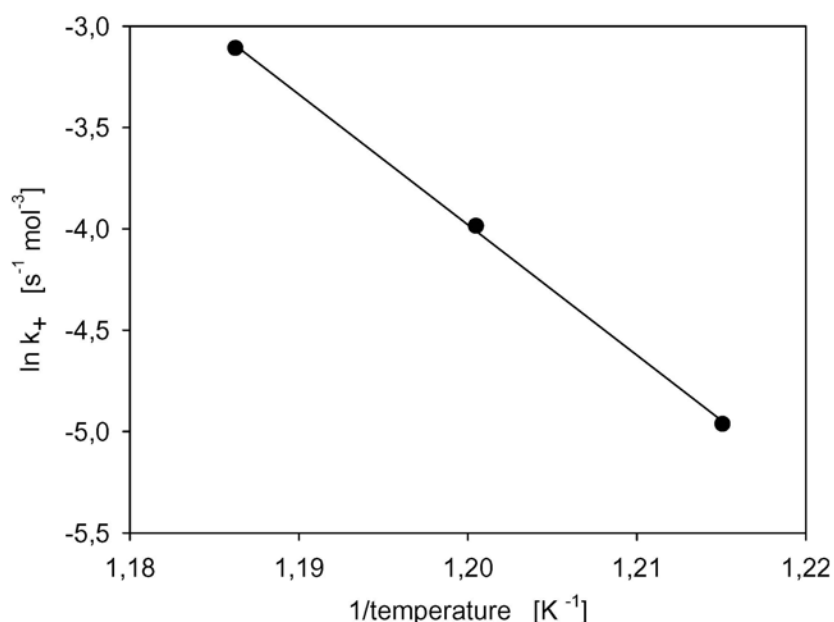


**Figure 47.** Arrhenius plot of the rate constant  $k_+$ .

Figure (48) shows results from numerical calculations for the cooling of the melt. The thick line is attributed to the equilibrium, while the thin lines were obtained for different cooling

rates, which were in the range from 1 to 2,000 K·min<sup>-1</sup>. At all these cooling rates, the system is in equilibrium at temperatures > 680 °C and the redox reaction is frozen in below 590 °C. The redox ratio of the cooled glass is attributed to the equilibrium value at 634 °C. In the following, these temperatures are denoted as fictive redox temperatures. The smaller the cooling rate, the lower the temperature at which first deviations from the equilibrium occur and the lower the fictive redox temperature.

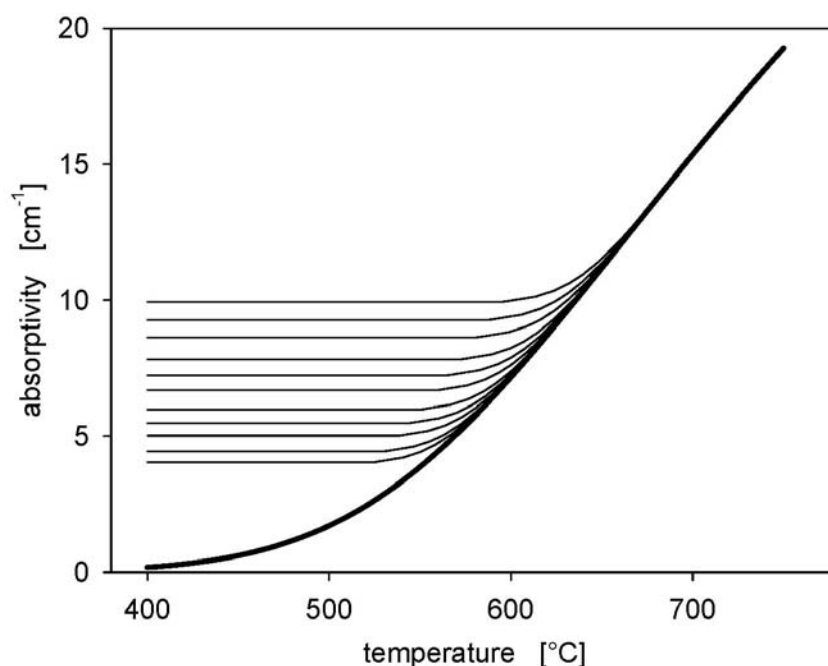


**Figure 48.** Theoretically calculated Cr<sup>6+</sup> absorptivities (normalized to room temperature for different cooling rates) full lines: 2000, 1000, 500, 200, 100, 50, 20, 10, 5, 2, 1 K·min<sup>-1</sup>. Thick line: equilibrium values.

The fictive redox temperature is shown in Fig. (49). Within the studied cooling rate range (0.05 to 2,000 K·min<sup>-1</sup>), it varies over more than 100 K.

In Fig. (50), the behaviour during heating of the sample is shown. For temperatures < 480 °C, the redox ratio is equal to that during cooling and does not change with temperature, while at temperatures > 650 °C, the redox ratio is equal to that of the equilibrium (see thick line). In between, the redox ratio is affected by the heating rate. It first decreases and after reaching the equilibrium value at the respective temperature increases again. The decrease in the absorption (corrected to room temperature) is largest at the smallest heating rate supplied. Here, it decreases from initially 10 cm<sup>-1</sup> to 3.5 cm<sup>-1</sup>, i.e., around the factor 3.

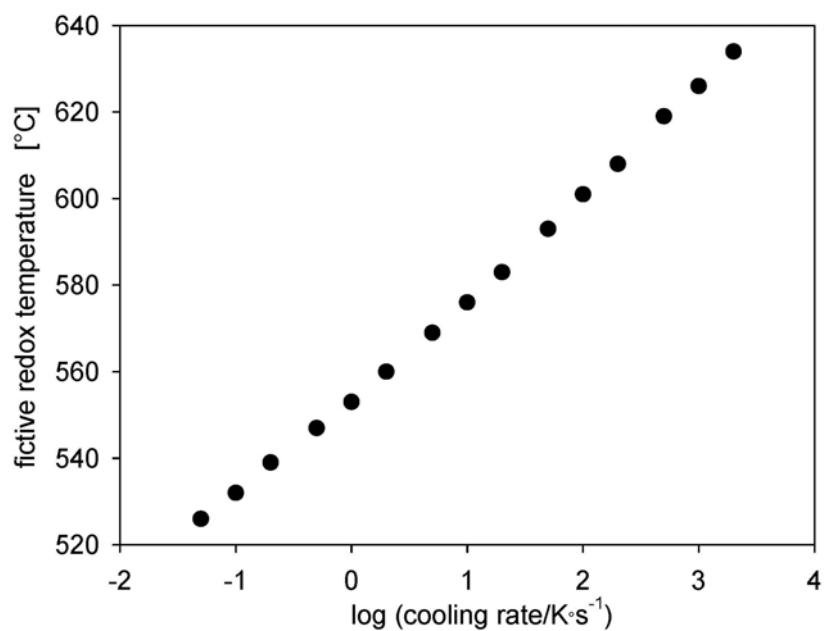


**Figure 49.** Calculated fictive redox temperatures as a function of the cooling rate.

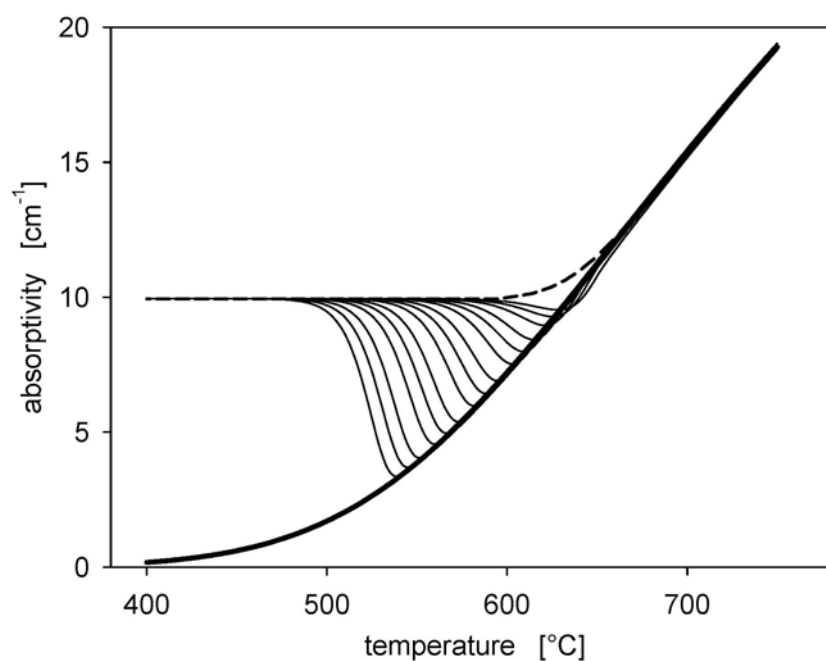


**Figure 50.** Theoretically calculated  $\text{Cr}^{6+}$  absorptivities (normalized to room temperature for different heating rates) full lines: 2000, 1000, 500, 200, 100, 50, 20, 10, 5, 2, 1, 0.5, 0.2, 0.1, 0.05  $\text{K}\cdot\text{min}^{-1}$  (from the top), dashed line: during cooling; thick line: equilibrium values.

## 6. Conclusions.

The redox behaviour of polyvalent elements in glasses with the base composition  $16\text{Na}_2\text{O}\cdot 10\text{CaO}\cdot 74\text{SiO}_2$  in temperature range between 25 and 800 °C was studied by means of high temperature UV-vis-NIR spectroscopy in the spectral range from 300 to 1 100 nm.

This soda-lime-silica composition is oft used as a base glass for many industrial glasses, therefore, gives not only a good approximation on the research level but also to introduce the results for practice.

As high-temperature UV-vis-NIR spectroscopy equipment two arrangements were used regarding the investigated spectral range (see Fig. (3)). For the range between 300 and 800 nm, a heating stage was coupled with a diode-array spectrometer (light source: Xe lamp), whereas, a modular spectrometer with chopper and amplifier (light source: halogen lamp) was used to investigate the spectral range between 450 and 1 100 nm. The later arrangement provides that the radiation from heated parts (sample, heating stage chamber) does not influence the measurement.

The chosen low concentrations of polyvalent element ( $< 2$  mol %) does not notably influence the optical basicity of the glass, i.e., the position and the half bandwidth of a particular absorption band of the element stays constant for different concentrations of polyvalent elements (see Figs. (12 & 25)). In the glass doped simultaneously with two polyvalent elements, the spectrum is composed as a superposition of particular bands. Therefore, Gaussian parameters obtained from absorption spectra of a glass doped with one polyvalent element (see Figs. (5 - 7)) are then used for decomposing the mixed spectra at certain temperature over the whole investigated spectral range (see Figs. (8 - 9)). For all investigated glasses, the UV absorption edge is shifted with increasing temperature towards longer wavelengths ((see Fig. (10)). This phenomenon is assumable caused by increasing of thermal vibration of the oxygen in the glass structure.

### 6.1. Glasses doped with copper or additionally with tin, antimony, arsenic.

Spectra recorded from CuO doped glasses show a well pronounced absorption band at  $12,660\text{ cm}^{-1}$  ( ${}^2\text{E} \rightarrow {}^2\text{T}_2$ ). The curves exhibit a near Gaussian shape (see Fig. (4)). Glasses simultaneously doped with CuO and SnO, Sb<sub>2</sub>O<sub>3</sub> or As<sub>2</sub>O<sub>3</sub>, respectively, show no influence



on the structure of  $\text{Cu}^{2+}\text{O}_6$ , i.e., the position and the half bandwidth of the  $\text{Cu}^{2+}$  absorption band remain constant (see Figs. (12 & 17)). This is independent on concentration and temperature (in the range studied in this work). Furthermore,  $\text{SnO}$ ,  $\text{Sb}_2\text{O}_3$  or  $\text{As}_2\text{O}_3$  do not absorb in the vis-NIR spectral range. Increasing temperatures led to a shift of the  $\text{Cu}^{2+}$  absorption band up to  $11,560\text{ cm}^{-1}$  at  $800\text{ }^\circ\text{C}$  (see Fig. (15)). Simultaneously, the band is becoming broader from  $7,220$  ( $25\text{ }^\circ\text{C}$ ) to  $7,580\text{ cm}^{-1}$  ( $800\text{ }^\circ\text{C}$ ) (see Fig. (16)). In glasses, solely doped with  $\text{CuO}$ , the intensity of the absorption band decreases slightly with temperature.

Glasses doped with  $\text{CuO}$  and  $\text{SnO}$  showed smaller absorption at room temperature and the temperature-depending behaviour is similar as in glasses solely doped with  $\text{CuO}$  (see Fig. (18)). This can be easily explained by the small standart reaction enthalpy ( $\Delta H_{\text{Cu/Sn}}^0 = 8\text{ kJ}\cdot\text{mol}^{-1}$ ) of the reaction:  $2\text{ Cu}^{2+} + \text{Sn}^{2+} \rightleftharpoons 2\text{ Cu}^+ + \text{Sn}^{4+}$ .

The absorptivity of glasses additionally doped with  $\text{CuO}$  and  $\text{Sb}_2\text{O}_3$  is comparably smaller than that of glasses doped with copper and tin at room temperature. During heating, the absorptivity showed a similar behaviour, however, from temperature over  $600\text{ }^\circ\text{C}$ , the absorptivity of the  $\text{Cu}^{2+}$  absorption band is significantly increasing (see Fig. (20)). This was explained by the redox reaction:  $2\text{ Cu}^{2+} + \text{Sb}^{3+} \rightleftharpoons 2\text{ Cu}^+ + \text{Sb}^{5+}$  ( $\Delta H_{\text{Cu/Sb}}^0 = 102\text{ kJ}\cdot\text{mol}^{-1}$ ). Decreasing temperature leads to a shift of the redox reaction to the right and hence, to a decrease in the  $\text{Cu}^{2+}$  concentration.

Glasses doped with  $\text{CuO}$  and  $\text{As}_2\text{O}_3$  show also more or less constant absorptivities up to  $600\text{ }^\circ\text{C}$ , in analogy to the glasses described above. However, with increasing temperature the absorptivity increases (see Fig. (22)). Likewise, by the glasses doped with  $\text{CuO}$  and  $\text{Sb}_2\text{O}_3$ , also here a redox reaction takes place:  $2\text{ Cu}^{2+} + \text{As}^{3+} \rightleftharpoons 2\text{ Cu}^+ + \text{As}^{5+}$  ( $\Delta H_{\text{Cu/As}}^0 = 46\text{ kJ}\cdot\text{mol}^{-1}$ ), which is shifted to the left with increasing temperature.

Thermodynamic calculations based on  $\Delta H^0$  and  $\Delta S^0$  values measured by high temperature square-wave voltammetry qualitatively and quantitatively explain the shift in the redox ratio observed during heating (or cooling) in the temperature range  $600$  to  $1500\text{ }^\circ\text{C}$ . The temperature of  $600\text{ }^\circ\text{C}$  is regarded as a fictive temperature under which the redox ratio does not change any more due to kinetic hindrance of the redox reaction.

## 6.2. Glasses solely doped with manganese or chromium or simultaneously with chromium and manganese.

Here, three sets of glasses were investigated: glasses solely doped with manganese or chromium and then glasses doped with both manganese and chromium in different concentrations.

High temperature absorption spectra recorded from chromium doped glasses showed generally that the intensity of the  $\text{Cr}^{6+}$  ( $T_1(\pi) \rightarrow {}^3T_2(\pi^*)$ ) band centred at  $27,460 \text{ cm}^{-1}$  ( $25 \text{ }^\circ\text{C}$ ) decreases with increasing temperature (see Fig. (27)). From  $T > 600 \text{ }^\circ\text{C}$  the decrease is even stronger (see Fig. (28)). The former effect can be explained by dissociation of chromate complexes. This is combined with the synproportional reaction of:  $2 \text{Cr}^{6+} + \text{Cr}^{3+} \rightleftharpoons 3 \text{Cr}^{5+}$ , which can be explained by the latter effect. The shift of the charge-transfer  $\text{Cr}^{6+}$  band differs only  $570 \text{ cm}^{-1}$  (up to  $800 \text{ }^\circ\text{C}$ ) (see Fig. (29)). Simultaneously, the band becomes broader about the value  $1,640 \text{ cm}^{-1}$  from  $3,840 \text{ cm}^{-1}$  ( $25 \text{ }^\circ\text{C}$ ) (see Fig. (30)).

The physical evaluation of the Gaussian parameter for the  $\text{Cr}^{3+}$ -band, centered at  $22,560 \text{ cm}^{-1}$  ( ${}^4A_2 \rightarrow {}^4T_1(F)$ ) with a halfwidth of  $3,270 \text{ cm}^{-1}$ , can be seriously discussed only in the temperature range where the synproportional reaction of  $\text{Cr}^{5+}$  does not take place ( $< 600 \text{ }^\circ\text{C}$ ), because the  $\text{Cr}^{5+}$ -absorption band has similar band position and thus, can strongly influence the  $\text{Cr}^{3+}$ -band. However, the band parameters are used for decomposing the spectra of glasses doped with chromium and manganese.

The last discussed chromium absorption comes from crossing region centered at  $15,240 \text{ cm}^{-1}$ . In this work it is described with only one band with the halfwidth  $3,000 \text{ cm}^{-1}$ , although, this consists two of spin-forbidden and one spin-allowed absorption band, and thus, the physical meaning of the values is disputable. In spite of that and the fact that the region can be described in good agreement with one Gaussian band over the whole investigated temperature range (see Fig. (7)), the function was later used as an auxiliary function for decomposing of spectra the chromium-manganese-doped glasses.

Although the Gaussian parameters of the last two  $\text{Cr}^{3+}$ -band have no physical meaning at higher temperature, they can still be taken as an auxiliary function parameter for modelling the high temperature emission spectra.

In the case of glasses doped with manganese, the absorption spectrum consists of one main peak at  $20,330 \text{ cm}^{-1}$  ( ${}^5E \rightarrow {}^5T_2$ ),  $5,940 \text{ cm}^{-1}$  broad, and its shoulder band at  $15,140 \text{ cm}^{-1}$ ,

FWHM  $4,850\text{ cm}^{-1}$ , caused by Jahn-Teller distortion (see Fig. (31)). The intensity ratio between them is  $\sim 4.3$ . The main peak is continuously shifted to smaller wavenumbers with increasing temperature by about the values of  $1,330\text{ cm}^{-1}$  (up to  $800\text{ }^{\circ}\text{C}$ ) and get broader from  $5,940$  to  $8,130\text{ cm}^{-1}$  within this temperature range (see Figs. (33 & 28-30)). The absorptivity slightly decreases about 10 % up to  $T < 700\text{ }^{\circ}\text{C}$ . The shoulder peak decreases more strongly in intensity up to  $T = 700\text{ }^{\circ}\text{C}$ . At temperatures above  $700\text{ }^{\circ}\text{C}$  it is no longer detectable. That means that the Jahn-Teller distortion with increasing temperature disappear and the  $\text{Mn}^{3+}$  absorption spectrum becomes a Gaussian-shape ((see Fig. (5)).

Using Gaussians parameters (peak center and the full width at half maximum) obtained from spectra collected from glasses solely doped with one polyvalent element, for different concentrations  $< 2\text{ mol}\%$ , it is possible to sufficiently describe the spectra collected from glasses doped with both polyvalent elements. In glasses doped with both, chromium and manganese, the same absorptions are observed as in glasses either doped with chromium or manganese. However, at room temperature absorptions attributed to  $\text{Cr}^{6+}$  are smaller than those in glasses without manganese and doped with the same chromium concentrations, while absorptions of  $\text{Mn}^{3+}$  are larger than in glasses solely doped with manganese. This is a notable difference and a hint at a shift in the redox ratios occurring during cooling of the melt to room temperature. During heating glasses doped simultaneously with chromium and manganese up to a temperature of  $600\text{ }^{\circ}\text{C}$ , the absorptions of the respective bands of  $\text{Cr}^{6+}$  and  $\text{Mn}^{3+}$  decrease in approximately the same manner as in glasses only doped with one of these polyvalent elements. It can be concluded that up to a temperature of  $600\text{ }^{\circ}\text{C}$ , the redox ratios do not change with temperature. At temperature  $> 600\text{ }^{\circ}\text{C}$ , the absorptions of the  $\text{Cr}^{6+}$  band at  $27,460\text{ cm}^{-1}$  increase again while those of the  $\text{Mn}^{3+}$  decrease more strongly as in glasses only doped with manganese (see Figs. (37 & 38)). This can be explained by a redox reaction:  $\text{Cr}^{3+} + 3\text{Mn}^{3+} \rightleftharpoons \text{Cr}^{6+} + 3\text{Mn}^{2+}$ .

From thermodynamic data of the  $\text{Cr}^{6+}/\text{Cr}^{3+}$  redox couple available in the literature and the absorption spectra, the molar extinction coefficient of  $\text{Cr}^{6+}$  at  $27,460\text{ cm}^{-1}$  can be calculated. Since the increase in the  $\text{Mn}^{3+}$ - and the decrease in the  $\text{Cr}^{6+}$ -concentration are directly correlated to each other by stoichiometry, also the molar extinction coefficient of  $\text{Mn}^{3+}$  at  $20,330\text{ cm}^{-1}$  can be calculated. This enables the calculation of the equilibrium constant of the  $\text{Mn}^{3+}/\text{Mn}^{2+}$  equilibrium at the melting temperature. From the respective molar extinction coefficients, the thermodynamic data of the  $\text{Cr}^{6+}/\text{Cr}^{3+}$  equilibrium, the equilibrium constant of

the  $\text{Mn}^{3+}/\text{Mn}^{2+}$  equilibrium at 1480 °C and a fitted standard enthalpy  $\Delta H^0 = 106.8 \text{ kJ}\cdot\text{mol}^{-1}$ ,  $\text{Cr}^{6+}$  and  $\text{Mn}^{3+}$  absorptivity were calculated.

Though the variation of the heating rate from 20 down to 1  $\text{K}\cdot\text{min}^{-1}$ , it is possible to get new important knowledge about the kinetics of the reaction between chromium and manganese in glasses. Using diode-array spectrometer, one spectrum can be taken in 0.3 s (!) which allowed more precise observing of the redox changes with time and temperature.

While changing the temperature, a redox reaction occurs at temperatures  $> 520 \text{ }^\circ\text{C}$ . With increasing temperature, this reaction is shifted towards  $\text{Cr}^{6+}$  and  $\text{Mn}^{2+}$ . At temperatures  $< 520 \text{ }^\circ\text{C}$ , the reaction is frozen in, while it is in equilibrium at temperatures  $> 600 \text{ }^\circ\text{C}$  (both within the time scale of the experiment performed) (see Fig. (41)). During thermal treatment of the sample at temperatures in the range from 530 to 600 °C, the absorptions caused by  $\text{Cr}^{6+}$  decrease with time, while those attributed to  $\text{Mn}^{3+}$  increase with time (see Figs. (42 - 45)). The relaxation times are in the range from 9,460 to 2,000 s for temperatures of 550 to 570 °C, respectively (see Figs. (48 & 50)). This is the first experimental evidence for chemical redox relaxation in glasses.

## 7. References.

- 
- [1] J.-H. Lee & R. Brückner: *Zum Redoxgleichgewicht Chrom – Mangan in Silicat- und Boratgläsern*. Glastechn. Ber. 57 (1984) 7-11.
- [2] A. Paul & R. W. Douglas: *Mutual interaction of different redox pairs in glass*. Phys. Chem. Glasses 7 (1966) 1-12.
- [3] M. Leister, D. Ehrh, G. Van der Gönna, C. Rüssel, F. W. Breitbarth: *Redox state and coordination of vanadium in sodium silicates melted at high temperatures*. Phys. Chem. Glasses 40 (1999) 319-25.
- [4] H. D. Schreiber & G. B. Balazs: *Mutual interaction of Ti, Cr, and Eu redox couples in silicate melt*. Phys. Chem. Glasses 22 (1981) 99-103.
- [5] O. Claußen, S. Gerlach, C. Rüssel: *Self-diffusivity of polyvalent ions in silicate melts*. J. Non-Cryst. Solids 253 (1999) 76-83.
- [6] C. Rüssel: *Redox reactions during cooling of glass melts – A theoretical consideration*. Glasstech. Ber. 62 (1989) 199-203.
- [7] H. Müller-Simon: *Electron exchange reactions between polyvalent elements in soda-lime-silica and sodium borate glasses*. Glastechn. Ber. Glass Sci. Technol. 69 (1996) 387-395.
- [8] G. Gravanis and C. Rüssel: *Redox reactions in  $Fe_2O_3$ ,  $As_2O_5$  and  $Mn_2O_3$  doped soda-lime-silica glasses during cooling – A high-temperature EPR investigation*. Glastechn. Ber. 62 (1989) 345-50.
- [9] L. Genzel: *Messung der Ultrarot – Absorption von Glas zwischen 20 und 1360 °C*. Glastechn. Ber. 24 (1951) 55-63.
- [10] N. Neuroth: *Der Einfluß der Temperatur auf die spektrale Absorption von Gläsern im Ultraroten*. Glastechn. Ber. 25 (1952) 242-249.
- [11] N. Neuroth: *Der Einfluß der Temperatur auf die spektrale Absorption von Gläsern im Ultraroten II*. Glastechn. Ber. 26 (1953) 66-69.
- [12] N. Neuroth: *Der Temperatureinfluß auf die optische Konstanten von Glas im Gebiet starker Absorption*. Glastechn. Ber. 28 (1955) 411-22.
- [13] J. Endrýs, F. Geotti-Bianchini & L. De Riu: *Study of the high-temperature spectral behavior of container glass*. Glastechn. Ber. Glass Sci. Technol. 70 (1997) 126-36.
- [14] M. Coenen: *Durchstrahlung des Glasbades bei Farbgläsern*. Glastechn. Ber. 41 (1968) 1-10.

- 
- [15] B. Wedding: *Measurements of high-temperature absorption coefficients of glasses*. J. Am. Ceram. Soc. 58 (1975) 102-5.
- [16] K. Mausbach, N. Nowack & F. Schlegeimilch: *UV/VIS- spectroscopy of aluminates in liquid and solid oxide slags*. Steel Research 68 (1997) 392-7.
- [17] S. Okretic, N. Nowack & K. Mausbach: *UV/VIS-spectroscopy of molten and solid CaO-MgO-SiO<sub>2</sub> - slags*. Steel Research 69 (1998) 259-267.
- [18] J.-Y. Tilquin, P. Duveiller, J. Glibert, P. Claes: *Comparison between high temperature UV-visible spectroscopy and electrochemistry for the in situ study of redox equilibria in glass-forming melts*. J. Non-Cryst. Solids 224 (1998) 216-224.
- [19] J.-Y. Tilquin, P. Glibert & P. Claes: *High-temperature study of multivalent elements in glass-forming melts: the particular case of iron*. Ber. Bunsenges. Phys. Chem. 100 (1996) 1489-92.
- [20] A. Paul, R. W. Douglas: *Ultra-violet absorption of chromium (VI) in binary alkali borate glasses*. Phys. Chem. Glasses 8 (1967) 151-9.
- [21] D. S. Goldman & J. I. Berg: *Spectral study of ferrous iron in Ca+Al-borosilicate glass at room and melt temperatures*. J. Non-Cryst. Solids 38&39 (1980) 183-8.
- [22] D. A. Nolet: *Optical absorption and Mössbauer spectra of Fe, Ti silicate glasses*. J. Non-Cryst. Solids 37 (1980) 99-110.
- [23] P. A. van Nijnatten, J. T. Broekhuijse & A. J. Faber: *High-temperature IR radiation conductivity of industrial glasses*. Ceram. Eng. Sci. Proc. 20 (1999) 47-56.
- [24] C. Ades, T. Toganidis and J. P. Traverse: *High temperature optical spectra of soda-lime-silica glasses and modelization in view of energetic applications*. J. Non-Cryst. Solids 125 (1990) 272-9.
- [25] C. Ades, R. Tsiava, J.-P. Traverse: *Spectral remote sensing method of temperature distribution in molten glass for optimising the glass manufacturing process*. Glastech. Ber. 62 (1989) 261-5.
- [26] M. Müller, A. Kriltz: *In situ investigation of phase formation in semiconductor microcrystal doped glasses*. Proc. XVII. Int. Congress on Glass, Beijing, China, 1995, vol. 2, 309-14.
- [27] M. Müller, A. Kriltz, T. Kittel: *Investigation of nucleation and crystal growth by in situ UV-vis spectroscopic measurements*. Glastech. Ber. Glass Sci. Technol. 68 C1 (1995) 163-8.

- 
- [28] F. Geotti-Blanchini, H. Geißler, F. Krämer, I. H. Smith: *Recommended procedure for the IR spectroscopic determination of water in soda-lime-silica glass*. *Glastech. Ber. Glass Sci. Technol.* 72 (1999) 103-111.
- [29] A. Paul: *Effect of thermal stabilization on redox equilibria and colour of glass*. *J. Non-Cryst. Solids* 71 (1985) 269-78.
- [30] H. Schirmer, M. Müller and C. Rüssel: *High-temperature spectroscopic study of redox reactions in iron- and arsenic-doped melts*. *Glass Sci. Technol.* 76 (2003) 1-7.
- [31] C. Rüssel, R. Kohl & H. A. Schaeffer: *Interaction between oxygen activity of Fe<sub>2</sub>O<sub>3</sub> doped soda-lime-silica glass melts and physically dissolved oxygen*. *Glastech. Ber.* 61 (1988) 209-13.
- [32] H. Scholze: *Glass (nature, structure, and properties)*. Springer-Verlag: New York, Berlin, Heidelberg, 1990.
- [33] H. L. Schläfer und G. Gliemann: *Einführung in die Ligandfeldtheorie*. Frankfurt am M.: Akademische Verlagsgesellschaft, 1967.
- [34] T. Bates, R. W. Douglas: *The absorption bands of Cr<sup>3+</sup>-ions in solutions, crystals and glasses*. *J. Soc. Glass Techn.* (1958) 289-307.
- [35] A. D. Liehr, C. J. Ballhausen: *Intensities in inorganic complexes*. *Phys. Rev.* 106 (1957) 1161-3.
- [36] E. Orgel: *Band widths in the spectra of Manganous and other transition-metal complexes*. *J. Chem. Physics* 23 (1955) 1824-6.
- [37] T. M. Dunn: *The visible and ultra-violet spectra of complex compounds*. *Modern Coordination Chemistry*, New York: Interscience Publ., 1960.
- [38] A. Paul: *Chemistry of glasses*. 2<sup>nd</sup> edition, London: Chapman&Hall, 1990.
- [39] T. Bates: *Ligand field theory and absorption spectra of transition-metal ions in glasses*. *Modern aspects of the vitreous state*. (1962), 2, 195-254.
- [40] M. Cable and Z. Xiang: *Extinction coefficient of the cupric ion in soda-lime-silica glasses*. *Glastech. Ber.* 62 (1989) 382-388.
- [41] D. Ehrt, M. Leister & A. Matthai: *Polyvalent elements iron, tin and titanium in silicate, phosphate and fluoride glasses and melts*. *Phys. Chem. Glasses* 42 (2001) 231-9.
- [42] M. Cable & Z. D. Xiang: *Cuprous-cupric equilibrium in soda-lime-silica glasses melted in air*. *Phys. Chem. Glasses* 30 (1989) 237-242.
- [43] W. Schmidt: *Optische Spectroskopie*. 2. Aufl., Weinheim: Wiley-VCH, 2000.

- 
- [44] G. Fuxi: *Optical and spectroscopic properties of glass*. Berlin: Springer, 1992.
- [45] W. A. Weyl: *Coloured glasses*. London : Dawson's of Pall Mall, 1967.
- [46] J. Wong, C. A. Angell: *Glass - structure by spectroscopy*. New York: Dekker, 1976.
- [47] R. Linn Belford, M. Calvin, and Geneva Belford: *Bonding in copper (II) chelates: solvent effect in their visible absorption spectra*. J. Chem. Physics 26 (1957) 1165-74.
- [48] C. R. Bamford: *The application of the ligand field theory to coloured glasses*. Phys. Chem. Glasses 3 (1962) 189-202.
- [49] M. Gitter, W. Vogel, H. Schütz und E. Stutter: *Zur Kupfer (II)-, Nickel (II)- und Kobalt (II)- Koordination in Oxidgläsern*. Wiss. Ztschr. FSU Jena, Math.-Naturwis. R., 32 (1983) 341-62.
- [50] S. Sakka, K. Kamiya and H. Yoshikawa: *Near-infrared electronic spectra of Cu<sup>2+</sup> ions in silicate, borate and germanate glasses*. J. Non-Cryst. Solids 27 (1978) 289-93.
- [51] J.-H. Lee und R. Brückner: *Optische und magnetische Eigenschaften Cu<sup>1+</sup> - und Cu<sup>2+</sup> - haltige Alkaliborat-, - germanat- und -silatgläser mit Bezug auf die Borsäure und Germanatanomalie*. Glastechn. Ber. 57 (1984) 30-43.
- [52] M. Cable & Z. D. Xiang: *The optical spectra of copper ions in alkali-lime-silica glasses*. Phys. Chem. Glasses 33 (1992) 154-160.
- [53] W. D. Johnson, A. Chelko: *Oxidation – reduction equilibria in molten Na<sub>2</sub>O·2SiO<sub>2</sub> glass in contact with metallic copper and silver*. J. Am. Ceram. Soc. 49 (1966) 562-4.
- [54] Z. D. Xiang & M. Cable: *Redox interactions between Cu and Ce, Sn, As, Sb in a soda-lime- silica glass*. Phys. Chem. Glasses 38 (1997) 167-172.
- [55] A. K. Bandyopadhyay: *A study of interaction between copper and manganese in a soda-borate glass by ESR*. J. Mater. Sci. 15 (1980) 1605 – 8.
- [56] C. Rüssel & E. Freude: *Voltametric studies of the redox behaviour of various multivalent ions in soda-lime-silica glass melts*. Phys. Chem. Glasses 30 (1989) 62-8.
- [57] C. Rüssel: *The electrochemical behaviour of some polyvalent elements in soda-lime-silica glass melts*. J. Non-Cryst. Solids 119 (1990) 303-9.
- [58] A. Wiedenroth, C. Rüssel. *Thermodynamics of the redox equilibrium Fe<sup>2+</sup>/Fe<sup>3+</sup> and the diffusivity of iron in 5Na<sub>2</sub>O·15MgO·xAl<sub>2</sub>O<sub>3</sub>·(80-x)SiO<sub>2</sub> (x=0-20) melts*. J. Non-Cryst. Solids 297 (2002) 173-81.
- [59] C. Rüssel, E. Freude: *Voltammetric studies in a soda-lime glass melt containing two different polyvalent ions*. Glastechn. Ber. 63 (1990) 149-53.



- 
- [60] O. Claußen, C. Rüssel: *Voltammetry in a sulfur and iron containing soda-lime-silica glass melt*. Glastechn. Ber. Glass Sci. Technol. 70 (1997) 231.
- [61] A. Paul: *Optical absorption of chromium (II) in glasses*. Phys. Chem. Glasses 15 (1974) 91-4.
- [62] D. Gödeke, Ma. Müller and C. Rüssel: *High-temperature UV-VIS-NIR spectroscopy of chromium-doped glasses*. Glastechn. Ber. Glass Sci. Technol. 74 (2001) 177-82.
- [63] P. Nath, A. Paul & R. W. Douglas: *Physical and chemical estimation of trivalent and hexavalent chromium in glasses*. Phys. Chem. Glasses 06 (1965) 203-6.
- [64] D. Gödeke: *Untersuchungen zum Lichtabsorptions- und Emissionsverhalten silicatischer Gläser bei Temperaturen bis 1400°C*. Thesis (2002) Friedrich-Schiller-University, Jena, Germany.
- [65] M. Casalboni, V. Ciafardone, G. Giuli et al.: *An optical study of silicate glass containing Cr<sup>3+</sup> and Cr<sup>6+</sup> -ions*. J. Phys.: Condens. Matter 8 (1996) 9056-69.
- [66] M. Herren, H. Nishiuchi, and M. Morita: *Cr<sup>5+</sup> luminescence from chromium-doped SiO<sub>2</sub> glass*. J. Chem. Phys. 101 (1994) 4461-2.
- [67] A. Elvers and R. Weißmann: *ESR spectroscopy – an analytical tool for the glass industry*. Glastechn. Ber. Glass Sci. Technol. 74 (2001) 32-8.
- [68] C. Nelson & W. B. White: *Transition metal ions in silicate melts – I. Manganese in sodium silicate melts*. Geochim. Cosmochimica Acta 44 (1980) 887-93.
- [69] K. Bingham, S. Parke: *Absorption and fluorescence spectra of divalent manganese in glasses*. Phys. Chem. Glasses 6 (1965) 224-32.

## **Danksagung. Acknowledgements.**

Herrn Prof. Dr. C. Rüssel danke ich für die Möglichkeit, an diesem Projekt zu arbeiten, und die jederzeit hervorragende fachliche Betreuung.

Frau Doz. Dr. D. Ehrh danke ich für Konsultations-Stunden und für die Bereitschaft, ein Gutachten für diese Dissertation zu erstellen.

Mein besonderer Dank gilt Herrn Dr. M. Müller für die direkte Betreuung und die Hilfe nicht nur auf wissenschaftlicher Ebene.

Außerdem gilt mein Dank allen Mitarbeiterinnen und Mitarbeitern des Otto-Schott-Institutes für das sehr angenehme Arbeitsklima und die vielfältige Unterstützung bei der Durchführung dieser Arbeit. Besonders danken möchte ich:

Herrn R. Weiß und Herrn L. Preißer für die Hilfe beim Umbau der Apparatur und anderen hilfreichen Konstruktionen;

Herrn Dr. W. Winzer für seine Beratung bei Schmelzen;

Frau G. Möller für die schnelle und ausgezeichnete Probenpräparation;

Frau B. Hartmann nicht nur für die optische Absorptionsmessungen.

Ich danke Frau B. Rambach und Herrn Dr. M. Friedrich für die Durchführung der EPR Messungen und Frau M. Machado für die EPR-Probenvorbereitung.

Frau G. Loesche und Frau C. Apfel danke ich für die Durchführung der DTA Messungen.

Der Deutschen Forschungsgemeinschaft und dem DAAD danke ich für die gewährte finanzielle Unterstützung.

Ebenfalls möchte ich mich bei den Herren Prof. Dr. H. A. Schaeffer, Dr. H. Reiß, Prof. M. Liška, Dr. D. Galúsek and Dr. R. Klement für ihre Hilfe bedanken.

Nicht zuletzt danke ich meiner Mutti und meiner Freundin Astrid für die Unterstützung besonderes in der Zeit der Fertigstellung dieser Arbeit.

## **Selbständigkeitserklärung:**

Ich erkläre, dass ich die vorliegende Arbeit selbständig und unter Verwendung der angegebenen Hilfsmittel, persönlichen Mitteilungen und Quellen angefertigt habe.

Jena, 18. Feb. 2005

Ladislav Kido

## LEBENS LAUF

---

Name: Kido

Vorname: Ladislav

Nationalität: slowakisch

Familiestand: ledig

Geburtsdatum und –ort: 14.05.1976, Povazska Bystrica, Slowakei

1982 - 1990 Grundschohle, Povazska Bystrica

1990 - 1994 Berufsschohle mit Abitur, Fachrichtung: Glas Technologie, Puchov

10/1995 – 06/2001 Anorganische Chemie, Spezialisazion: Glass und Keramik; Slowakische Technische Universitat, Bratislava

06.06.2001 Diplom-Ingenieur

01.07.2001-30.09.2001 Wissenschaftliche Mitarbeiter der Trencin Universitat, Trencin

01.10.2001-31.12.2004 Promotion mit DAAD Stipendium der Fachrichtung Glaschemie, Otto-Schott-Institute FSU Jena, Deutschland

Jena, den 17. Feb. 2005

Ladislav Kido